Technische Universität München
Fakultät für Chemie
WACKER Lehrstuhl für Makromolekulare Chemie

Cobalt Porphyrin Catalysts Utilised in the Copolymerisation of CO_2 and Propylene Oxide

Wei Xia

Vollständiger Abdruck der von der Fakultät für Chemie der Technischen Universität München zur Erlangung des akademischen Grades eines

Doktors der Naturwissenschaften
(Dr. rer. nat.)
genehmigten Dissertation.

Vorsitzender: Univ. -Prof. Dr. K. Köhler

Prüfer der Dissertation: 1. Univ. -Prof. Dr. Dr. h.c. B. Rieger
2. Univ. -Prof. Dr. Th. F. Fässler

Die Dissertation wurde am 18.12.2014 bei der Technischen Universität München eingereicht und durch die Fakultät für Chemie am 19.02.2015 angenommen.

Acknowledgements

I would like to first thank Prof. Dr. Dr. h.c. Bernhard Rieger for giving me the chance to do my Ph. D. thesis in this group and for the academic freedom that I have enjoyed for the last three years. Dr. Carsten Troll is thanked for his help in the maintenance of lab equipment and in various lab issues. Dr. Sergei Vagin is acknowledged for his help in the revision of my manuscript and for many useful discussion in chemistry.

I would also like to thank several former group members, Dr. Carly Anderson, Dr. Konrad Hindelang, Dr. Christian Anger, Victor Bretzler, for the good time we have enjoyed together. My lab mate Abdussalam Quarosh is thanked for the nice lab atmosphere I have shared with him.

Julian Kehrle, Maximilian Knaus, Stefan Weidle are acknowledged for their kind help in chemicals and lab equipment. Andriy Plikhta is thanked for his help in crystal growth. Of course I am grateful to every one of my colleagues for the time we spent together during the last three years.

Thanks also give to Dr. Ning Zhang, Dr. Yang Li, former KAUST members, Dr. Antoine Monassier, Dr. Khalifah Salmeia, Dr. Tina Lee and many others whom I met during my life in Germany and with whom I enjoyed the time.

Last, but not least, special thanks give to my mom and my girlfriend, Zenghui Zhang for their continuous support of this thesis.

献给胡志林先生

Abbreviations

BDI	beta-diiminate
CHO	cyclohexene oxide
DCM	dichloromethane
DDQ	2,3-Dichloro-5,6-dicyano-1,4-benzoquinone
DLS	dynamic light scattering
DMAP	4-dimethylaminopyridine
DMAQ	dimethylaminoquinoline
DMF	dimethylformamide
EDX	energy-dispersive X-ray spectroscopy
eq.	equivalence
ESI	electrospray ionization
FTIR	fourier transform infrared spectroscopy
GPC	gel permeation chromatography
HCl	hydrochloric acid
H-T%	head to tail percentage
IR	Infrared
MALDI	matrix-assisted laser desorption/ionization
MeOH	metahnol
MTBD	7-methyl-1,5,7-triazabicyclo[4.4.0]dec-5-ene
NBu_4Br	tetrabutylammonium bromide
NBu_4Cl	tetrabutylammonium chloride
NBu_4OAc	tetrabutylammonium acetate

NEt_3	triethylamine
NEt_4^+	tetraethylammonium cation
N-MeIm	N-methyl imidazole
NMR	nuclear magnetic resonance
PCy_3	tricyclohexylphosphine
PDI	polydispersity index
PDMS	polydimethylsiloxane
PO	propylene oxide
PPC	poly(propylene carbonate)
PPh_3	triphenylphosphine
$PPNBF_4$	bis(triphenylphosphine)iminium tetrafluoroborate
PPNCl	bis(triphenylphosphine)iminium chloride
$(PPN)ClO_4$	bis(triphenylphosphine)iminium perchlorate
$PPNN_3$	bis(triphenylphosphine)iminium azide
PPO	poly(propylene oxide)
SEM	scanning electron microscope
THF	tetrahydrofuran
TOF	turnover frequency
TON	turnover number
TPP	tetraphenylporphyrin
TPPAlCl	tetraphenylporphyrin aluminium(III) chloride
TPPCoCl	tetraphenylporphyrin cobalt(III) chloride
TPPCoOMe	tetraphenylporphyrin cobalt(III) methoxide
TPPFeCl	tetraphenylporphyrin iron(III) chloride

TPP-NH_2	5-para-aminophenyl-10, 15, 20-triphenylporphyrin
TPP-NO_2	5-para-nitrophenyl-10, 15, 20-triphenylporphyrin
UV-Vis	ultraviolet–visible
VPO	vapor pressure osmometry
$ZnEt_2$	diethyl zinc(II)

1. Introduction

1.1 Current Research Interests in CO_2 Transformation

Carbon dioxide is an attractive molecule owing to the fact that it is an ideal C-1 feedstock for chemical reactions. This molecule is abundant in the air atmosphere and is non-toxic. Carbon dioxide is considered to be the major source causing the greenhouse effect. The side effects of the high-concentration CO_2 in the air atmosphere, despite the global warming, include the rise of the sea level caused by the melting of the polar ice and the more acidic sea water due to the dissolution of CO_2 to form carbonic acid with water.

Therefore, the utilisation of CO_2 in various important chemical productions is an ideal way not only of industrial concerns, but also of environmental concerns. However, carbon dioxide is relatively stable. Up to date, the following CO_2 transformations are under continuous investigations, and for a more detailed summary of the utilisation of CO_2, a review published in 2011 is referred.[1] Herein, several major chemical reactions involving CO_2 as a building block are briefly introduced as follow:

1. The coupling of CO_2 with olefin compounds by using nickel based catalysts (Scheme 1) was first discovered by Hoberg, Walther and their co-workers.[2] During this reaction, a five-membered ring is initially formed and an HCl aqueous solution is subsequently utilised to cleave down the final product (carboxylic acid) from the nickel centre.

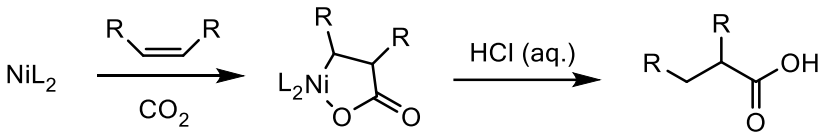

Scheme 1. The reaction of olefin and CO_2 to afford carboxylic acid.

2. The transformation of CO_2 and olefins into acrylic acids is an ideal reaction to afford these synthetically useful compounds (Scheme 2). However, despite the numerous efforts being made during last several decades,[3-7] the following catalytic reaction (Scheme 2) has not been fully realized hitherto. The key hindrance lies in the difficulty of β-H elimination of

the nickelalaction to afford nickel hydride since the five-membered ring is relatively stable and rigid which prevents the approach of the nickel centre to the β hydrogen.

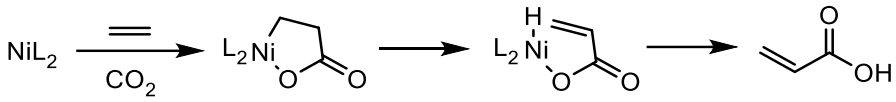

Scheme 2. The formation of acrylic acid from CO_2 and olefin.

3. Palladium phosphine complex has been proved to be able to catalyse the coupling reaction of CO_2 and cyclopropanes (Scheme 3), a reaction which was initially discovered by Inoue *et al.*.[8] During this catalytic cycle, a side reaction has been found, in that C-H bond in the product can be further activated to form a C-C coupling by product.[9] Binger, Weintz and co-workers modified the reaction conditions and successfully suppresses this undesirable side reaction.

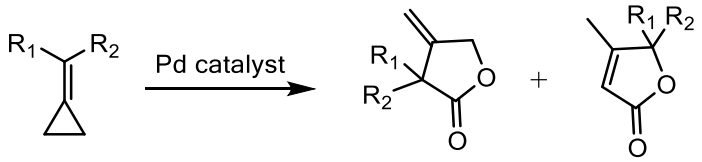

Scheme 3. The coupling of CO_2 and cyclopropane catalysed by palladium-based complexes.

4. Palladium(0) complexes have also been proved to be active for the coupling reaction of CO_2 and diene (Scheme 4).[10] Besides palladium as the metal centre, nickel complexes have also been explored and evaluated for their activities towards such a reaction.[11]

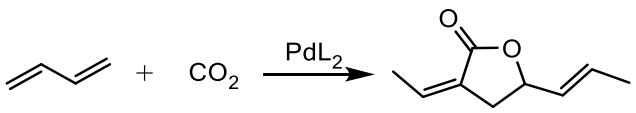

Scheme 4. The coupling of CO_2 and diene.

In addition to the reactions involving CO_2 as a building block mentioned above, the copolymerisation of epoxides and CO_2 is also of great importance (Scheme 5). It was initially discovered by Inoue *et al.* in 1969.[12] Since then, various catalysts with different metal centres

and organic ligands have been designed and investigated aiming to further enhance the polymerisation activity, to suppress the formation of by products (cyclic carbonate and polyether which is formed via repeating insertion of PO into the growing polymer chain), as well as to tune the microstructures for the fulfilments of the required physical properties.[13-19]

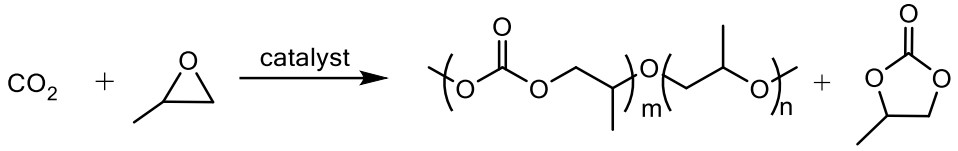

Scheme 5. The copolymerisation of propylene oxide and CO_2.

1.2 Homogeneous Catalysts Applied in PO/CO_2 Copolymerisation

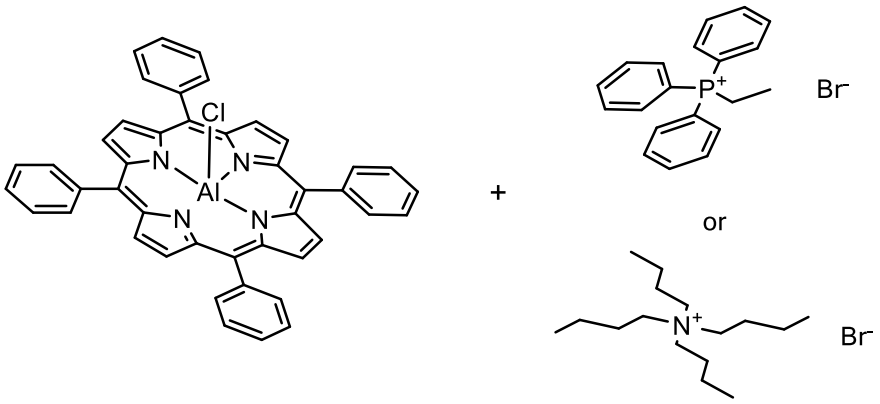

Figure 1. Catalytic system of TPPAlCl and onium salts developed by Inoue.

The first homogeneous catalyst for such a polymerisation was designed by Inoue *et al.* in 1986 wherein tetraphenylporphyrin aluminium(III) chloride with a quaternary ammonium salt as a co-catalyst (Figure 1) is demonstrated to be active for poly(propylene carbonate) formation.[20] Polymers with very narrow molecular weight distribution are afforded by using such a catalyst as determined by GPC measurements (PDI< 1.1). On the other hand, high catalyst concentration is essential to keep the polymerisation at an efficient level (upon elevated dilution of the catalyst concentration, the catalytic activity shows a gradual loss), and a large amount of ether linkage is found in the polymer as evidenced by NMR spectroscopy.

Darensbourg *et al.* developed a zinc phenoxide catalyst[21] (Figure 2) which is able to produce copolymers with higher carbonate content compared with TPPAlCl. However, the molecular weight distribution of the afforded poly(propylene carbonate) is much broader.

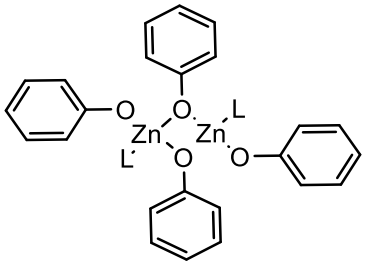

Figure 2. The structure of zinc phenoxides.

Zinc β-diiminate compounds designed by Coates and co-workers (Figure 3) show good activities towards CHO/CO_2 copolymerisation.[22] In addition, minor modifications of the ligand lead to significant changes in the catalytic activities, including the fact that PO/CO_2 copolymerisation has been made possible with this catalyst.

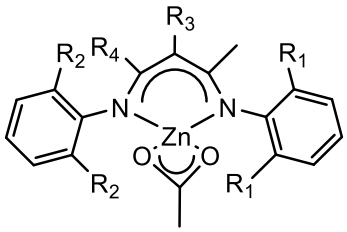

Figure 3. Zinc β-diiminate designed by Coates.

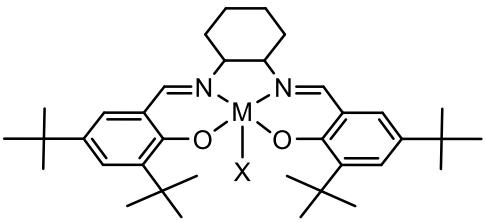

Figure 4. The structure of metal salens.

Metal salen complexes (cobalt(III), chromium(III) as the metal centres) are one of the most effective catalysts up to date (Figure 4). This catalyst is adopted from Jacobsen's chromium(III)

complex which was originally applied in the hydrolytic kinetic resolution of racemic epoxides.[23] In 2003, Coates and co-workers introduced the first cobalt(III)-based salen complex active for epoxides/CO_2 copolymerisation with high selectivity and good region-selectivity.[24]

Although the activity of salenCo(III) does not surpass the zinc BDI catalyst, the formation of cyclic carbonate is successfully suppressed below 1%. Moreover, if a co-catalyst is introduced, such as an onium salt comprising a nucleophilic anion or a Schiff base (e.g. DMAP, N-MeIm), the activity of the polymerisation is significantly enhanced with a highest TOF of 620 h^{-1}.[25]

Due to the fact that many traditional metal complexes, which are capable of copolymerizing epoxides and CO_2, are relatively toxic (e.g. cobalt, chromium), explorations on environmentally friendly metal complexes with superior polymerisation activities become highly desirable. Our group designed a bimetallic zinc catalyst (Figure 5) which is able to catalyse the copolymerisation of CHO and CO_2 with an unprecedently high TOF (9130 h^{-1}).[26] This phenomenon is explained by similar energy barriers between the epoxide ring opening and the CO_2 insertion as suggested by the shift of the rate determining step between these two steps in accordance with the variation of the applied CO_2 pressure. Besides, the synthetic approach of this catalyst is facile and straightforward (three-step syntheses from the commercially available precursor) and this binuclear catalyst overcomes the commonly observed catalytic activity loss upon the dilution of the catalyst concentration with many traditional monometallic catalysts, implying a bimetallic mechanism working behind the chain propagation. Although this di-zinc complex shows nearly no activity towards PO and CO_2 copolymerisation, further ligand modifications as well as detailed mechanistic studies are in progress in our laboratory in order to achieve an even higher catalytic activity in poly(cyclohexane carbonate) formation and to explain the reason behind the fact that it fails to polymerize PO and CO_2 in its current ligand structure.

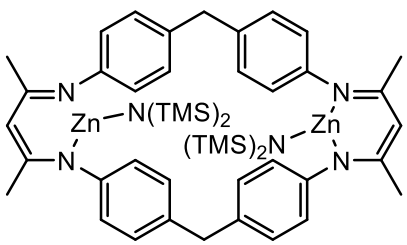

Figure 5. The structure of the binuclear-zinc catalyst.

Cobalt(III) porphyrin complexes are initially considered not to be ideal choices for serving as active catalysts in such a copolymerisation, since they exhibit relatively low affinities towards PO binding in the gas phase as proved by Chisholm *et al.* by using mass spectrometry.[27] In 2008, Sugimoto[28] and Wang[29] independently demonstrated that in the presence of either an onium salt or a Schiff base (e.g. DMAP) as a co-catalyst, tetraphenylporphyrin cobalt(III) chloride complex (Figure 6) polymerizes PO/CO_2 with high carbonate content in the polymer (up to >99%), high selectivity against cyclic carbonate formation (up to 99%) and good region-selectivity (>90% H-T). In addition, TPPCoCl/DMAP system is a bi-functional catalyst active for both CHO/CO_2 and PO/CO_2 copolymerisation. The catalytic activity is moderate with a TOF of 188 h^{-1}.

Following these two initial publications on cobalt(III)-based porphyrin catalysts, modifications of the porphyrin periphery with the introductions of a series of alkoxy groups onto the para-position of the phenyl rings show an enhancement of the overall activity.[30] In contrast, covalent tether of either electron-withdrawing or electron-donating groups onto the ortho-position of the phenyl rings exhibits a drawback with respect to the yield of cyclic carbonate.[31] This phenomenon is explained by the steric effect of the ortho-position-modified catalyst, in that the coordination of the monomer as well as CO_2 insertion are hindered.

The activity of the polymerisation by using cobalt(III)-based porphyrin complexes is sensitive to the change of the temperature. If the reactions are performed at 60 ^oC, the cyclic carbonate formation increases apparently. Based on a thermodynamic viewpoint, the cyclic carbonate formation has a higher energy barrier compared with the polymer formation, and as a consequence, at high temperature, the cyclic carbonate formation rate is naturally enhanced. Further, variation of the applied CO_2 pressure also strongly influences the copolymerisation rate. It has been demonstrated that 30 bar is the best pressure point for a high-speed polymer formation. Copolymerisation reactions conducted over or below this pressure point lead to an obvious decrease of the catalytic activity.

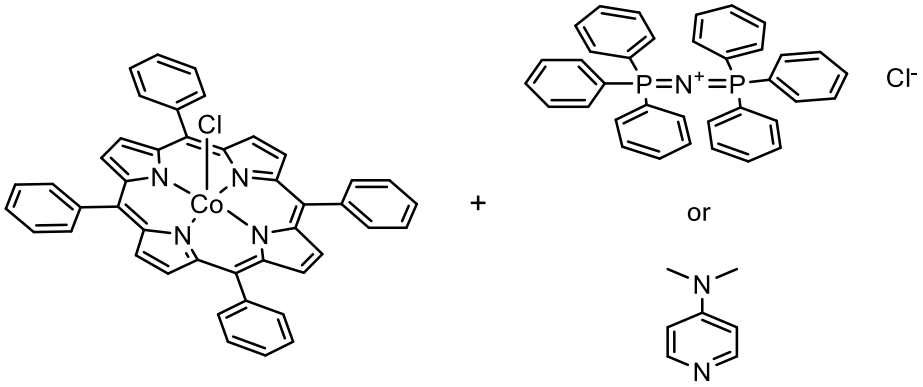

Figure 6. The catalytic system of TPPCoCl with its co-catalysts.

1.3 Reaction Mechanism Concerning PO/CO_2 Copolymerisation

Since the initial discovery of this polymerisation reaction, it has been more than forty years and numerous homogeneous catalysts have been developed and investigated for a further understanding of the copolymerisation mechanism. However, the full images of the catalytic cycle for certain catalysts have not been built up yet.

The reaction pathways for PO/CO_2 copolymerisation are illustrated in Scheme 6, despite the formation of poly(carbonate), poly(ether) and cyclic by product are also possible to be generated during the reaction. The copolymer is formed through a continuous cycle of the ring opening of the epoxide and CO_2 insertion (Scheme 6, middle route). Large amounts of ether linkage, due to the repeating ring opening of the monomer, are found in the polymer while some catalysts (e.g. TPPAlCl) are applied (Scheme 6, left route). No continuous incorporation of CO_2 into the growing polymer chain has ever been reported. Another by product of this polymerisation is cyclic propylene carbonate. It is considered most likely to be afforded through a back-biting side reaction, in that the nucleophilic oxygen atom (either from an alcoholate chain end or a carbonate chain end, we do not specified if it is coordinated or dissociated) is able to attack the nearest electron deficient carbon of the growing polymer chain and a five-membered-ring compound is thus formed (Scheme 6, right).

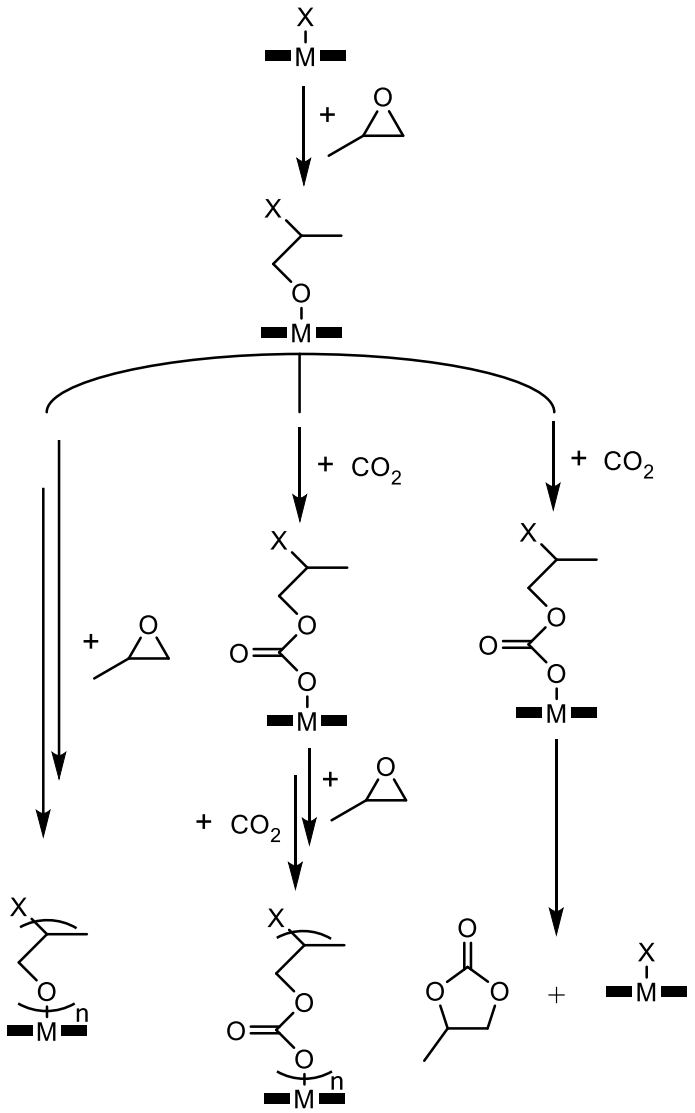

Scheme 6. The possible pathways for the formations of copolymer, poly(ether) and cyclic carbonate in PO/CO_2 copolymerisation.

1.3.1 Initiation Pathways

The initiation of epoxides/CO_2 copolymerisation is commonly considered to be the ring opening of the epoxide by either the axial nucleophile on the catalyst or an additional one (e.g. from onium salts or Schiff bases). The nucleophilic attack of the initiator could take place on either the methylene carbon or the methine carbon of the monomer (Figure 7) and, as a result, leads to two different ring-opening isomers. The ring-opening position of PO by an initiator depends on many factors e.g. the nucleophile, reaction temperature, etc. The selectivity of

the ring-opening position has a strong influence on the polymer regioregularity which makes the polymers exhibiting distinct mechanical properties.

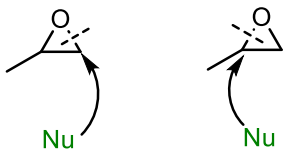

Figure 7. Different ring-opening position of PO by an initiator.

Previous publications[23,32-34] suggest that the ring opening of the epoxides may involve two metal centres of two catalyst molecules which allows to establish a bimetallic initiation pathway. In this case, one epoxide pre-coordinates to one metal centre and the axial nucleophile on another catalyst conducts the nucleophilic attack to accomplish the ring opening (Scheme 7, right). This mechanism of initiation was first proposed by Jacobsen *et al.* in the asymmetric ring opening of epoxides catalysed by a chiral salenCr(III) complex.[23,35]

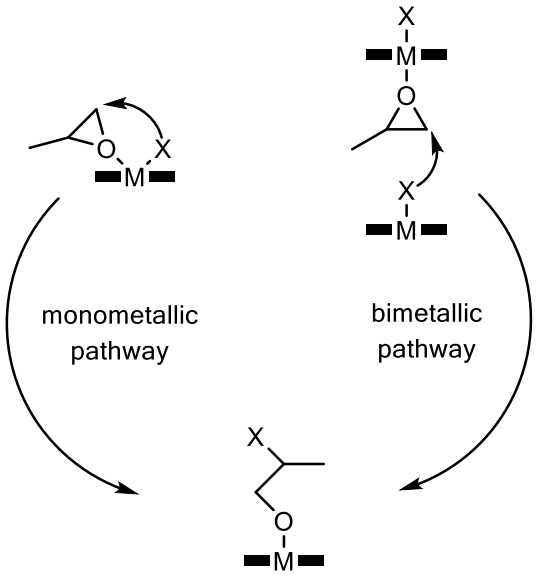

Scheme 7. Two possible pathways of initiation in PO/CO_2 copolymerisation.

Another ring-opening mechanism suggests that the initial ring opening takes place exclusively on one catalyst (Scheme 7, left). A kinetic study on a TPPAl(III)-alkoxide-catalysed ring opening of PO supports such a monometallic initiation as reported by Chisholm *et al.*.[36]

If a co-catalyst is introduced, a binary initiation may take place as illustrated in Scheme 8 (upper route).[18,28,37-53] The additional co-catalyst could attack the pre-coordinated PO and thus finishes the ring opening. Meanwhile, the axial nucleophile on the catalyst would also undergo either a monometallic pathway or a bimetallic pathway to initiate the polymerisation. However, if the polymer chain is able to grow on both sides of the metal centre while in the presence of a co-catalyst is still under debate.[54,55]

The extra nucleophiles could also function as additional ligands which coordinate to the metal centre and improve its Lewis acidity (Scheme 8, lower route). An equilibrium of coordination between PO and the additional nucleophiles towards the metal complex should be formed. Although unasserted, the labilization effect on the metal-nucleophile bond through *trans*-coordination of a strong nucleophile, a phenomenon that may facilitate the PO ring opening, has been suggested in previous publications.[18,49]

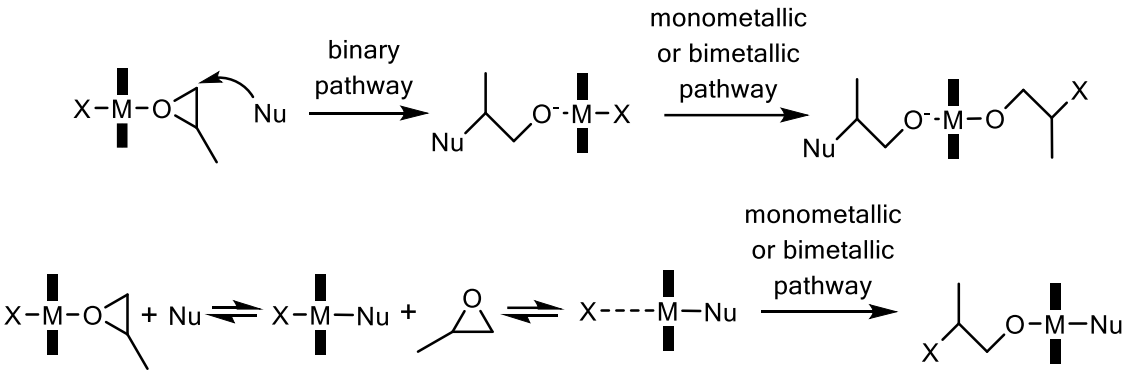

Scheme 8. Pathways of initiation in PO/CO_2 copolymerisation while in the presence of a co-catalyst.

1.3.2 Chain Propagation Pathways

The production of poly(propylene carbonate) involves a series of epoxide ring opening and CO_2 insertion. After initiation, carbon dioxide incorporates into the generated metal alkoxides and a carbonate chain end is thus formed. Then, the epoxide is again ring-opened by this carbonate chain end and via repeating these procedures, the copolymer is formed.

Monometallic chain propagation (Scheme 9, upper route) suggests that the chain growth takes place exclusively on one catalyst.

Due to the fact that many traditional monometallic catalysts will lose their catalytic activities under highly diluted conditions while in contrast to this, the binuclear catalysts designed by Nozaki *et al.* and our group are able to maintain their activities upon the dilution of the catalyst concentration, a bimetallic chain propagation (Scheme 9, lower route) has thus been proposed.[56,57] The stability of the growing polymer may also be enhanced in this bimetallic mechanism since it is always able to coordinate to one metal centre.

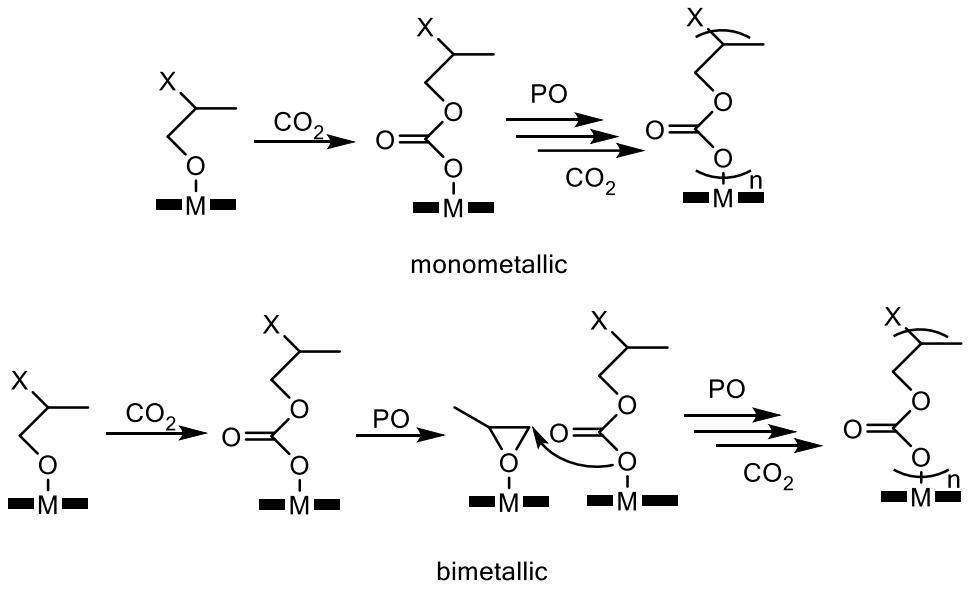

Scheme 9. Monometallic and bimetallic pathways during chain propagation.

In the presence of a co-catalyst, the polymerisation rate has been enhanced significantly. Although the mechanism behind such a rate enhancement has been discussed by many groups,[37,49,52] the reason for such an observation remains obscure.

1.4 Development of Cobalt(III) Porphyrin Catalysts for PO/CO_2 Copolymerisation

Cobalt(III) porphyrins were traditionally considered to have low affinities towards PO binding in the gas phase proved by using mass spectrometry,[27] the capability of these catalysts for PO/CO_2 copolymerisation was thus questioned. In 2008, two independent publications from Wang[29] and Sugimoto[28] demonstrated that tetraphenylporphyrin cobalt(III) chloride with an onium salt (e.g. PPNCl) or a Schiff base (DMAP) is indeed an active catalyst for the poly(propylene carbonate) formation.

In order to start the polymerisation, it is essential for cobalt(III) porphyrin complexes to be accompanied by a co-catalyst. The reactions by using TPPCoCl as a catalyst are carried out mostly at room temperature and a highest TOF of 188 h^{-1} has been reported with a molar ratio of 1500:1:1 between PO, catalyst and co-catalyst. Under such conditions, the copolymer is nearly the exclusive product and the carbonate content in the polymer reaches as high as 99%. Further, the molecular weight distribution of the copolymer, as determined by GPC measurements, shows a very narrow characteristic (PDI=1.2). A bimodal molecular weight distribution of polycarbonates, determined by GPC measurements, is observed, indicating that the polymers have two distinct molecular weights. This may due to a chain transfer caused by trace amounts of water in the reaction mixture. Copolymers with a head-to-tail microstructure reach more than 90% (Figure 8), suggesting an excellent regio-selectivity of the TPPCoCl catalyst.

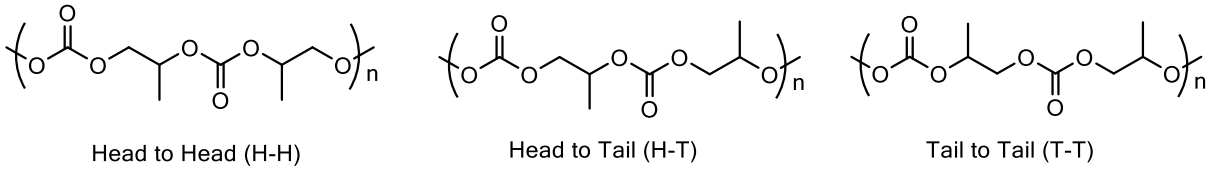

Figure 8. The microstructures of poly(propylene carbonate).

Variations of the reaction conditions lead to the changes in the polymer formation rate, the carbonate content in the polymer structure and the formation rate of the cyclic carbonate. Detailed results are summarized as follow:

By increasing the reaction temperature, the overall catalytic activity of TPPCoCl decreases and the formation of cyclic carbonate increases simultaneously, due to the instability of the polymer chain under such conditions, leading to the depolymerisation via a chain back-biting reaction.

Increasing CO_2 pressure from 20 bar to 50 bar results in a gradual loss of the catalytic activity. This phenomenon is explained as a volumetric expansion of the polymerisation mixture under high CO_2 pressure, leading to the dilution of the catalyst concentration.[58]

Moreover, variation of the axial nucleophile on the catalyst has been proved to influence the polymerisation rate significantly, with strong nucleophiles exhibiting a higher polymer formation rate. Correspondingly, co-catalysts comprising Cl^- or Br^- as the anion show nearly

the same activity compared with each other, whereas co-catalysts containing I^- are completely incapable of assisting the polymer formation.

The molar ratio of catalysts and co-catalysts has also been demonstrated to be a crucial factor to achieve high activities. Detailedly, more than 4 or less than 1 equivalents of co-catalyst leads to an obvious decrease of the polymer formation rate. However, polymerisation with 4 equivalents of co-catalyst increase the cyclic carbonate formation rate.

Interestingly, polymerisations performed in the presence of different solvents show very distinct reaction rates. For instance, an addition of a chlorinated solvent (e.g. DCM, chloroform) decelerates the poly(propylene carbonate) formation. On the contrary, an addition of toluene further enhances the polymer formation rate.

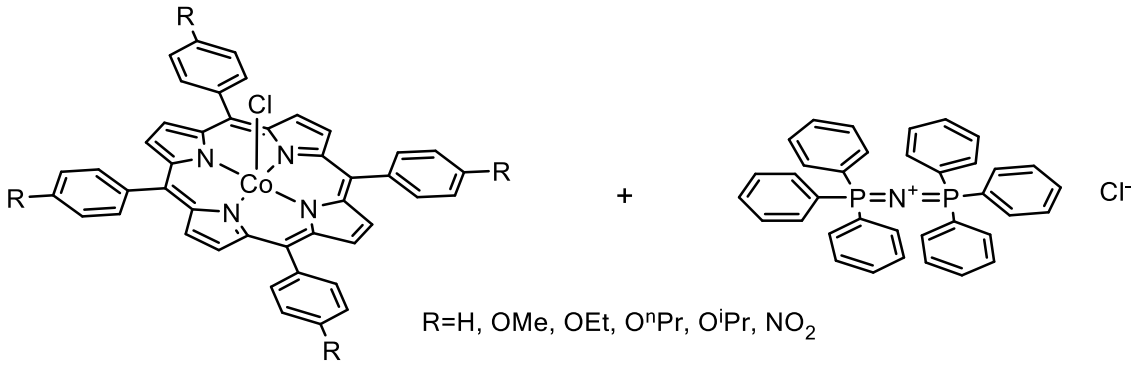

Figure 9. Modified cobalt(III) catalysts.

The combination of TPPCoCl and DMAP serves as a bi-functional initiator, which is effective for both PO/CO_2 and CHO/CO_2 copolymerisation. The influences on such a polymerisation by changing the reaction conditions are stated below:

Without the addition of DMAP, nearly pure poly(cyclohexene oxide) is afforded by TPPCoCl alone. Further, the variation of the co-catalyst with a variety of Schiff base and quaternary ammonium salts has been tested to examine their influences on the polymerisation rate. Conclusively, DMAP shows the highest activity among all of them. The addition of 0.5-1 equivalent of DMAP has been demonstrated to be most suitable for a rapid polymer formation.

The formation of poly(cyclohexene carbonate) catalysed by TPPCoCl and DMAP favours high temperature and high CO_2 pressure. The cyclic carbonate formation is well suppressed below 1% under such conditions. On the contrary, the back-biting reaction seems to take place more

easily in the PO/CO_2 copolymerisation catalysed by TPPCoCl/DMAP. This observation may be attributed to the more bulky backbone of cyclohexene oxide compared with propylene oxide. As a result, the back-biting reaction to produce cyclohexene carbonate is sterically hindered.Following these two publications, further modifications of the porphyrin periphery have been conducted in order to achieve an even faster polymer formation. A series of alkoxy groups has been introduced into the para-position of four phenyl rings (Figure 9) and a slight increase of the catalytic activity has been reported by our group.[30] On the other hand, if the substituent is an electron-withdrawing group (e.g. -NO_2), a decrease in the catalytic activity has been observed.

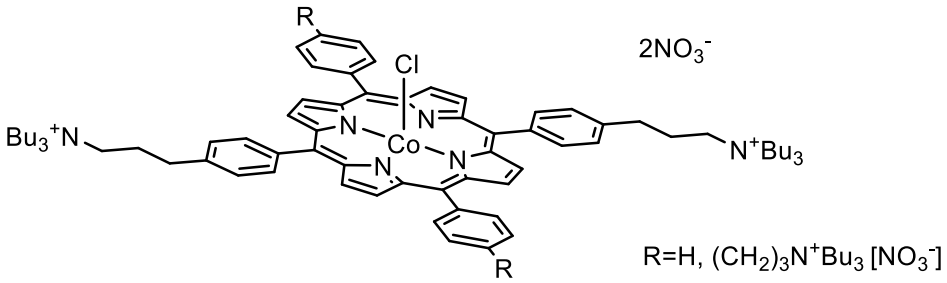

Figure 10. Cobalt(III) porphyrin catalysts tethered with two or four quaternary-ammonium-salts arms on its periphery.

Interestingly, the above-mentioned modifications of the porphyrin ligand with electron-donating groups lead to the formation of the homopolymer (poly(propylene oxide)) in the presence of PO with a TOF of <10 h^{-1}. In contrast, the non-modified cobalt(III) porphyrin catalyst (TPPCoCl) as well as the catalysts modified by electron-withdrawing groups (-NO_2) both show no activity for poly(propylene oxide) formation.

The modified catalysts also exhibit a better selectivity for polymer against by products with a cyclic carbonate formation below 5%.

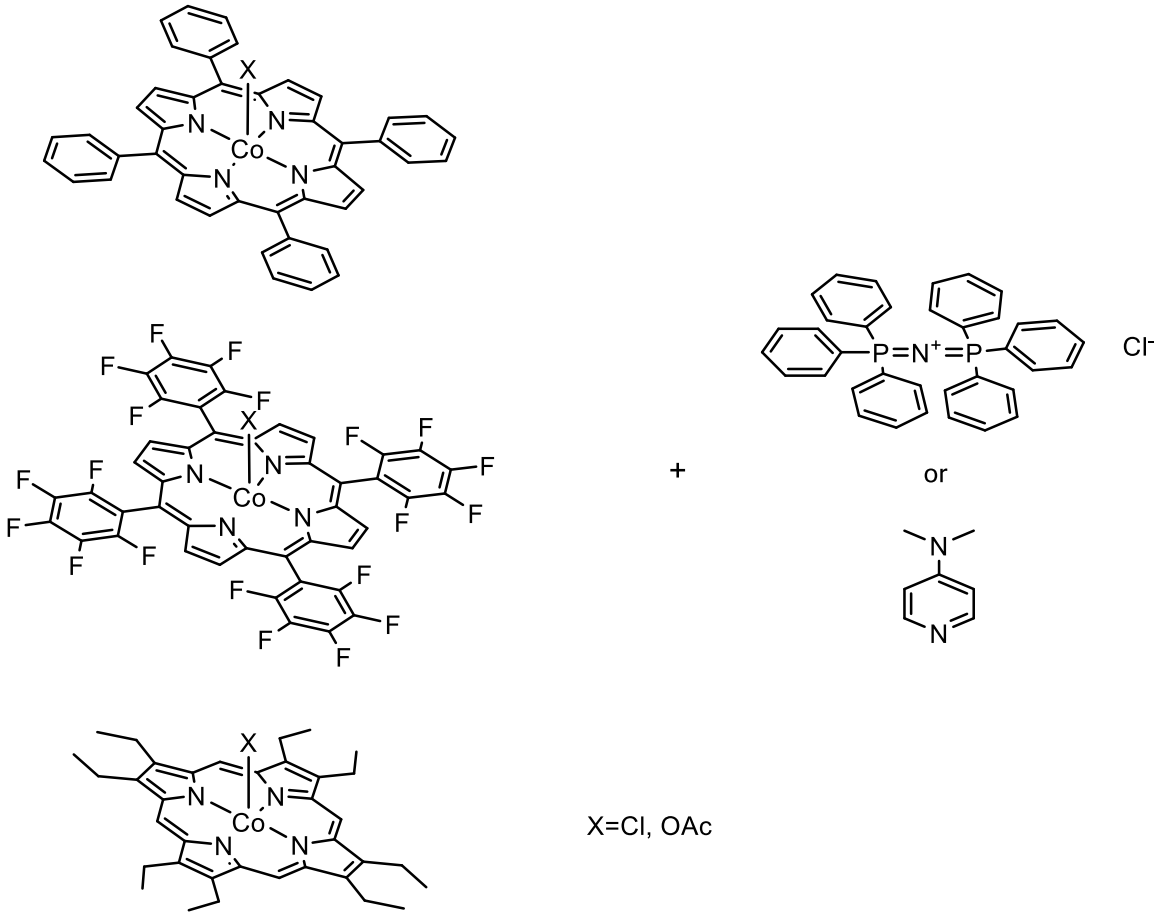

Figure 11. Three cobalt(III) porphyrin catalysts with ligands and their co-catalysts.

By covalent tether of quaternary ammonium salts on the periphery of the cobalt(III) salen catalysts, a significant enhancement of the polymer formation rate has been observed.[59-65] The similar method has also been tentatively applied to cobalt(III) porphyrin catalysts. Wang and co-workers have successfully synthesised two cobalt(III) porphyrin catalysts bearing two or four quaternary-ammonium-salts arms on the periphery (Figure 10).[35] In the absence of a co-catalyst, both of these two catalysts are able to produce poly(propylene carbonate) under various polymerisation conditions. Although these catalysts show better selectivity for the copolymer formation against cyclic carbonate at high temperature, no significant improvements of the catalytic activity has been achieved compared with non-tethered TPPCoCl/PPNCl, reflected from the similar TOF between them.

These two tethered catalysts, compared with each other, also have different catalytic behaviour. For instance, the di-substituted cobalt(III) porphyrin complex fails to maintain its catalytic activity upon dilution whereas the tetra-substituted cobalt(III) porphyrin does not

lose its activity under such conditions. Moreover, further tether from two arms of quaternary ammonium salts to four leads to a slight decrease in activity.

A comparison between cobalt(III) porphyrin complexes with different ligands (Figure 11) applied in both homopolymerisation of PO and PO/CO_2 copolymerisation has been made by Chisholm *et al.*.[24] A reduction reaction of TPPCoCl to TPPCo(II) in the presence of PO has been observed. This side reaction may lead to the deactivation of the catalyst during the polymerisation.

Variation of the axial nucleophiles influences strongly on the homopolymerisation behaviour of cobalt(III) porphyrin complexes. As mentioned in the previous text, TPPCoCl shows no activity towards PO homopolymerisation even in the presence of a co-catalyst. On the other hand, TPPCo-acetate with PPNCl is able to produce a regioregular poly(propylene oxide).[24]

Variation of the porphyrin ligand from tetraphenylporphyrin to octaethylporphyrin and tetra(pentafluorophenyl)porphyrin shows a decrease in the polymerisation rate.

1.5 Influences of Co-catalysts in Combination with Various Catalysts on Epoxides/CO_2 Copolymerisation

A co-catalyst, introduced into the copolymerisation of epoxides/CO_2, is either an onium salt comprising a nucleophilic anion (e.g. PPN^+Cl^-, $NBu_4^+Br^-$) or a Schiff base such as DMAP. Bulky and charge-delocalized cations show better activities in such a polymerisation. As a consequence, they usually appear to be PPN^+, NBu_4^+, NEt_4^+ and some bulky phosphonium cations.

In most cases, the addition of a co-catalyst accelerates the polymerisation. On the other hand, negative effects have also been observed, such as the enhanced formation of cyclic carbonate and the increased PPO incorporation into the polymer chain. The mechanisms behind such observations have been discussed in many previous publications. The major hypotheses are that it either serves as a coordinating ligand which binds to the metal altering its Lewis acidity or initiates an additional polymer chain (Scheme 10).

In 1982, Inoue and co-workers introduced an aluminium(III) porphyrin catalyst active for epoxide/CO_2 copolymerisation. However, ether-rich polymers are afforded if the reaction is

catalysed by this aluminium porphyrin alone.[66] On the other hand, the addition of a co-catalyst, such as triphenylethylphosphonium bromide or tetrabutylammonium bromide (Figure 12), efficiently increases the carbonate content in the polymer.[20] In the absence of a catalyst, neither polymer nor cyclic carbonate can be produced by a co-catalyst alone. Inoue *et al.* proposed a mechanism for the polymerisation performed in the presence of a co-catalyst, in that the ionic co-catalysts serve as extra initiators (Scheme 10) which start additional polymer chains.[20] For Schiff-base co-catalysts, an *in-situ* formation of an onium salt from triphenylphosphine has been claimed, although such a result remains disputable.[20]

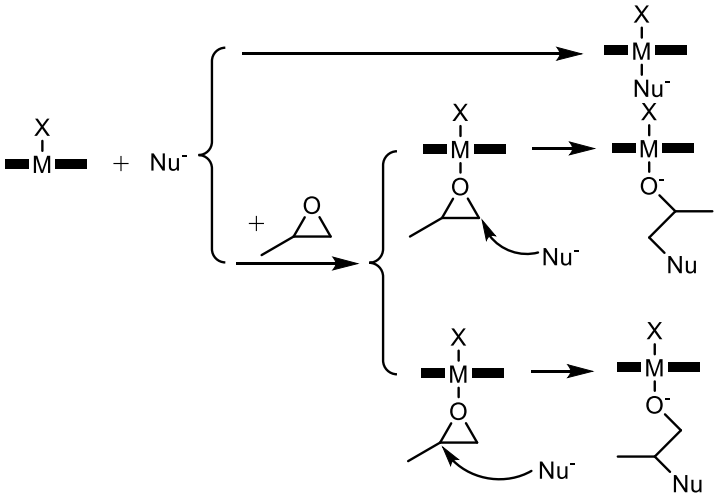

Scheme 10. Proposed functionalities of a co-catalyst in PO/CO_2 copolymerisation.

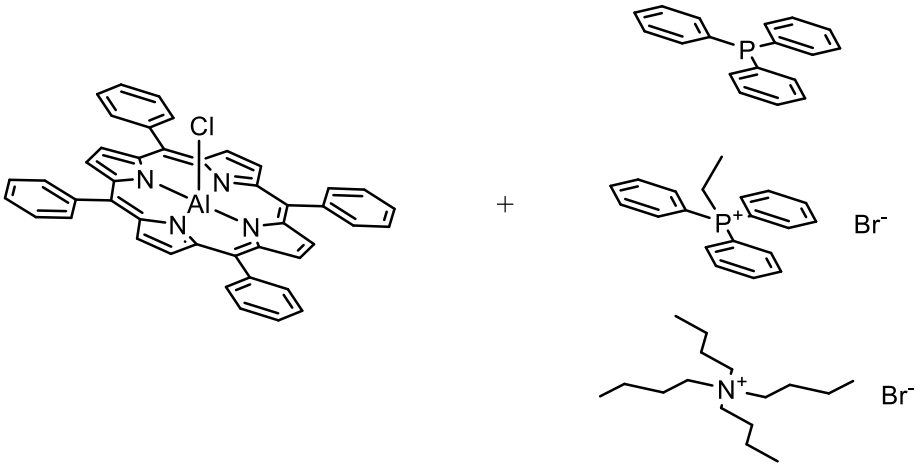

Figure 12. TPPAlCl/co-catalyst designed by Inoue in epoxide/CO_2 copolymerisation.

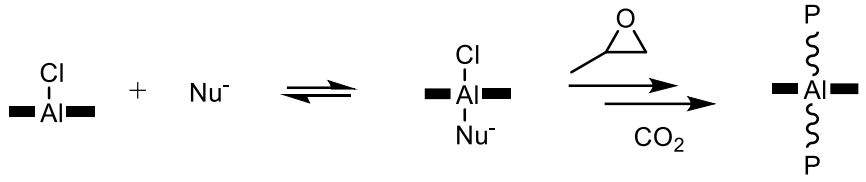

Scheme 11. Dual-site chain propagation proposed by Inoue.

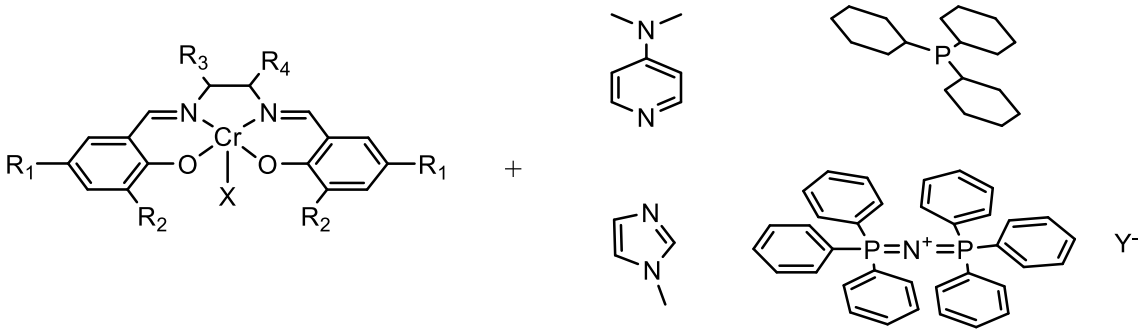

Figure 13. The structure of salenCr(III) catalysts and their co-catalysts.

As reported by Nguyen and co-workers in 2001, a salenCr(III) complex with DMAP is an active catalyst for the coupling of PO and CO_2 to produce cyclic carbonate (Figure 13). During the investigations of this catalyst in our group, the ratio between the salenCr(III) complex and DMAP is demonstrated to be crucial for a selective formation of copolymer. With 2 equivalents of DMAP, cyclic carbonate is the exclusive product. On the other hand, a decrease of the co-catalyst loading to 0.5 equivalent successfully affords poly(propylene carbonate) with high selectivity by using a salenCr(III) complex with conjugated backbone (R_3, R_4=phenyl ring).

With a high loading of DMAP (>1 equivalent), the formation of cyclic carbonate is supposed to take place via a chain back-biting mechanism, in that DMAP displaces the growing polymer chain through a competitive coordination towards the chromium centre, and the alcoholate chain end nucleophilically attacks the nearest electron-deficient carbon to form a five-membered-ring compound. Increase of CO_2 pressure efficiently suppresses this back-biting side reaction. This phenomenon may be explained by the lower nucleophilicity of the carbonate chain end, compared with alcoholate, leading to a slower depolymerisation.

Darensbourg *et al.* applied a salenCr(III) catalyst (with non-conjugated backbone (R_3, R_4=cyclohexane)) in the production of poly(cyclohexene carbonate).[18] A TOF of 10.4 h^{-1}

(R_1=R_2=tert-Bu, X=Cl) is obtained from the polymerisation performed in the absence of a co-catalyst. On the other hand, in the presence of 2.25 equivalents of 1-methylimidazole, the activity of the polymerisation shows a three-time enhancement with a decreased ether-linkage formation.

Variation of the co-catalyst loading from 2.25 equivalents of N-MeIm to 1 equivalent of $PPNN_3$ shows a remarkable boost of the polymer formation rate (TOF=1150 h^{-1}). Darensbourg attributed the functionality of the co-catalyst to a coordinating ligand which binds to the metal centre altering its Lewis acidity and as a consequence, benefits a rapid copolymer formation.

In addition to the selection of the co-catalyst, the amount of the co-catalyst has also been proved to influence the polymerisation rate significantly. Increase of N-MeIm loading up to 10 equivalents accelerates the reaction whereas further additions lead to longer induction periods as detected by *in-situ* IR spectroscopy.[18]

By utilizing a salenCr(III) complex having conjugated backbone (R_3, R_4=phenyl ring) in the copolymerisation of PO and CO_2, increasing PCy_3 loading from 1 equivalent to 2 equivalents results in a decrease of the polymerisation rate. In contrast to this, highly excessive additions of a co-catalyst in CHO/CO_2 copolymerisation does not show such a decrease in the polymer formation rate. Further, the most effective co-catalyst, $PPNN_3$, in a rapid poly(cyclohexene carbonate) production is also able to enhance the reaction rate of PO/CO_2 copolymerisation, however, to a limited extent (1 eq. $PPNN_3$, TOF=190 h^{-1}) in comparison with CHO/CO_2 copolymerisation (TOF=1150 h^{-1}).

Shortly after Coates and co-workers presented the first cobalt(III)-based salen catalysts active for PO/CO_2 copolymerisation,[45] Lu and co-workers examined the binary catalytic system comprising cobalt(III) salen dinitrophenolate (Figure 14) and a series of quaternary ammonium salts bearing different nucleophilic anions (Cl^-, Br^-, I^- or OAc^-). For all of the onium salts tested, higher TOF, compared with the ones acquired in the absence of them, are obtained.

NBu_4Cl and NBu_4OAc show excellent selectivity for the copolymer formation (99%) among all examined co-catalysts. The values of TOF obtained under the same experimental conditions by using different co-catalysts are in an order as follow: Cl (257 h^{-1})=Br (289 h^{-1})=I (272 h^{-1})>OAc (167 h^{-1}). By varying the reaction temperature and CO_2 pressure, a highest TOF of 371 h^{-1} for this cobalt(III) salen/onium salts catalyst is achieved under 40 ^oC and 40 bar pressure by using NBu_4Cl as a co-catalyst.

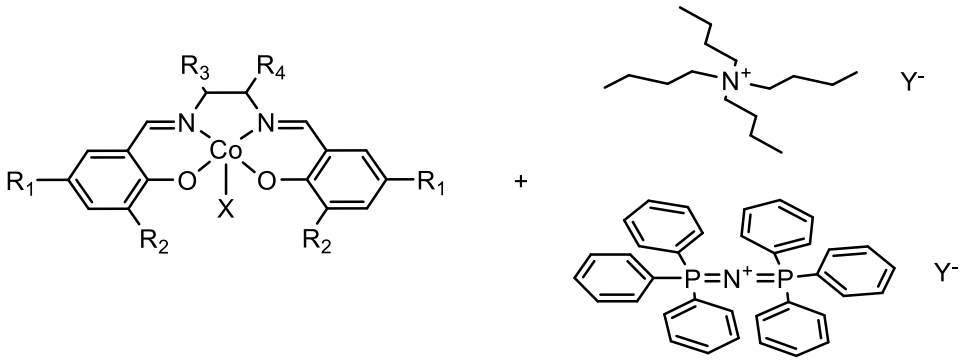

Figure 14. The structure of salenCo(III) catalysts and their co-catalysts.

A similar enhancement in activity upon the addition of a co-catalyst has been observed by Coates and co-workers as well by using salenCo(III) complexes in CHO/CO_2 copolymerisation.[44] The highest TOF of 440 h^{-1} for this catalyst is achieved via the optimisation of the polymerisation conditions (70 ^{o}C and 6.8 bar CO_2 pressure) in the presence of 1 equivalent of PPNCl.

Darensbourg and co-workers examined the catalytic activity of salenCr(III) azide complexes in combination with a variety of co-catalysts (PPNCl, $PPNN_3$ and PCy_3) in PO/CO_2 copolymerisation.[48] Distinct characteristics have been observed compared with CHO/CO_2 copolymerisation. Above 1 equivalent of co-catalyst loading, the polymerisation rate decreases sharply for all co-catalysts examined, with 2 equivalents of $PPNN_3$ or PPNCl being completely inactive for the copolymer formation and yielding exclusively cyclic carbonate. A chain-degradation mechanism in the presence of excessive onium salts has been proposed to explain this phenomenon, in that a di-co-catalyst substituted salenCr(III) complex is formed and the free polymer anion gradually depolymerised through the chain back-biting reaction to afford the cyclic compound (Scheme 12). $PPNN_3$ while mixed with propylene oxide in the absence of a catalyst has no activity for the formation of either cyclic carbonate or copolymer after pressuring CO_2. This observation is in consistency with the result reported by Inoue, as discussed in the previous text, that co-catalyst alone is not able to form any product in this copolymerisation.

0.5 equivalent of co-catalyst loading is demonstrated to be most active for a high-speed PO/CO_2 copolymerisation with salenCr(III) azide as a catalyst. A further addition to 1 equivalent slightly slows down the reaction rate. Darensbourg supposed that the additional

nucleophile may serve as a bridging ligand which links two chromium salen molecules together to form an active dimer for the polymer formation (Scheme 13).[48] The lone pairs of the chloride anion are able to alter the Lewis acidity of both metal centres. However, all attempts to crystalize this proposed complex were unsuccessful.

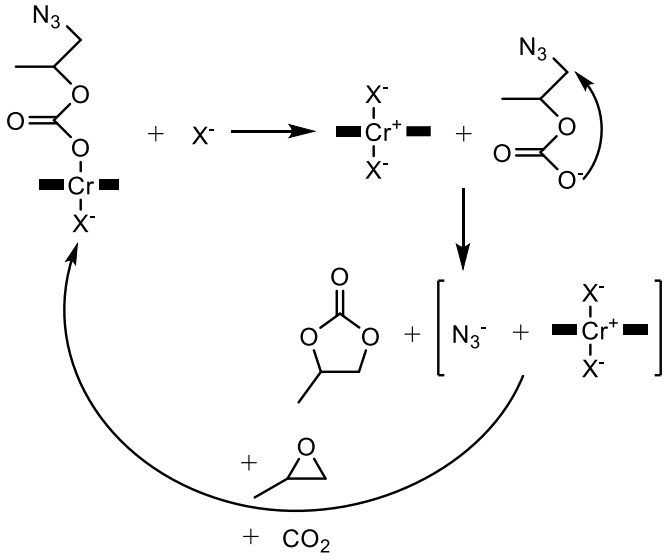

Scheme 12. The possible mechanism of the back-biting to form cyclic carbonate in the presence of excessive onium salts (>1 equivalent).

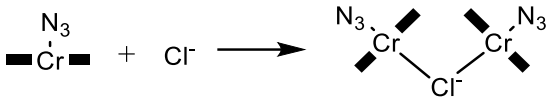

Scheme 13. A possible active species comprising two salenCr(III) catalysts bridged with one chloride anion.

If phosphine compounds are utilised as co-catalysts (e.g. PCy_3, PPh_3), relatively weak bindings of these species towards the chromium centre have been demonstrated by using IR spectroscopy. This observation may explain the fact that a higher catalyst loading (1 equivalent), compared with onium salts (0.5 equivalent), is essential for phosphine compounds to achieve a rapid polymerisation. Kinetic studies suggest that the real effective co-catalyst, when using PCy_3, is a phosphonium zwitterion afforded from the ring opening of the epoxide by phosphine compounds. This phenomenon is also able to explain the fact that with higher amounts of PCy_3, a longer induction period is observed, which is due to the initial

formation of such a phosphonium zwitterion. This result is consistent with what has been observed by Inoue *et al.*, that a phosphonium zwitterion is formed during the polymerisation.[20]

Nguyen and co-workers tested salenCr(III) complexes with dimethylaminoquinoline (DMAQ) as a co-catalyst in PO/CO_2 copolymerisation and this catalytic system shows a moderate activity under mild conditions (e.g. 10 bar CO_2, room temperature).[42] On the other hand, Coates and co-workers found that under the same experimental conditions, the same catalyst in the absence of a co-catalyst is inactive in such a polymerisation. Nguyen attributed the functionality of a co-catalyst to a coordinating ligand which binds to the metal centre leading to a labilization of the metal alkoxide bond.

The molar ratio between salenCr(III) complexes and DMAQ has been found to be important to achieve a fast and highly selective polymerisation, with 2 equivalents of DMAQ being most suitable. A decrease of the DMAQ loading to 1 equivalent significantly lowers the catalytic activity by more than 50%. Conversely, an increase of the DMAQ loading to more than 2 equivalents also leads to a slight decrease of the polymerisation rate. (R)-(+)-4-(dimethylamino)pyridinyl(pentaphenylcyclopentadienyl) iron complex has been found to be a highly effective co-catalyst (TOF value= 589 h^{-1}, while combined with a salenCr(III) nitrate). This result may be explained by an increased Lewis basicity of such an iron complex compared with DMAQ.[67]

Lu and co-workers examined the salenCo(III) complexes with a series of onium salts bearing either a nucleophilic anion (I^-, Br^-, Cl^-, F^-or N_3^-) or an anion with a poor nucleophilicity (e.g. ClO_4^-) in epoxides/CO_2 copolymerisation.[39] A co-catalyst comprising a bulky cation and an anion with a high nucleophilicity and a good leaving ability (e.g. I^- or Br^-) shows an improved catalytic activity (TOF up to 314 h^{-1}). On the other hand, the selectivity for the copolymer when using these co-catalysts is not satisfactory (65%-75%).

By using a co-catalyst bearing a nucleophilic anion with a poor leaving ability (e.g. Cl^-), this problem of selectivity is successfully overcome (PPC up to >99%). Further, a co-catalyst bearing an anion with a poor nucleophilicity (e.g. ClO_4^-) has nearly no activity in the coupling of PO and CO_2.

The variation of the cations also influences the polymerisation rate. If the anion of the co-catalyst remains the same, among PPN^+, NBu_4^+ and NEt_4^+, PPN^+ shows the highest catalytic activity under the same experimental conditions.

Interestingly, strong organic bases with sterically hindered orientations (e.g. 7-methyl-1,5,7-triazabicyclo[4.4.0]dec-5-ene (MTBD)) have been found to be able to copolymerize PO and CO_2 if combined with a salenCo(III) catalyst. However, the TOF (77 h^{-1}) is not as high as the one obtained with onium salts. In contrast to CHO/CO_2 copolymerisation by using a salenCr(III) complex and N-MeIm, nearly no activity in PO/CO_2 copolymerisation is obtained with the same catalyst.

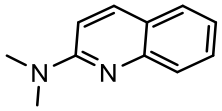

Figure 15. The structure of dimethylaminoquinoline (DMAQ).

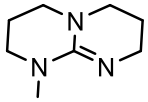

Figure 16. The structure of 7-methyl-1,5,7-triazabicyclo[4.4.0]dec-5-ene (MTBD).

The mass spectrum (recorded in the cation mode) of the poly(propylene carbonate) produced from the salenCo(III)/MTBD-catalysed PO/CO_2 copolymerisation shows a series of polymer signals. The molar mass of the chain end is thus able to be determined via a simple mathematic calculation. The calculated value fits well to the molar mass of MTBD, implying that MTBD serves as an initiator. On the other hand, no signals of the copolymers initiated by dinitrophenolate (from the salenCo(III) complex) are detected in both cation and anion modes. Lu proposed a mechanism of PO/CO_2 copolymerisation catalysed by salenCo(III)/MTBD, in that MTBD conducts the ring opening and a zwitterion is thus formed, followed by the chain propagation. This result is in agreement with the reaction mechanisms proposed by Inoue[20] and Coates,[25] in that the co-catalysts are additional initiators.

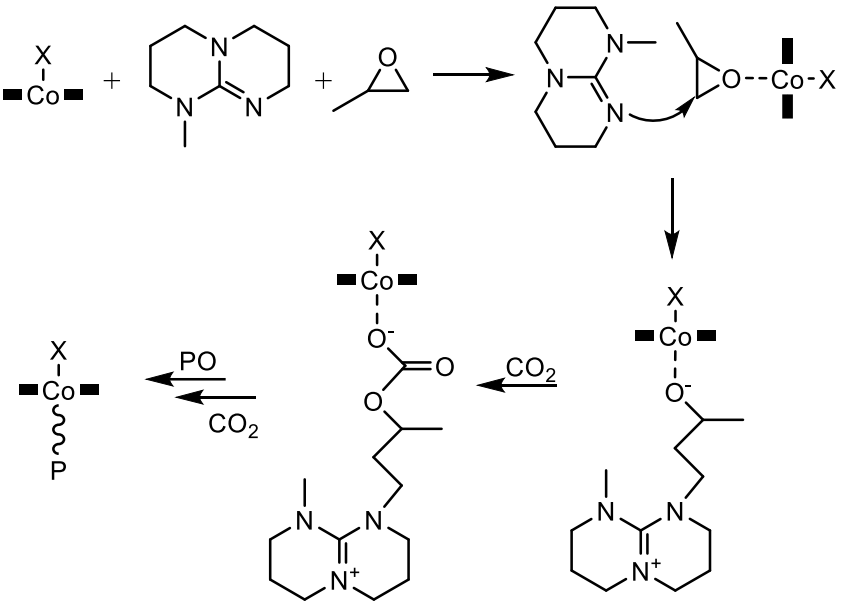

Scheme 14. Role of MTBD in the copolymerisation of PO/CO_2 proposed by Lu.

Lu and co-workers suspected that the polymer formation may take place on both sides of the metal centre in the presence of a co-catalyst if the catalyst comprises a nucleophilic axial ligand (e.g. Cl^-). However, this proposal finds itself difficult to explain why salenCo(III) chloride with (PPN)ClO_4 or N-MeIm is not able to induce the polymerisation.[39]

The depolymerisation of poly(cyclohexene carbonate) in the presence of different amounts of a co-catalyst (PPNCl) has been tested by Darensbourg and co-workers.[47] The formation of cyclic carbonate via the degradation of the polymer chain may take place in two different pathways, namely a metal-mediated degradation (the polymer chain is coordinated to the metal centre in this route) and a back-biting reaction of free (non-coordinated) anion chains.

Upon the addition of excessive co-catalysts (e.g. 2 equivalents of PPNCl), the coordinated polymer chains may be displaced by the co-catalysts, leading to free (non-coordinated) polymer anions. The depolymerisation of a free polymer chain has a lower energy barrier compared with a coordinated polymer chain and hence, this pathway of the polymer degradation is considered to proceed more rapidly (Scheme 15). Indeed, in the presence of 2 equivalents of PPNCl, the rate for the cyclic carbonate formation from polymer is higher than the rate obtained from the experiment performed with 1 equivalent of PPNCl.

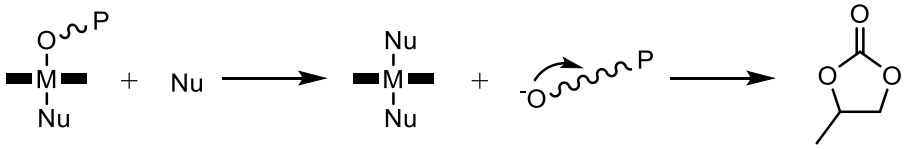

Scheme 15. Chain degradation via a competitive coordination by an additional nucleophile.

Niu and co-workers explored a catalytic system comprising salenCo(III) and DMAP in PO/CO_2 copolymerisation.[43] This combination has been demonstrated to be efficient and exceeds the activity of salenCo(III)/NBu_4Br under the same polymerisation conditions (TOF=112 h^{-1} for DMAP, 43.1 h^{-1} for NBu_4Br). By optimizing the reaction conditions, a highest TOF of 501 h^{-1} for this catalyst is achieved (60 ^oC, 20 bar CO_2 pressure).

Lu and co-workers compared the difference between the binding of DMAP towards salenCr(III) and salanCr(III) (Figure 17) complexes by using ESI-Mass spectrometry.[37] Upon the variation of the molar ratio between salenCr(III)/salanCr(III) and DMAP, a di-DMAP-coordinated complex is found to be dominate with salenCr(III)/DMAP whereas a mono-DMAP-coordinated complex is the major species with salanCr(III)/DMAP (even at a molar ratio of salanCr(III):DMAP=1:10). This phenomenon is explained by the steric hindrance of the salan ligand leading to a lower affinity of DMAP towards salanCr(III).

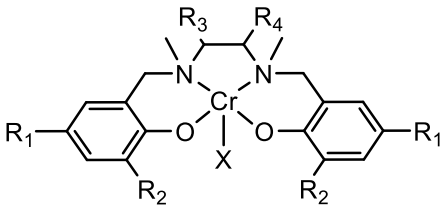

Figure 17. The structure of salanCr(III) complexes.

By using mass spectrometry, molar masses of the polymers with DMAP end groups have been detected in salenCr(III)/DMAP catalysed epoxide/CO_2 copolymerisation, suggesting that DMAP serves as an initiator.[37] Since in the absence of a co-catalyst, a salenCr(III) nitrate complex alone is capable of producing poly(propylene carbonate), the polymer formation on both sides of the metal by using salenCr(III) and DMAP is thus proposed by Lu as illustrated in Scheme 16.[37]

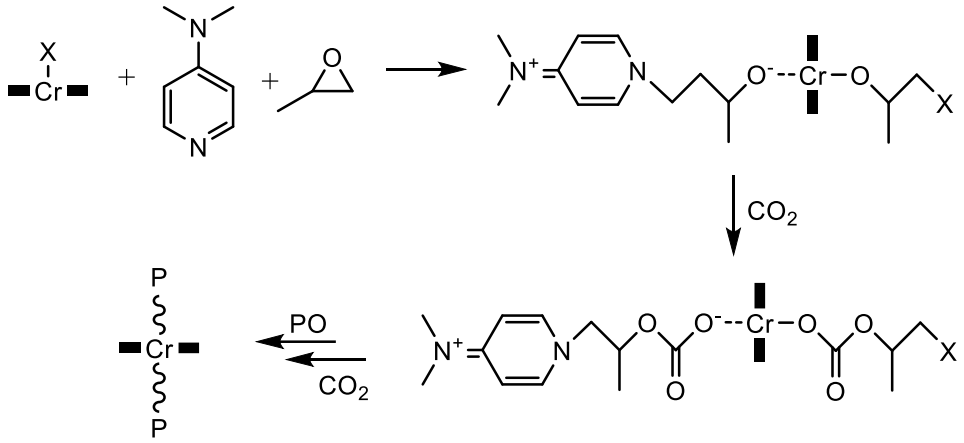

Scheme 16. The mechanism of dual-site chain growth when using DMAP as a co-catalyst.

1.6 Identifications and Analyses of the Products from PO/CO_2 Copolymerisation

PO/CO_2 copolymerisation catalysed by organic metal complexes yield both the desired product, poly(propylene carbonate), and several by products, namely poly(propylene oxide) (which comes from repeating insertions of PO into the growing polymer chain) and cyclic carbonate (which is formed via a chain back-biting reaction).

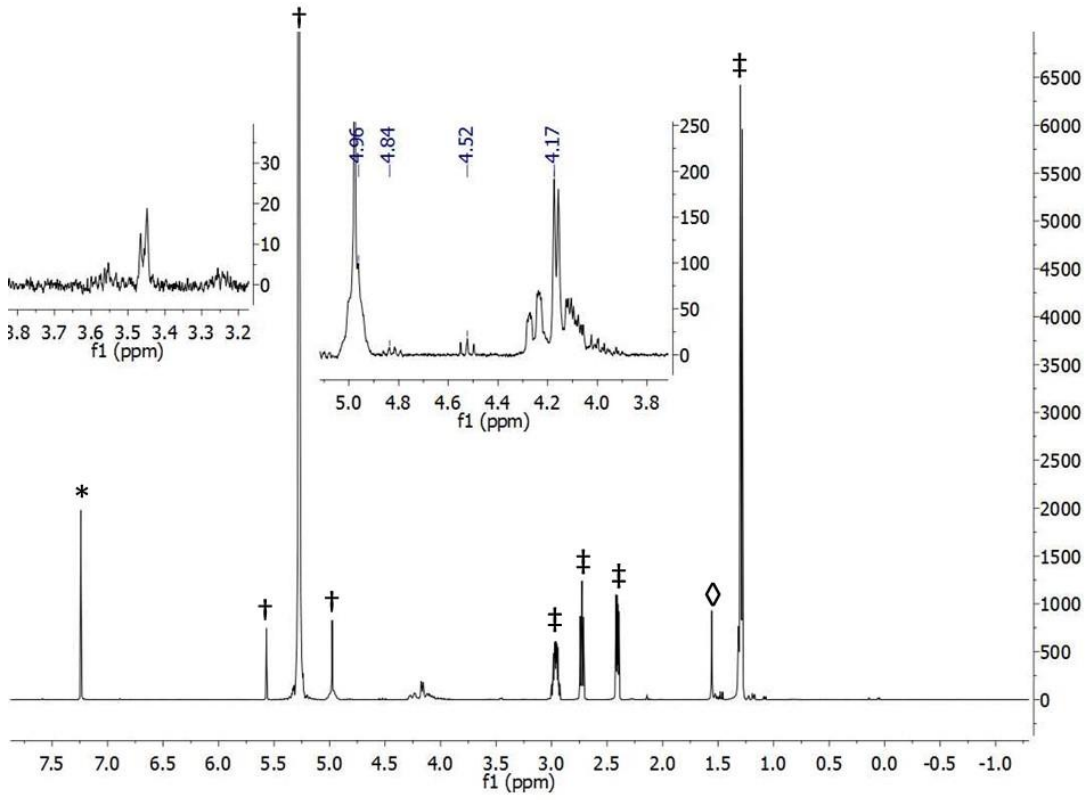

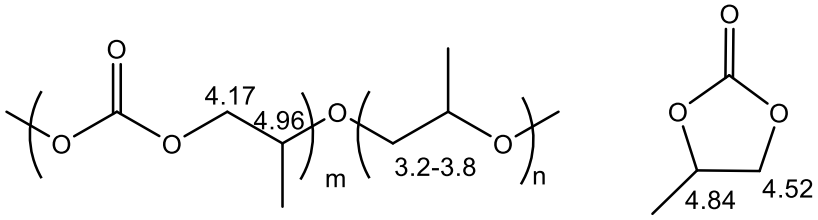

Figure 18. A typical ^{1}H NMR spectrum of the polymerisation products in $CDCl_3$ (25 ^{o}C, 300 MHz, expanded from -1 ppm to 7.5 ppm) and the assignments of the NMR signals (*=CD_2HCl, †=residual DCM, ‡=residual PO, ◊=water).

The identifications of all these products are achieved mainly by using ^{1}H NMR spectroscopy. As shown in Figure 18, NMR signals of poly(propylene carbonate), poly(propylene oxide) and cyclic carbonate can be clearly assigned in the ^{1}H NMR spectrum of the raw product. Poly(propylene carbonate) shows two proton signals at 4.98 and 4.17 ppm, corresponding to the CH and the CH_2 groups respectively. On the other hand, proton signals for the CH and the CH_2 groups in the ether linkages locate between 3.2 to 3.8 ppm. In addition, within this chemical-shift range, proton signals of the polymer chain end could also be found. Cyclic carbonate exhibits two proton signals at 4.52 and 4.84 ppm. According to the ratio of the integrations, the selectivity of the copolymer against cyclic carbonate as well as the percentage of the ether linkages in the copolymer could be determined.

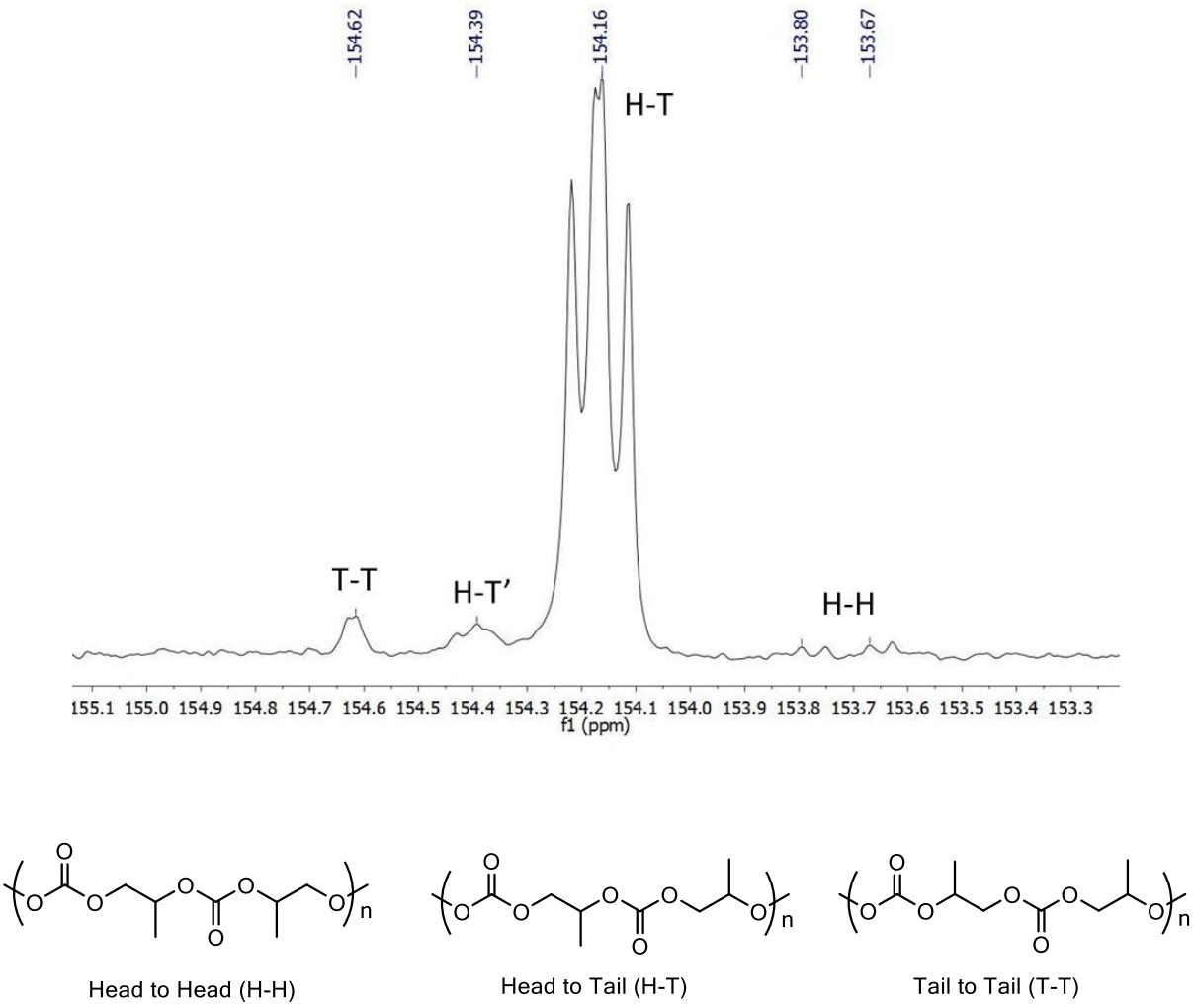

Figure 19. The determination of the regio-selectivity by ^{13}C NMR spectroscopy and the illustration of three microstructures.

The yield of the copolymer was determined by weighing the isolated pure polymer product. The ratio of the integrations between the copolymer and the residual PO is not an accurate value of the polymer yield due to the fact that PO is highly volatile.

The regioselectivity (head-to-tail percentage) of the polymer is determined by using ^{13}C NMR spectroscopy. As shown in Figure 19, poly(propylene carbonate)s with different microstructures show distinct chemical shifts in the ^{13}C NMR spectrum. The H-T% is thus calculated by using the ratio of the integrations between the NMR signals of different microstructures.

The molecular weight of the obtained poly(propylene carbonate) is determined by GPC measurements (THF as the eluent, calibrated with a poly(styrene) standard). As shown in Figure 20, a bimodal molecular weight distribution has often been observed for the

poly(propylene carbonate) produced by cobalt(III) porphyrins. Other useful information of the polymer properties, besides the molecular weight, (e.g. PDI) can also been obtained by GPC measurements.

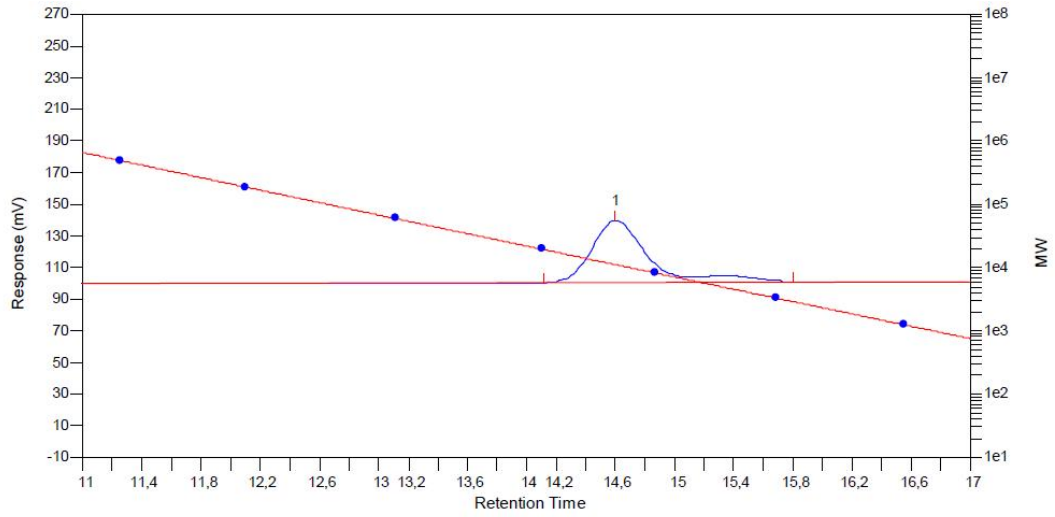

MW Averages

Peak No	Mp	Mn	Mw	Mz	Mz+1	Mv	PD
1	11123	9193	10205	10948	11493	10077	1.11008

Figure 20. A representative GPC report.

2. Motivation

Since the publications by Wang and Sugimoto concerning cobalt(III) porphyrin complexes catalysed PO/CO_2 copolymerisation, very few successive reports on further investigations of such catalysts hitherto emerge.

As suggested by substantial previous publications, in order to achieve even higher activities of epoxide/CO_2 copolymerisation, further developments of the catalysts lie in linked catalytic systems, comprising either two or more catalysts or catalysts and co-catalysts.

Up to date, the most frequently used method to achieve this purpose is covalent tether. This method builds up a single catalyst molecule which is easy to be characterized and handled. On the other hand, in some cases, the synthetic approaches may be too complex which reduces the value of the linked catalysts towards commercial applications. As a result, besides the covalent tether, the utilisation of intermolecular interactions (e.g. coordination, hydrogen bonding, etc.) are also possible paths to build up multi-metal-centred catalysts.

In this Ph.D. thesis, novel cobalt(III) porphyrin complexes, with mono-, di-, tri-metal centres, tethering amide side groups have been synthesised and well characterised. Dynamic light scattering, FTIR spectroscopy and vapour pressure osmometry have been applied to detect if there exist intermolecular interactions between the catalysts. A series of copolymerisation reactions of PO/CO_2 has been performed and the results are compared with a representative catalyst, TPPCoCl, and are discussed in detail.

The second part of this Ph. D. thesis refers to kinetic studies of the PO/CO_2 copolymerisation catalysed by TPPCoCl/PPNCl by using *in-situ* IR technology. Reaction orders of catalyst, co-catalyst, monomer as well as CO_2 pressure have been determined.

Mechanistic studies on the copolymerisation of propylene oxide and CO_2 catalysed by cobalt(III) porphyrin complexes have rarely been reported in literature. Hence, the third part of this thesis consists of spectroscopic studies on the initial ring opening of PO by TPPCoCl, aiming to gain a deeper insight into the mechanism of initiation. Further, the deactivation pathway of cobalt(III) porphyrin catalysts to cobalt(II) species in the presence of PO is investigated detailedly. The results are included in the last part of this thesis.

3. Syntheses of Cobalt(III) Porphyrin Catalysts Tethering Amide Side Groups and Their Behaviour in Epoxide/CO_2 Copolymerisation

3.1 Introduction

Since the initial discovery of the copolymerisation of CO_2/PO by Inoue and co-workers,[68] substantial mechanistic studies have been made, in order to gain a deeper understanding of the reaction mechanism. Traditional monometallic catalysts often suffer from the losses of activities upon dilution of the catalyst concentration. Therefore, a bimetallic mechanism in the chain propagation has been proposed in many previous publications.[13,69,70] Covalently linked catalysts have been proved to efficiently overcome such losses in catalytic activities at low catalyst concentrations.[56,57]

Metalloporphyrins are an important class of catalysts in the productions of various useful chemical compounds including polymers.[54] TPPAl(III)Cl is the first effective homogeneous catalyst active for the copolymerisation of PO/CO_2.[20,66] In addition, this catalyst is also able to polymerize lactones, lactides to give polyesters with narrow molecular weight distributions.[71-76] Zinc-centred N-substituted porphyrins have been proved to be active in the homopolymerisation of epoxides.[77] If combined with a co-catalyst, cobalt(III) porphyrins are effective catalysts for PO/CO_2 copolymerisation. Modifications of the porphyrin ligands show influences on the catalytic activities.[30]

Despite covalent link of two catalysts to overcome the loss of the activity upon dilution, self-assembly by using intermolecular interactions (e.g. coordination bonding, π-π stacking, hydrogen bonding and ionic interactions) is an ideal pathway to build up supramolecular structures.[78]

Cobalt(III) porphyrin catalysts (**1**-**3**) bearing amide side groups are designed, synthesised and possible intermolecular interactions (face to face π-π stacking between porphyrin rings, hydrogen bonding via amide side chains) have been tested by using dynamic light scattering, vapour pressure osmometry as well as IR spectroscopy.

3.2 Syntheses of Amide Side Group Linked Cobalt(III) Porphyrin Complexes (1-3)

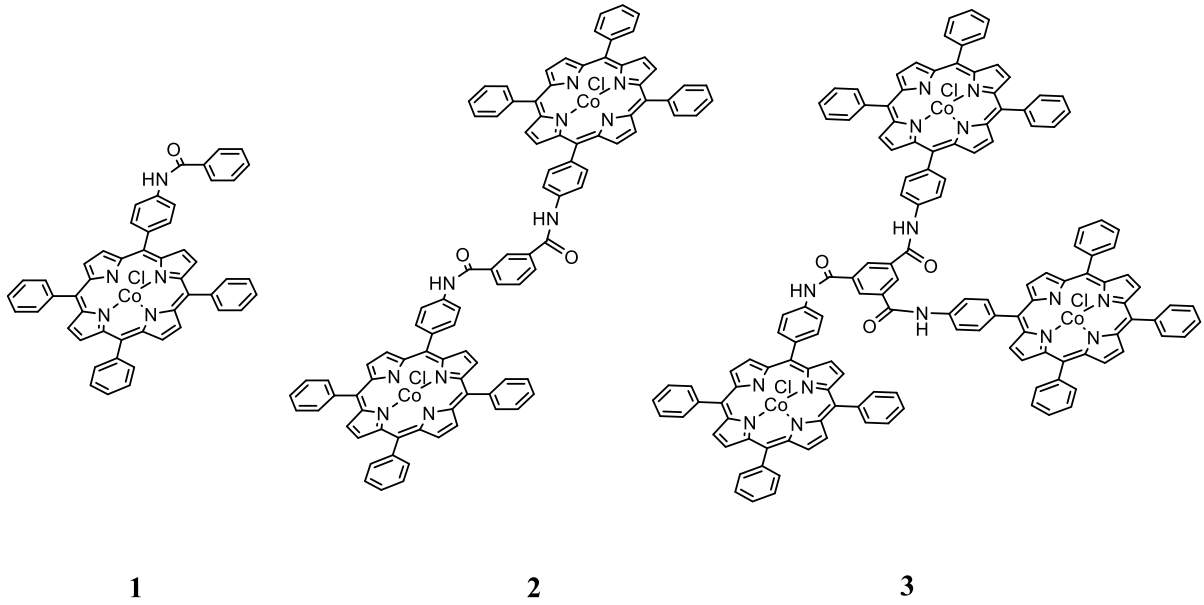

Figure 21. The linked cobalt(III) porphyrin complexes **1**-**3**.

The porphyrin precursor for the syntheses of **1**, **2** and **3** is a mono-nitro-substituted tetraphenylporphyrin (TPP-NO_2). It is synthesised by using a traditional synthetic route designed by Lindsey (Scheme 17).[79] This synthetic pathway, compared with Adler's method,[80] only requires a condition of room temperature and avoids a high-temperature refluxing (130 ^{o}C). In addition, dichloromethane is used as the reaction solvent, which abandons the irritating propionic acid.

Schlenk technique is used during the synthetic process due to the sensitivity of this reaction towards air and moisture. The stoichiometry of pyrrole, benzaldehyde and 4-nitro benzaldehyde applied in the reaction equals to the theoretical value (4:3:1). A solution of boron trifluoride diethyl etherate serves as an acid catalyst. After its addition, the colour of the reaction solution gradually turns from colourless/light yellow to dark purple/black. DDQ is then added as a solid to oxidise the produced porphyrinogen and a fully conjugated porphyrin macrocycle is thus afforded (Scheme 18).

During the reaction, undesired by products are generated as black precipitates. Hence, through vacuum filtration, the raw product is obtained as a purple solid after drying the filtrate under *vacuo*. Column chromatography (silica gel, eluent: DCM/hexane) is then performed to purify the product. TPP comes out of the column as the first eluate followed by the desired

product, TPP-NO_2. Other by products (e.g. multi-nitro-substituted porphyrins) also exist which comes out of the column after TPP-NO_2 due to their higher polarities.

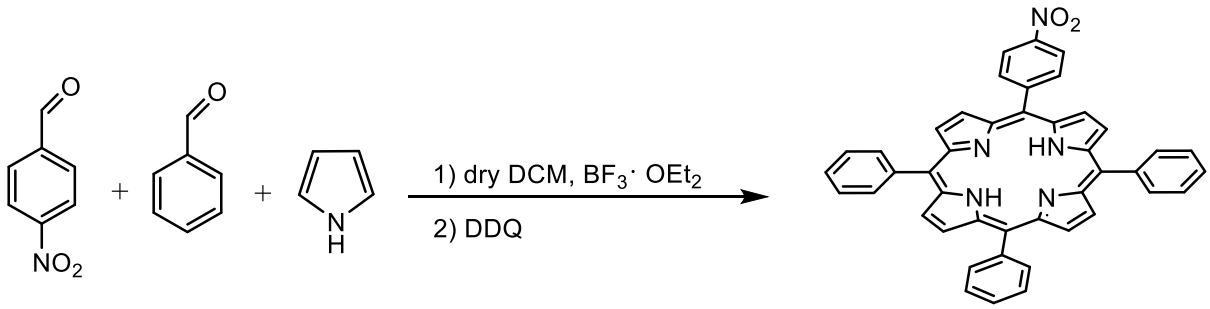

Scheme 17. The synthetic pathway for TPP-NO_2.

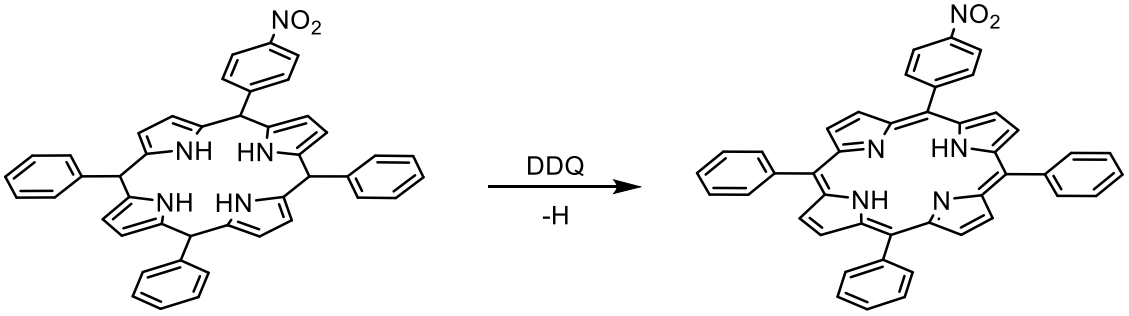

Scheme 18. The oxidation of the porphyrinogen by DDQ to afford the porphyrin macrocycle.

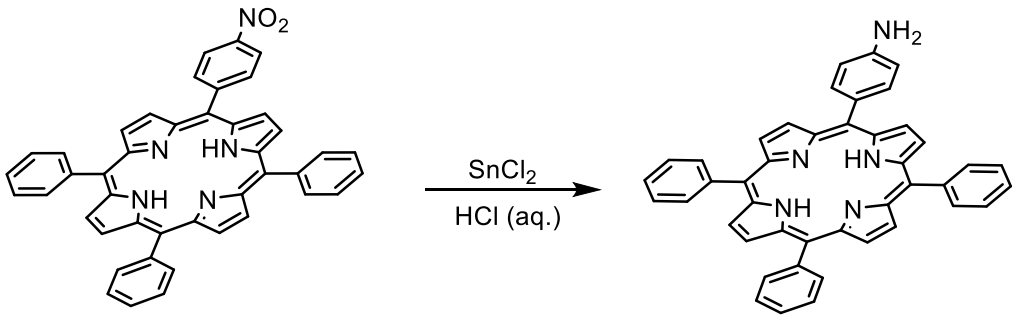

Scheme 19. The reduction of TPP-NO_2 to TPP-NH_2.

The reduction of TPP-NO_2 to form TPP-NH_2 is achieved in a concentrated HCl aqueous solution. Tin(II) chloride dihydrate is added as a reducing agent. In this aqueous suspension, the colour of the porphyrin turns from purple to green presumably due to the formation of a porphyrin

cation species with HCl. After the reaction finishes, an ammonia aqueous solution (25%) is utilised to neutralise the suspension. Due to the highly exothermal nature of the reaction between HCl and NH_3, ice bath as well as a slow addition of the NH_3 solution are essential to avoid a potential boiling of this aqueous suspension. The yield of the porphyrin product is satisfactory (>90%), and as indicated by mass spectrometry, no unreacted TPP-NO_2 exists in the product.

The covalent links of one to three TPP-NH_2 with a series of acryl chloride compounds have been successfully achieved (Scheme 20).[81] Triethylamine is used in the reaction to scavenge the generated HCl and consequently shifts the reaction equilibrium towards the product formation. Argon gas is used to protect the reaction from air and moisture.

The tris-porphyrin ligand has a relatively poor solubility in DCM and thus precipitates out of the solution during the condensation of TPP-NH_2 with acryl chloride. Therefore, instead of DCM, chloroform is applied as the eluent in column chromatography for the purification of the tris-porphyrin ligand. The yields of mono-, bis-, tris-porphyrin ligands is in such an order as mono>bis>tris.

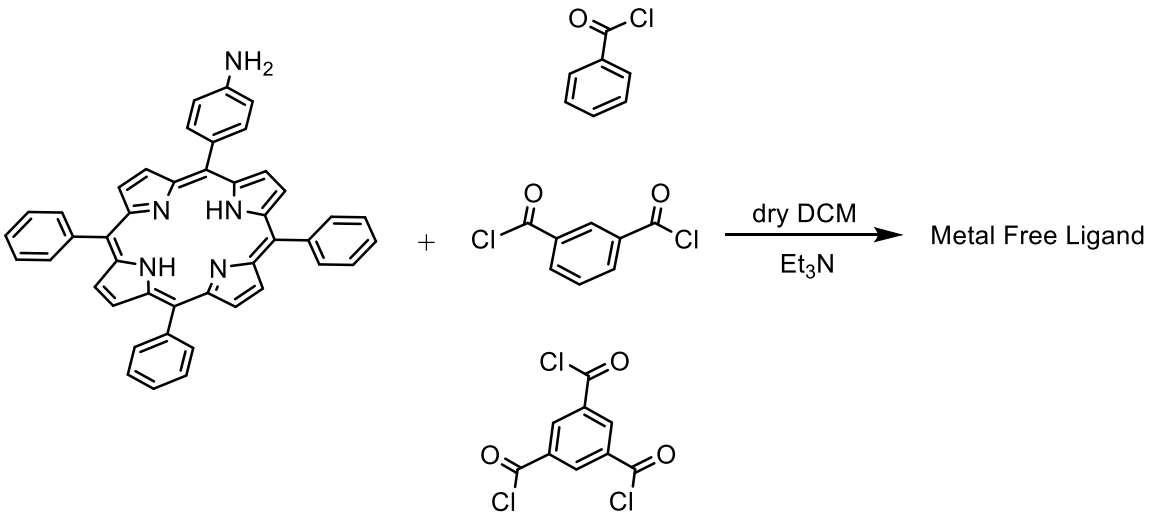

Scheme 20. The synthetic route of metal-free ligands of **1**, **2** and **3.**

The metalation of the ligands is performed by using the same method for TPP ligand.[82] DMF has been proved to be a suitable reaction solvent. The accomplishment of the metalation is indicated by the disappearance of the signals of the porphyrin ligands in the ESI-Mass

spectrum. Afterwards, the produced cobalt(II) complexes are used directly for the oxidation of the metal centre.

The oxidation of cobalt(II) porhyrins to cobalt(III) species is achieved in a methanol solution with HCl as a counter-ion supplier. During the purifications, a saturated $NaHCO_3$ aqueous solution is utilised to neutralise the obtained products.

3.2.1 Characterisations of Cobalt(III) Porphyrin Complexes (1-3)

The ^1H NMR spectrum of TPP-NO_2 is collected in $CDCl_3$ solution. All the signals in the spectrum can be assigned either to the product or to the residual solvents (e.g. water, chloroform, PDMS) (Figure A1). The collected spectrum of TPP-NO_2 shows identical characteristics compared with literature results.[83] Proton signals of the N-H group in the pyrrole rings appear at -2.80 ppm. Such a high-field shift is due to the shielding effect of the aromatic ring current (Figure 22).[84]

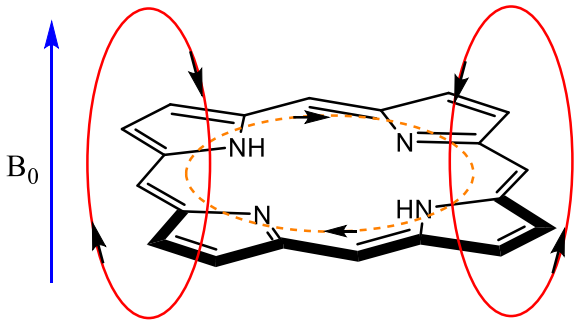

Figure 22. The illustration of the ring current induced by applying external magnetic fields (B_0=the external magnetic field; orange dash curve= the induced ring current; red curve=the magnetic field produced by the ring current).

The ^1H NMR spectrum of TPP-NH_2 (Figure A2) shows similar characteristics compared with literature results.[83] The proton signals of the amine group is detected at 4.01 ppm.

The ^1H NMR spectrum of the ligand of **1**, collected in a $CDCl_3$ solution, shows slight broadenings of the proton resonances (Figure A3). On the other hand, if THF-d_8 is used as the NMR solvent, no noticeable broadenings of the NMR signals are detected in the collected spectrum (Figure A4). This observation is explained by a potential aggregation between the porphyrin macrocycles in a $CDCl_3$ solution, whereas if a coordinating solvent, such as THF-d_8, is used, a

hexacoordinate species should be formed, which prevents such an aggregation due to a steric hindrance.

The ^{1}H NMR spectrum of the ligands of **2** and **3** (Figure A6, A7) are collected in a $CDCl_3$ solution and the chemical shifts of the proton signals are similar to the literature results.[81,85]

All the UV-Vis spectra of the ligands of **1**, **2** and **3** show similar characteristics (Figure A8-10) compared with each other, implying that covalent links of porphyrins do not result in significant changes in the property of their visible-light absorption. The results of the elemental analyses for the ligands of **2** and **3** indicate that small binding molecules (e.g. water, methanol) may co-exist with these two ligands, although both of the species have been dried at 60 ^{o}C under *vacuo* overnight.

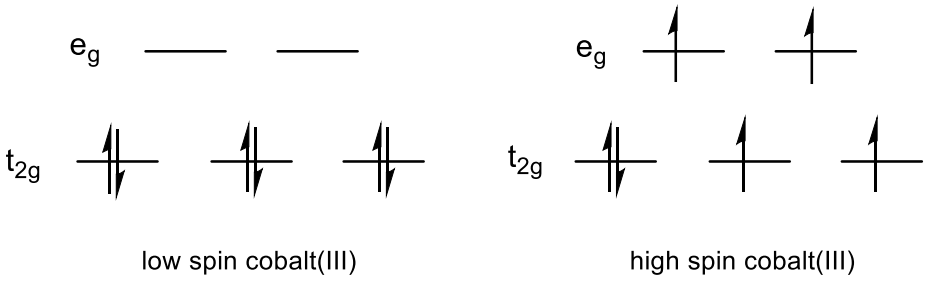

Figure 23. The spin-crossover of cobalt(III) complexes.

The ^{1}H NMR spectra of the cobalt(III) porphyrin complexes (**1**-**3**) show intense line broadenings of the detected proton signals (Figure A11-14). It is well known that metalloporphyrins have higher tendencies to form aggregated species, compared with their metal-free ligands. Even in a coordinating solvent, such as THF-d_8, the proton signals of complexes **2** and **3** still show slight broadenings. A possible explanation for such an observation may be that the covalent links of two or three porphyrins leads to stronger abilities for aggregations.

Another explanation for the detected line broadenings of complexes **2** and **3** is a spin-crossover between the diamagnetic low-spin cobalt(III) and the paramagnetic high-spin cobalt(III) species (Figure 23). Huet attributed the line broadenings of the NMR signals of cobalt(III) porphyrin complexes in a non-coordinating solvent to a disproportionation reaction which generates a paramagnetic cobalt(II) porphyrin and a cobalt(III) π-cation radical.[86]

The molar mass of the complex **3** exceeds 2000 and is out of the range of the ESI-Mass spectrometer in our laboratory. On the other hand, signals of 1/2 and 1/3 molar mass of the complex **3** are detected. This is due to double or triple charges of one porphyrin. MALDI-TOF mass spectrometry is also applied to characterize the complex **3**. The result of this measurement further confirms the formation of the tris-porphyrin cobalt(III) complex (Figure A15).

The existence of the axial ligand (Cl) on the cobalt(III) porphyrin catalysts are confirmed by EDX measurements. Further, no other elements which are heavier than the nitrogen atom, despite cobalt and chlorine, are detected during the measurements.

The SEM images of complexes **2** and **3** show plate-shaped structures, and the size of each plate varies from hundreds of nanometres to hundreds of micrometres (Figure 24). However, these plate-shaped structures are amorphous and are not suitable for X-ray measurements to determine their molecular structures.

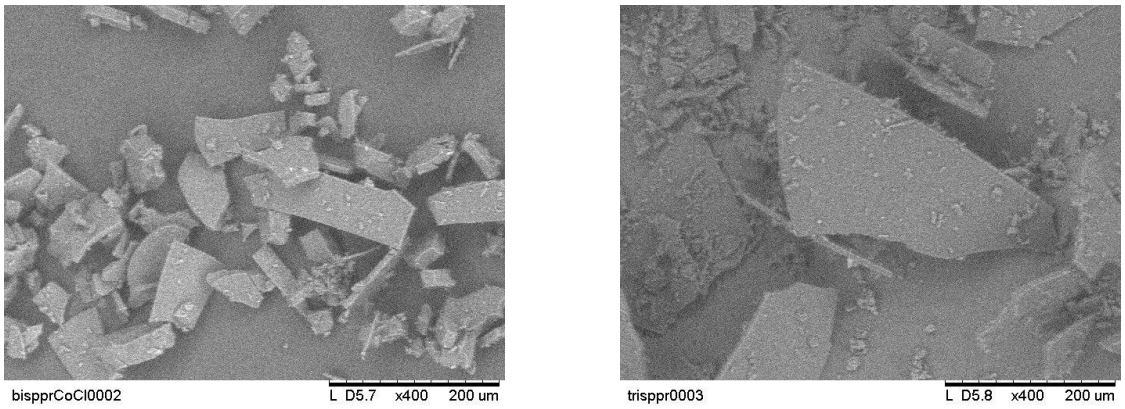

Figure 24. The SEM images of **2** (left) and **3** (right).

3.2.2 DLS, VPO, Solution IR Measurements of Cobalt(III) Porphyrin Complexes (1-3)

Previous studies on the chain propagation mechanism in the copolymerisation of epoxides and CO_2 often suggest a bimetallic reaction pathway,[13,69,70,87,88] in that an epoxide pre-coordinates to the metal centre of the catalyst and the growing polymer chain on another catalyst conducts the ring opening. Many traditional monometallic catalysts suffer losses in activities upon the dilution of the catalyst concentrations. Thereby, in order to overcome this

problem, covalently linked catalysts[5762] are of great interests in the current developments of novel catalysts. Cobalt(III) porphyrin catalysts (**1**-**3**) have been designed and synthesised to test if intermolecular interactions (e.g. hydrogen bonding, π-π stacking etc.) exists in solution. Due to the spacers between the porphyrin rings are relatively rigid, little or no intramolecular interactions between porphyrins in one molecule are expected to take place.

Dynamic light scattering measurements are first performed for complex **1** in a dichloromethane solution. However, the results show poor reproducibility and the detected particle size varies significantly under the same experimental conditions. The size for a single cobalt(III) porphyrin molecule (**1**) is approximately 2 nm as predicted by Chemdraw. One experiment shows that the particle size of **1** in DCM is 6 micrometres. Such a highly aggregated structure (>3000 molecules forms one supramolecular structure) seems unlikely.

If the applied solvent is changed to a PO/DCM mixture (1:1), the detected particle size is reduced to 15 nm. However, this result still has a poor reproducibility. Highly aggregated particles are again detected under the same experimental conditions.

The light source of the DLS machine has a wavelength of 565 nm. Porphyrins are organic dyes, so the cobalt(III) porphyrin complexes (**1-3**) show absorptions from approximately 500 to 600 nm, corresponding to the so-called Q band. In addition, metallopophyrins are known for their fluorescence properties. Combining these two facts, the poor reproducibility of the detected particle size may be due to the absorption and the subsequent emission by the porphyrins. Hence, dynamic light scattering is probably not a suitable method to detect the existence of intermolecular interactions between the porphyrin molecules.

Vapour pressure osmometry measurements are conducted to determine the molecular weight of complex **1** in a THF solution. A model complex with no amide side chain, TPPCoCl, is also applied in these measurements for comparison. As shown in Figure 25, both cobalt(III) porphyrin complexes show aggregations in THF solution as indicated by their detected molecular weights. If the concentrations exceed 10 mM, the detected molecular weights do not show a further increase and the average molecules aggregated to form a supramolecular structure are between 2 and 3. Upon dilution, an obvious decrease of the detected molecular weights is noticed. Since the detected molecular weights of both **1** and TPPCoCl are always similar to each other with the variation of their concentrations in THF, the hydrogen bonding between amide side chains has nearly no effect on building up supramolecular structures in

THF solutions. The difficulty of building up hydrogen bonds between amide groups may be due to the solvent, THF, since it is a competitive hydrogen-bond acceptor. The intermolecular interactions behind such an aggregation remain obscure.

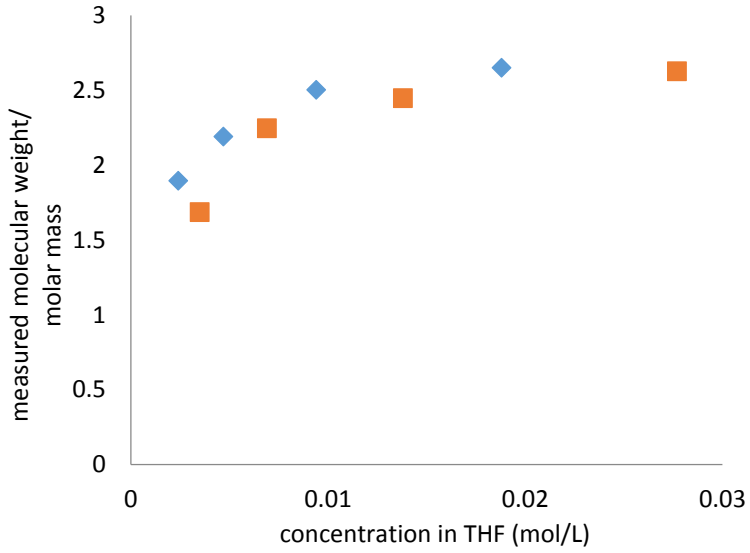

Figure 25. The results of vapour pressure osmometry for **1** (blue rhomb) and TPPCoCl (orange cube).

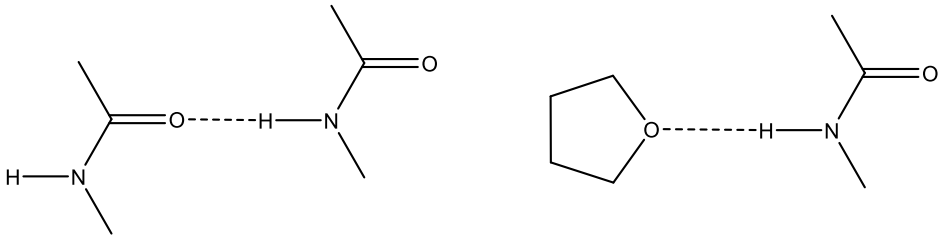

Figure 26. The Illustration of the hydrogen bondings between two amides (left) and between THF and the amide group (right).

The free N-H stretching band of the amide side group usually appears at ca. 3300 cm^{-1} in the IR spectrum. If hydrogen bonding is formed between two amide groups, this band exhibits a lower-wavenumber shift.[89] Solution IR measurements are carried out for complex **2** in THF. Since THF is a competitive hydrogen-bond acceptor, the self-assembly between two amide groups is thus considered difficult (Figure 26). A broad IR band is observed at ca. 3500 cm^{-1} for complex **2** in THF (Figure 27). With the variation of the concentrations of **2**, this band does not

exhibit a noticeable shift and no other additional bands between 3000 cm^{-1} and 4000 cm^{-1} is detected. Thereby, the band at 3500 cm^{-1} is assigned to the N-H stretching band of the amide groups which form hydrogen bonds with THF. The reason for the observed split of this band is hitherto unknown. And the ratio of the intensities between these two split bands never changes with the variation of the concentration of complex **2** in THF. IR measurements for complex **2** in its solid state are performed and the N-H stretching band is shifted towards lower wavenumbers compared with **2** in THF (Figure A16). A hydrogen bonding between amide groups in the solid state most probably exists, whereas upon the addition of a hydrogen-bond acceptor, such as THF, the hydrogen bonds between two amide side groups are very likely hard to be maintained.

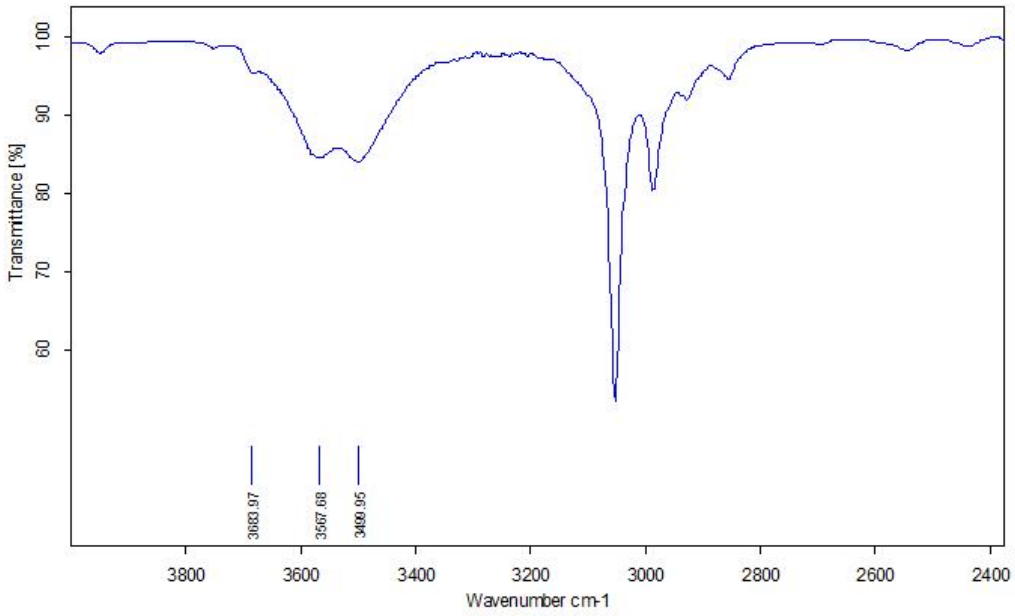

Figure 27. The IR spectrum of **2** in THF.

3.3 Results of PO/CO_2 Copolymerisation Reactions Catalysed by Cobalt(III) Porphyrin Complexes (1-3)

A series of PO and CO_2 copolymerisation reactions is performed by using catalysts **1**, **2** and **3** under different CO_2 pressures. The reaction time is kept constant as 24 hours and neat PO is utilised without additional solvents. As shown in Table 1, under 10 bar CO_2 pressure, catalyst **1** exhibits the highest polymer formation (59%) among all three catalysts examined. The

activities of catalysts **2** and **3** under the same conditions are much lower (PPC formation: 10% for **2**, 21 % for **3**). However, the cyclic carbonate formation in Entry 1 is 11% which indicates the back-biting reactions takes place more easily with catalyst **1** compared with the other two catalysts. Covalently linking two or three porphyrins overcomes this back-biting reaction to a great extent (Entry 4 and Entry 7, cyclic carbonate formation: 2%).

Under 20 bar CO_2 pressure, the polymer formation by using catalysts **1** and **3** is nearly equal (60% and 61% respectively). The back-biting reaction, if catalyst **1** is used, occurs and 18% cyclic carbonate is afforded. Catalyst **2** shows the lowest activity under the same experimental conditions with a polymer formation of 48% (60% and 65% for catalyst **2** and **3** respectively). The formation of cyclic carbonate by using catalysts **2** and **3** is well suppressed below 2%.

Entry	**Catalyst**	**Pressure**	**Conversion**		**Activity**	**Carbonate**
			PPC	CC	TON	**Linkages**
1	1	10 bar	59%	11%	1180	97%
2	1	20 bar	60%	18%	1200	98%
3	1	40 bar	84%	<1%	1680	>99%
4	2	10 bar	10%	2%	200	99%
5	2	20 bar	48%	2%	960	99%
6	2	40 bar	65%	<1%	1300	/
7	3	10 bar	21%	2%	420	94%
8	3	20 bar	61%	1%	1220	98%
9	3	40 Bar	88%	<1%	1776	98%

Table 1. PO/CO_2 copolymerisation by using catalyst **1**, **2** and **3** under different CO_2 pressure for long term reaction (polymerisation conditions: neat PO; PO:Cat.:PPNCl=2000:1:1; T=25 ^{o}C; reaction time=24 hours. Polymer conversion is determined by the weight of the isolated poly(propylene carbonate). TON=turnover number, (polymer conversion*mole of monomer)/(mole of catalyst). Cyclic carbonate conversion and carbonate linkage are determined by ^{1}H NMR spectroscopy.).

If the applied CO_2 pressure is further increased to 40 bar, the formation of the cyclic carbonate is well controlled below 1% for all three catalysts examined. A high pressure of CO_2 is able to keep the polymer chain end mostly at a carbonate group and such a carbonate chain end has

a higher energy barrier for the back-biting reaction compared with an alcoholate group. The polymer formation by using catalysts **1** and **3** is again very similar to each other (84% and 88% respectively). Catalyst **2** shows a slightly lower activity with a PPC formation of 65%.

The carbonate content in the final polymer reaches as high as >99%. As proved in our previous work, TPPCoCl is inactive in the homopolymerisation of PO to produce poly(propylene oxide) even in the presence of a co-catalyst.[30] This may be an explanation for such a high carbonate content in the polymer since the repeating insertion of PO to form ether linkages is extremely slow.

Entry	Catalyst	Pressure	Conversion		Activity		Carbonate
			PPC	CC	TON	TOF	Linkages
10	**1**	20 bar	37%	<1%	740	246	99%
11	**1**	40 bar	27%	<1%	557	185	/
12	**1**	60 bar	14%	<1%	280	93	>99%
13	**2**	20 bar	15%	1%	300	100	97%
14	**2**	40 bar	11%	1%	220	73	98%
15	**3**	20 bar	33%	1%	660	220	97%
16	**3**	40 bar	21%	<1%	420	140	92%

Table 2. PO/CO_2 copolymerisation by using catalyst **1**, **2** and **3** under different CO_2 pressure with short reaction time (polymerisation conditions: neat PO; PO:Cat.:PPNCl=2000:1:1; T=25 ^{o}C; reaction time=3 hours. Polymer conversion is determined by the weight of isolated poly(propylene carbonate). TON=turnover number, (polymer conversion*mole of monomer)/(mole of catalyst); TOF=turnover frequency, TON/reaction time (h^{-1}). Cyclic carbonate conversion and carbonate linkage are determined by ^{1}H NMR spectroscopy.).

Copolymerisation reactions of CO_2 and PO are subsequently explored with a shorter reaction time (3 hours) under different CO_2 pressures by using catalysts **1**-**3**. As shown in Table 2, cyclic carbonate formations are well controlled below 1% for all polymerisations performed. If comparing Entry 2 in Table 1 and Entry 10 in Table 2, for catalyst **1**, the polymer anion chain gradually becomes unstable over a long period of time.

Under 20 bar CO_2 pressure, catalysts **1** and **3** show similar activities towards the polymer formation. Catalyst **2** exhibits only half of the TOF value compared with **1** and **3** under the same polymerisation conditions. The catalytic activities under 20 bar CO_2 pressure for short-term reactions follow the same order (**1**=**3**>**2**) as for long-term reactions.

If the CO_2 pressure is increased from 20 bar to 40 bar, a decrease in the catalytic activity is observed for all these three catalysts. A volumetric expansion upon increasing CO_2 pressure to more than 35 bar has been proposed in previous literature[58]. This effect causes the dilution of the catalyst concentration and consequently slows down the polymerisation reaction. Increase of the CO_2 pressure to 60 bar intensifies this effect as reflected in the further decrease of the catalytic activity (Entry 12).

If comparing the PPC formation under the same polymerisation conditions for both short-term and long-term polymerisations, the reactions show obvious decelerations for the long-term polymerisations. Since no extra solvent is added, as the formation of the polymer continues, the viscosity of the reaction mixture gradually increases. As a consequence, the diffusion of either PO or CO_2 towards the active metal centre becomes more and more difficult which slows down the polymerisation.

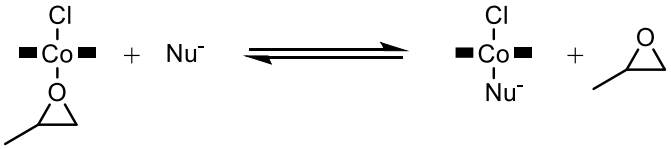

Scheme 21. Coordination equilibrium between PO and additional nucleophile towards cobalt centre.

A series of copolymerisation reactions of PO/CO_2 is then performed by varying the ratio between PO, catalysts and co-catalysts (Table 3). If the concentrations of catalyst **1** and PPNCl are both reduced to half (Entry 10 in Table 2, Entry 17 in Table 3), the TOF values maintain constant and the cyclic carbonate formations, in both cases, are well controlled below 1%. If the amount of the co-catalyst, PPNCl, is reduced to half while keeping the catalyst concentration constant (Entry 17, Entry 18), only a very slight decrease of the catalytic activity is observed. If the amount of PPNCl is further reduced to 0.1 equivalent, a significant decrease of the TOF value is observed (Entry 18, TOF=219 h^{-1}; Entry 19, TOF=53 h^{-1}). Additional

nucleophilic anions, such as Cl^-, are supposed to be able to bind to the sixth coordination site of the cobalt centre (Scheme 21) and labilizes the Co-Cl bond, thereby, accelerates the polymerisation reaction.[49] This hypothesis has not been fully confirmed yet, although has been frequently discussed in previous publications. Hence, the low activity when applying 0.1 equivalent of PPNCl may result from the shift of the equilibrium towards PO coordination as illustrated in Scheme 21 (postulated mechanism). Besides this explanation, there exist also other possible mechanisms, e.g. co-catalysts as initiators (for details, please refer to section 1.5).

Entry	Catalyst	PO:Cat:PPNCl	Conversion		Activity		Carbonate
			PPC	CC	TON	TOF	Linkages
17	**1**	4000:1:1	18%	<1%	748	249	97%
18	**1**	4000:1:0.5	16%	<1%	658	219	98%
19	**1**	4000:1:0.1	4%	<1%	160	53	97%
20	**1**	8000:1:1	9%	<1%	720	240	97%
21	**1**	20000:1:1	2%	/	388	129	/
22	**2**	4000:1:1	9%	<1%	360	120	98%
23	**3**	4000:1:1	8%	<1%	342	114	95%

Table 3. PO/CO_2 copolymerisation by using catalyst **1**, **2** and **3** under different PO:Cat:PPNCl ratio (polymerisation condition: neat PO; 20 bar CO_2 pressure; T=25 ^oC; reaction time=3 hours. Polymer conversion is determined by the weight of isolated poly(propylene carbonate). TON=turnover number, (polymer conversion*mole of monomer)/(mole of catalyst); TOF=turnover frequency, TON/reaction time (h^{-1}). Cyclic carbonate conversion and carbonate linkage are determined by ^1H NMR spectroscopy.).

If a PO:cat:PPNCl ratio of 8000:1:1 is applied (Entry 20), the activity of the catalyst does not decrease compared with Entry 17 (4000:1:1). On the other hand, a further dilution of the concentration of catalyst **1** and PPNCl shows an obvious decrease of the TOF value (Entry 21, 20000:1:1, TOF=129 h^{-1}). A polymer formation of 2% is achieved under such conditions after a 3-hour reaction.

Catalyst **2** maintains its activity upon one-time dilution (for both the catalyst and the co-catalyst concentrations) (Entry 13 in Table 2, Entry 22 in Table 3). On the contrary, catalyst **3**

shows an obvious decrease in its activity if half amounts of **3** and PPNCl are utilized (Entry 15 in Table 2, TOF of 220 h^{-1}; Entry 23 in Table 3, TOF of 114 h^{-1}).

Upon the dilution of catalysts and co-catalyst concentrations, the carbonate content in the copolymer does not show a sharp change.

A copolymerisation reactions by using catalyst **2** at 50 ^{o}C is performed (Table 4). The reaction time is 24 hours. After the reaction, no polymer is found and cyclic carbonate is the exclusive reaction product (53%). Since the formation of cyclic carbonate has a higher energy barrier compared with the copolymer formation. As a result, at high temperature, the selectivity for cyclic carbonate increases.

Entry	Catalyst	Temperature (^{o}C)	Conversion		Activity		Carbonate
			PPC	CC	TON	TOF	Linkages
24	**2**	50	/	53%	/	/	/

Table 4. PO/CO_2 copolymerisation by using catalyst **2** under 50 ^{o}C (polymerisation conditions: neat PO; PO:Cat.:PPNCl=2000:1:1; 20 bar CO_2 pressure; reaction time=24 hours. Cyclic carbonate conversion is determined by ^{1}H NMR spectroscopy.).

Entry	H-T%	Mn	Mw	PDI
4	93%	24996	31515	1.26
6	97%	32355	43588	1.35
9	91%	19596	27354	1.4

Table 5. H-T% and the molecular weights of the polymer as determined by GPC.

The polymers obtained from Entry 4, 6 and 9 show narrow molecular weight distributions (PDI<1.4) as determined by GPC measurements. The copolymers also have high head-to-tail percentages (Figure 28) (>90%) as determined by ^{13}C NMR measurements. The molecular number of the polymer generated by catalyst **2** is much higher, under the same polymerisation conditions, compare with the polymer produced by catalyst **3** (Entry 6 and Entry 9 in Table 5).

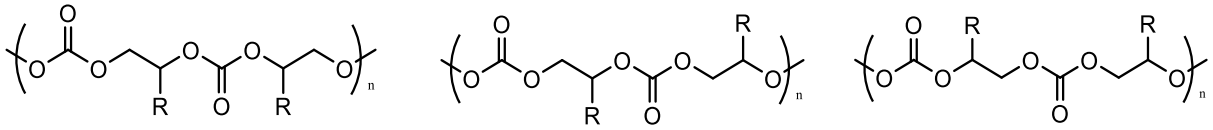

Head to Head (H-H) Head to Tail (H-T) Tail to Tail (T-T)

Figure 28. The microstructures of poly(propylene carbonate).

3.4 Results of CHO/CO_2 Copolymerisation Reactions Catalysed by Cobalt(III) Porphyrin Complexes (1 and 2)

Entry	Catalyst	Pressure	Temperature	Conversion		Activity	Carbonate
				PPC	CC	TON	Linkages
1	**1**	20 bar	25 ^{o}C	5%	/	64	77%
2	**1**	45 bar	80 ^{o}C	72%	/	1078	98%
3	**2**	45 bar	80 ^{o}C	18%	/	539	97%

Table 6. CHO/CO_2 copolymerisation by using catalyst **1** and **2** (polymerisation conditions: neat CHO; CHO/cat/PPNCl=1500:1:1 for Entry 1 and 2, CHO/cat/PPNCl=3000:1:1 for Entry 3; reaction time=24 hours. Polymer conversion and carbonate linkage are determined by ^{1}H NMR spectroscopy. TON=turnover number, (polymer conversion*mole of monomer)/(mole of catalyst).).

The copolymerisation reactions of CHO/CO_2 are investigated by using catalysts **1** and **2** (Table 6). Under mild polymerisation conditions (Entry 1, 20 bar, 25 ^{o}C), only small amounts of polymer are obtained after a 24-hour reaction by using catalyst **1**. The polymer product contains ca. 25% ether linkages due to the repeating insertion of CHO into the growing polymer chain. If the polymerisation is performed under 80 ^{o}C and 45 bar CO_2 pressure, a polymer formation of 72% is achieved with a significant increase of the carbonate content (98%, Entry 2). Under the same experimental conditions, the bis-porphyrin (**2**) shows a much lower activity (Entry 3, TON=539; Entry 2, TON=1078). The cyclic carbonate formation usually is not observed in CHO/CO_2 copolyemrisation. This observation is explained by a more bulky

backbone of CHO compared with PO, which prevents the back-biting reaction due to the steric hindrance.

3.5 *In-situ* IR Monitored PO/CO_2 Copolymerisation Catalysed by Cobalt(III) Porphyrin Complexes (1-3)

In-situ IR technology is powerful in the studies of an ongoing reaction. By collecting time-resolved IR spectra of the reaction mixture, a graphic of the intensity of an IR band versus the reaction time could be obtained. Poly(propylene carbonate) has a strong C=O-stretching band at 1748 cm^{-1} in the IR spectrum. On the other hand, the cyclic by product has a C=O-stretching band at 1810 cm^{-1}.

A series of copolymerisation reactions of PO/CO_2 is performed by using catalysts **1**, **2** and **3** under various reaction conditions monitored by *in-situ* IR spectroscopy. If an onium salt is applied as a co-catalyst, nearly no induction period is observed, which has also been reported in previous literatures.[49]

If the pressure of CO_2 exceeds 25 bar, the graphics of the polymer formation versus the reaction time show abnormal characteristics for all porphyrin catalysts examined (Figure 29). The intensity of the carbonyl-stretching band of poly(propylene carbonate) increases rapidly within the first several hours, and after 8 hours, the C=O-stretching band shows a sharp decrease.

This phenomenon is explained by the precipitation of the catalysts on the sensor which is located on the bottom of the autoclave. During the first several hours of polymerisation, the polymer chain is relatively short and this causes a problem of solubility of the catalysts which bear the growing chains. On the other hand, high CO_2 pressure is able to reduce the polarity of the reaction mixture which can also be a reason for the precipitation of the catalysts. As the reaction goes on, the polymer chain becomes longer which increases the solubility of the catalysts and the reaction mixture becomes again homogeneous.

If the CO_2 pressure is reduced to 20 bar, no such abnormal graphics is obtained. A low CO_2 pressure avoids this undesirable precipitation of the catalysts as mentioned above. Therefore, the determination of the catalyst order is successfully achieved under 20 bar CO_2 pressure by using *in-situ* IR technology.

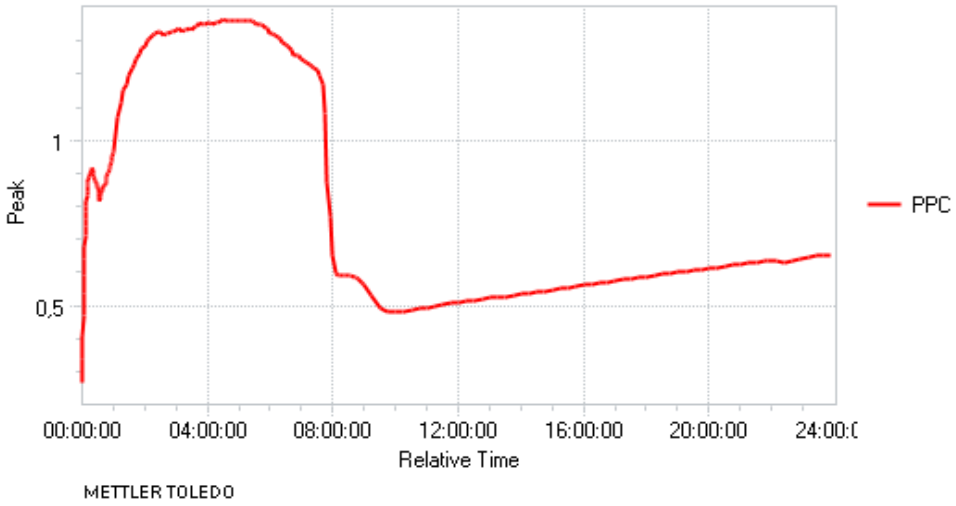

Figure 29. A Graphic of reaction time vs. polymer formation when CO_2 pressure is higher than 25 bar.

4. Kinetic Studies on the Determination of the Reaction Orders for TPPCoCl Catalysed PO/CO_2 Copolymerisation

4.1 Introduction

In-situ IR technology is ideal for kinetic studies in polymerisation reactions. Poly(propylene carbonate) exhibits a C=O-stretching band at 1748 cm^{-1} while the cyclic by product has a C=O-stretching band at 1810 cm^{-1}. Figure 30 (left) shows a typical graphic collected by the *in-situ* IR for a copolymerisation reaction of PO/CO_2, which illustrates the changes of the IR spectra with respect to the reaction time. A continuing growth of a band at 1748 cm^{-1} implies the poly(propylene carbonate) formation and the C=O-stretching band of cyclic carbonate at 1810 cm^{-1} has only very low intensity, suggesting nearly no cyclic by product is produced. The time interval is set to either 30 s or 1 min in this study.

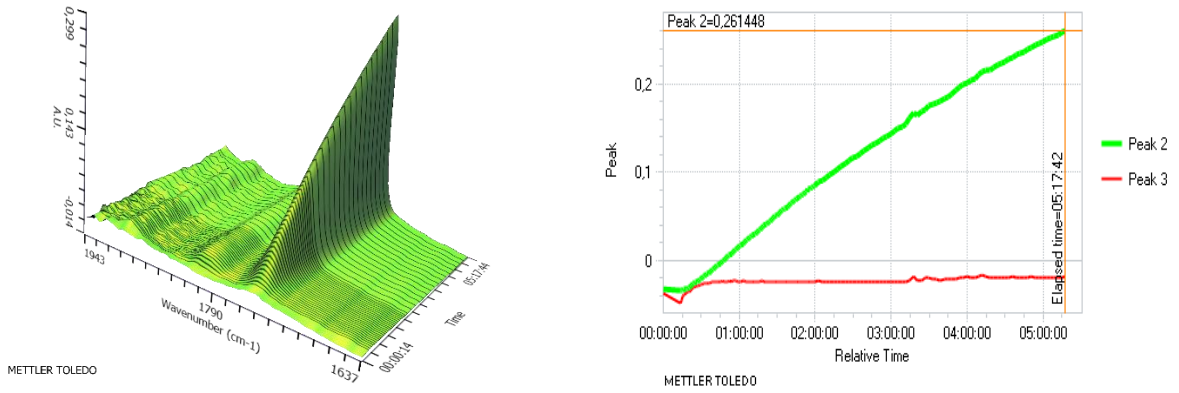

Figure 30. A tpical *in-situ* IR graphic collected from copolymerisation of PO/CO_2 (left) and a 2D graphic for both the formation of polymer (peak 2, 1748 cm^{-1}) and cyclic carbonate (peak 3, 1810 cm^{-1}).

A simplified 2D graphic for the formation of poly(propylene carbonate) and cyclic carbonate with the reaction time is shown in Figure 30 (right). For cobalt(III) pophyrin catalysts with PPNCl as a co-catalyst, usually no induction period is found after pressurizing CO_2. The cyclic carbonate band only increases at the beginning of the polymerisation (several minutes to several hours depending on the reaction conditions) and maintains constant for the rest of the reaction period. The rate of the polymer formation shows only very little decrease in the

first several hours which can be used for the kinetic study. A further decrease of the reaction rate is noticed for the rest period of the reaction. This may due to the increase of the viscosity of the reaction mixture caused by the formation of the polymer.

The rate equation of TPPCoCl catalysed PO/CO_2 copolymerisation is shown below.

$$r=k[cat.]^a[PO]^b[CO_2]^c[co\text{-}cat.]^d$$

In the case of the cobalt(III) porphyrin as the catalyst, without the addition of a co-catalyst, the polymerisation shows nearly no activity. The reaction rate is influenced by the catalyst concentration, the monomer concentration, the CO_2 pressure and the co-catalyst concentration and k is the rate constant. To determine the values of a, b, c and d, polymerisations with the variation of one parameter (e.g. the catalyst concentration) while fixing the rests are performed and the results are discusses in detail.

4.2 The Reaction Order of TPPCoCl

A series of copolymerisation reactions by varying the initial TPPCoCl concentration is performed to determine the order of the catalyst. The reactions are carried out under 20 bar CO_2 pressure and room temperature. 5 mL PO and 10.41 mg PPNCl (4000:1) are utilized for all the reactions performed. 5 mL DCM is added to reduce the viscosity of the polymerisation mixture caused by the formation of the polymer. The catalyst loading varies from 0.25 equivalent to 4 equivalents.

As shown in Figure 31, the double logarithmic plot of the initial reaction rate and the catalyst concentration fits in a linearity with a slope of 1, implying a pseudo-first order in TPPCoCl.

As discussed in previous literatures, two possible mechanisms of chain propagation have been proposed: monometallic and bimetallic pathways. The former route suggests that one polymer chain propagates exclusively on one metal centre. On the other hand, a bimetallic chain propagation requires the cooperation of two metal centres for the polymer growth. In such a bimetallic mechanism, the growing polymer chain should be more stable, compared with the monometallic route, since it is always able to coordinate to one metal centre (For more details of the mechanisms of the chain propagation, please refer to section 1.3.2).

The pseudo-first order in TPPCoCl may indicate that the polymer formation takes place exclusively on one metal centre. However, due to the presence of the co-catalyst, this proposal is not fully confirmed yet. A change in the mechanism, if a co-catalyst is used, has been observed by Nozaki *et al.*. A bimetallic mechanism is supported by kinetic studies while applying linked cobalt(III) salen catalysts. On the other hand, if a co-catalyst (PPNCl) is combined with the linked catalysts, the order of the catalysts changes from a pseudo-second order to a pseudo-first order.[56]

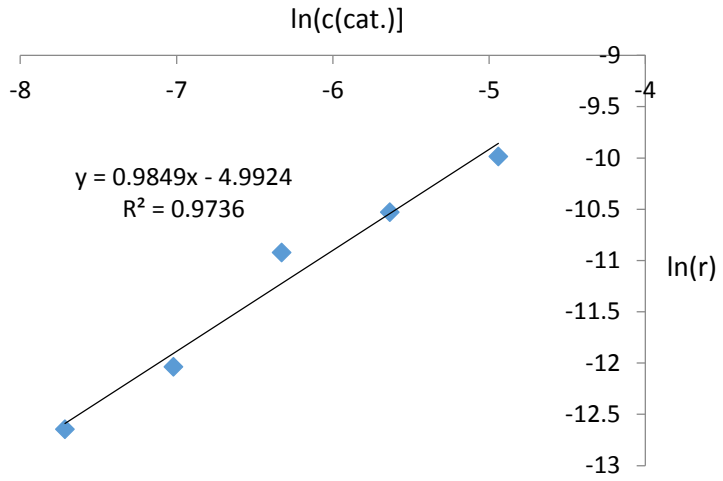

Figure 31. The graphic of ln(r) vs. ln[c(cat.)].

4.3 The Reaction Order of PO

By varying the ratio of PO and DCM, while keeping the total volume of the liquid as 10 mL, a series of copolymerisation reactions are carried out. The amounts of TPPCoCl and PPNCl are 12.64 mg and 10.41 mg respectively (1:1 molar ratio) for all reactions performed. The reactions are carried out under 20 bar CO_2 pressure and room temperature. The volume of PO differs from 1 mL to 7 mL.

As shown in Figure 32, the double logarithmic plot of the initial rate versus the PO concentration fits well in a linearity with a slope of 1, implying a pseudo-first order in PO. Meanwhile, the formation of cyclic carbonate increases with the decrease of the PO concentration, as shown in Figure 33. The back-biting reaction seems to take place more easily

under the low concentrations of the monomer. The coordination of PO towards the cobalt centre is considered a fast process.

Although an obvious explanation of the determined pseudo-first order in PO seems obscure, some factors may have influences on such a result. Since the ratio of DCM and PO is varies in this study, the change of the properties of the solvent (e.g. dielectric constant) may be influential towards the polymerisation reactions. Besides, the equilibrium of the coordination towards the metal centre between PO and the additional nucleophile (PPNCl) presumably exists and the decrease of the PO concentration shifts this equilibrium towards a PPNCl-coordinated cobalt(III) species and thus may have an impact on the order of PO.

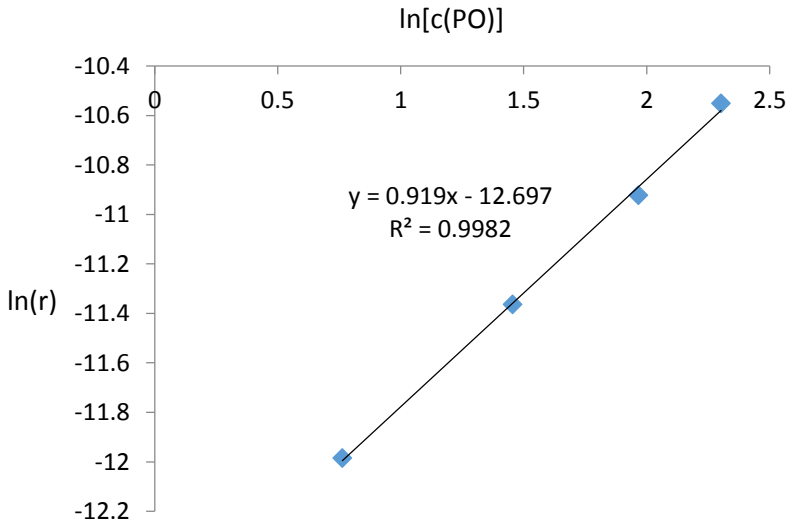

Figure 32. The graphic of ln(r) vs. ln[c(PO)].

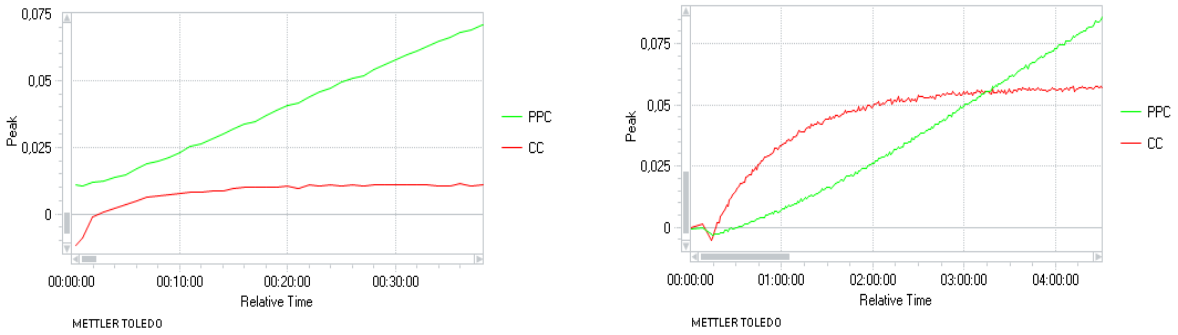

Figure 33. Graphics showing PPC and CC formation by varying the initial PO concentration (left: 7 mL; right: 1.5 mL).

4.4 The Reaction Order of CO_2 Pressure

As has already been mentioned in the previous text, the increase of CO_2 pressure to higher than 25 bar causes abnormal *in-situ* IR graphics probably due to the precipitation of the catalysts on the sensor. An addition of an extra solvent (e.g. DCM), aiming to increase the solubility of the catalysts and the polymer, does not solve this problem. Thus, the determination of the order of the CO_2 pressure by using *in-situ* IR technology is not successfully achieved.

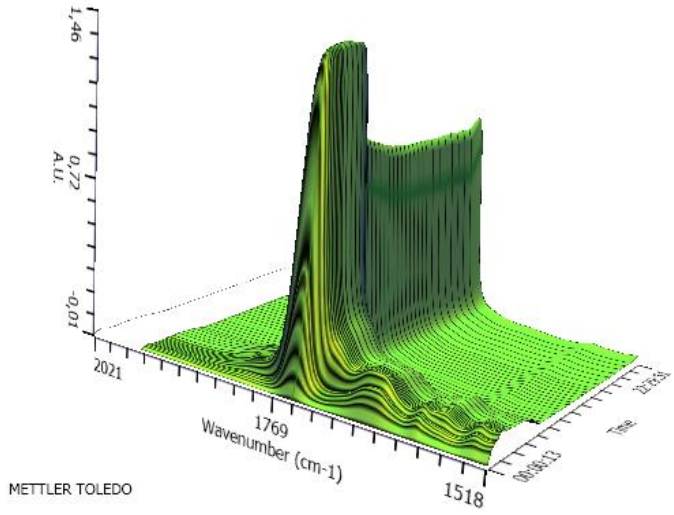

Figure 34. An abnormal *in-situ* IR spectrum showing significant increase and decrease of the band at 1748 cm^{-1}.

4.5 The Reaction Order of PPNCl

A series of copolymerisation reactions is performed by varying the initial co-catalyst concentrations. The co-catalyst loading varies from 0.25 equivalent to 4 equivalents. 12.64 mg TPPCoCl, 5 mL PO (1:4000) and 5 mL DCM are utilized for all reactions performed. All polymerisation reactions are carried out under 20 bar CO_2 pressure and room temperature.

As shown in Figure 35 (left), upon the increase of the co-catalyst loading to higher than 2 equivalents, the polymer formation rate is not further enhanced. This phenomenon may due

to an obvious increase of the cyclic carbonate formation under high co-catalyst loadings (>1 equivalent).

The double logarithmic plot of the reaction rate and the co-catalyst concentration fits well in a linearity within the range of the co-catalyst loading from 0.25 equivalent to 2 equivalents and a pseudo-first order of PPNCl is established (Figure 35, right).

Although the functionality of the co-catalyst is not fully understood hitherto, it is apparent that the variation of the co-catalyst concentration influences strongly on the reaction rate even if the catalyst concentration is constant.

As suggested by previous literatures, the nucleophilic anion of the co-catalyst is able to coordinate to the cobalt centre altering its Lewis acidity. Other hypothesis attributes the role of the co-catalyst to an additional initiator. For more detailed information of the functionality of the co-catalyst, please refer to section 1.5.

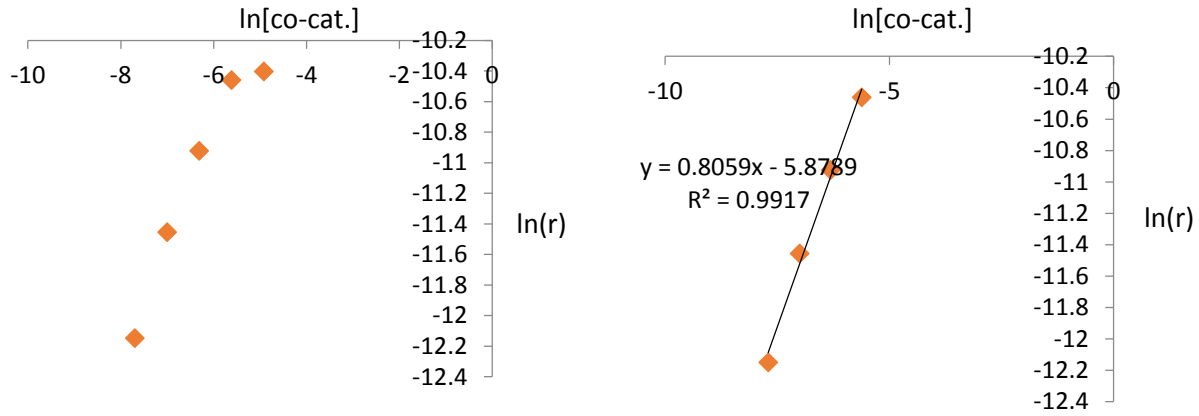

Figure 35. Graphics of ln(r) vs. ln[co-cat.].

4.6 Conclusions

In summary, the TPPCoCl catalysed PO/CO_2 copolymerisation has a rate equation as shown below,

$$r=k[cat.]^1[PO]^1[CO_2]^c[co\text{-}cat.]^1$$

The reaction order of the co-catalyst is valid in the range of less than 2 equivalents. Although the order of CO_2 pressure is not able to be determined by *in-situ* IR technology due to an unexpected precipitation of the catalyst. According to the polymerisation results obtained by using a hand autoclave, via the increase of the CO_2 pressure from 20 bar to 30 bar, the polymer formation maintains constant. This observation may indicate that CO_2 insertion is not the rate determining step in such a copolymerisation within the range of 20 bar to 30 bar.

Since the orders of the catalyst, the monomer and the co-catalyst are the same. The variation of each of them has equal influences on the rate of the polymer formation.

Many publications suggest that the chain propagation takes place via a cooperation of two metal centres.[23,32-34] As indicated by this kinetic study, the pseudo-first order of the catalyst may either infers a monometallic chain propagation by TPPCoCl/PPNCl or be due to the presence of the co-catalyst.

The variation of the ratio of PO and DCM shows a pseudo-first order of the monomer. This may result from the change of the solvent properties or the shift of the equilibrium of the coordination between PO and PPNCl towards the metal centre.

TPPCoCl alone shows nearly no activity in both the copolymer and cyclic carbonate formations. PPNCl alone without a catalyst is also not able to give any product after the polymerisation. To further understand this copolymerisation reaction, continuous efforts are still being made.

5. Ring Opening of Propylene Oxide Catalysed by a Cobalt(III) Porphyrin Complex

5.1 Introduction

Epoxides are useful intermediates for organic syntheses due to their high reactivity towards a large amount of electrophiles and nucleophiles.[90] For instance, asymmetric ring opening of various racemic epoxides produces highly enantiopure compounds.[23] Copolymerisation of propylene oxide and carbon dioxide is also considered to be an excellent way to utilise this greenhouse gas and the afforded poly(propylene carbonate) is biodegradable which meets the environmental considerations.[91]

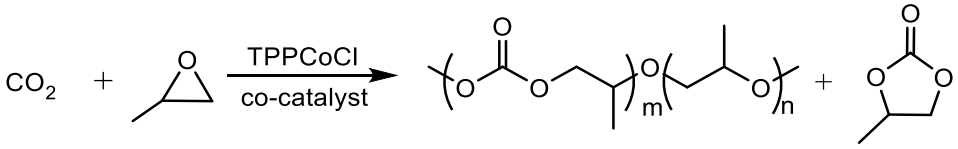

Scheme 22. Copolymerisation of propylene oxide and carbon dioxide by TPPCoCl.

Following the initial discovery of this copolymerisation by Inoue,[68] numerous catalysts have been developed to improve the catalytic activities as well as the selectivity for the copolymer and to modify the microstructures for the requirements of specific physical properties.[91] Cobalt(III) tetraphenylporphyrin chloride has been proved to be an active catalyst for poly(propylene carbonate) formation (Scheme 22). It was first discovered by Wang[29] and Sugimoto[28] independently with either PPNCl or DMAP as a co-catalyst. Modifications of the porphyrin ligand with the introductions of a series of electron-withdrawing groups conducted by our group show a slight increase in the catalytic activity.[30]

Inoue introduced aluminium(III) tetraphenylporphyrin chloride (TPPAlCl) with quaternary salts as co-catalysts which are able to copolymerise propylene oxide and CO_2 in 1986.[20] Chisholm studied the mechanism of such a copolymerisation by using NMR spectroscopy in 2005.[36] Up to date, very few mechanistic studies by using cobalt(III) porphyrins has been reported for PO/CO_2 copolymerisation.

In this chapter, the initial ring opening of PO is studied with TPPCoCl as a model catalyst by using ^{1}H NMR spectroscopy. A series of onium salts is introduced into the ring-opening system to examine their influences on the ring-opening rate. Onium salts comprising nucleophilic anions are commonly used as co-catalysts for poly(propylene carbonate) formation which accelerates the reaction rate.[18,37-40,42-48,50-53,92] The possible role of the co-catalyst is either a coordinating ligand or an extra initiator (Scheme 23). The reaction pathways both in the absence and presence of onium salts are discussed in detail.

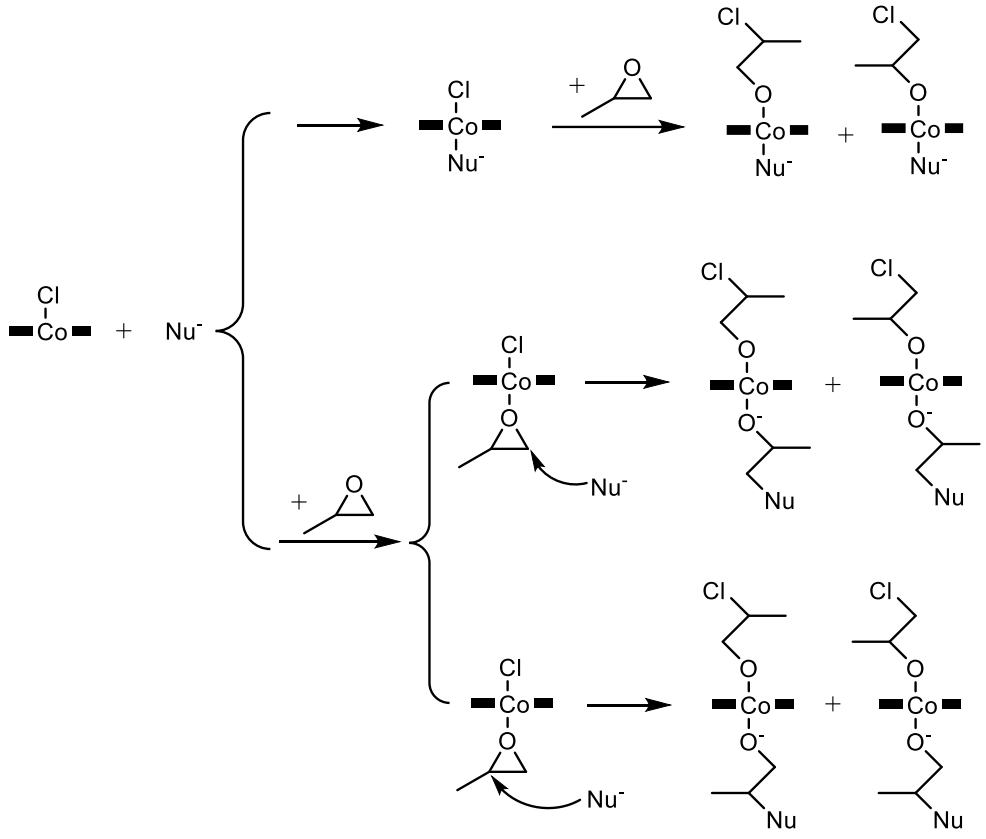

Scheme 23. Possible ring-opening pathways in the presence of additional nucleophiles.

5.2 Synthesis and Crystal Structure of TPPCoCl

The ligand (TPP) is purchased from TCI-Europe and the method of the metalation is adopted from Adler's work wherein DMF was proved to be the most suitable solvent (Scheme 24).[82] The air oxidation of the metal centre from cobalt(II) to cobalt(III) is performed in methanol (250 mL) at room temperature and a concentrated HCl aqueous solution (ca. 7 mL) is added to supply the counter ion, Cl^-.

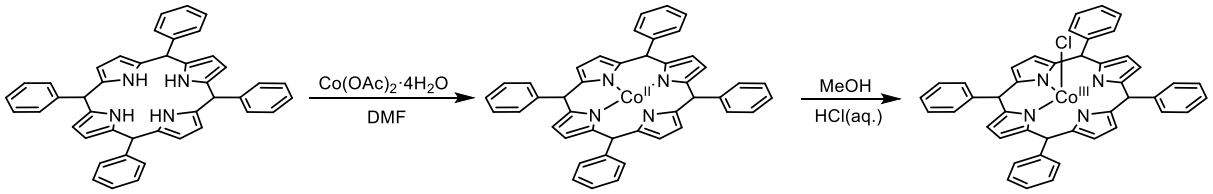

Scheme 24. The metalation and oxidation of TPP ligand.

During the purification, Millipore water is utilised to wash out the remaining inorganic salts in the product followed by the neutralization with a saturated $NaHCO_3$ aqueous solution and more wash with water. The solid is dried under air atmosphere overnight and is redissolved in acetone. After the filtration of this acetone solution, the final product is obtained as a purple solid via the rotary evaporation. In addition, the single crystal of TPPCoCl-acetone has been successfully grown through a slow diffusion of hexane into an acetone solution and the molecular structure has been resolved by X-ray crystallography.

Elemental analysis is performed to characterise the product and the detected values of carbon, hydrogen and nitrogen contents are very similar to the theoretical values which assures the purity of the product. ^{1}H NMR measurements are conducted for TPPCoCl in both CD_2Cl_2 and CD_2Cl_2+THF-d_8. Distinguishing characteristics have been observed between these two collected NMR spectra. Broad protons signals of TPPCoCl are found if CD_2Cl_2 is used as the NMR solvent (Figure A17). On the other hand, upon the addition of THF-d_8, these proton resonances become sharp (Figure A18). The broad NMR signals in CD_2Cl_2 may result from the paramagnetism of a high-spin cobalt(III).[93] Upon the addition of a coordinating solvent, such as THF, a hexacoordinate species is formed stabilizing the metal centre on a low-spin state. Huet attributed the line broadenings of the NMR signals in non-coordinating solvents to a disproportionation reaction of TPPCoCl which generates paramagnetic TPPCo(II) and TPPCo(III) π-cation radical (Scheme 25).[86]

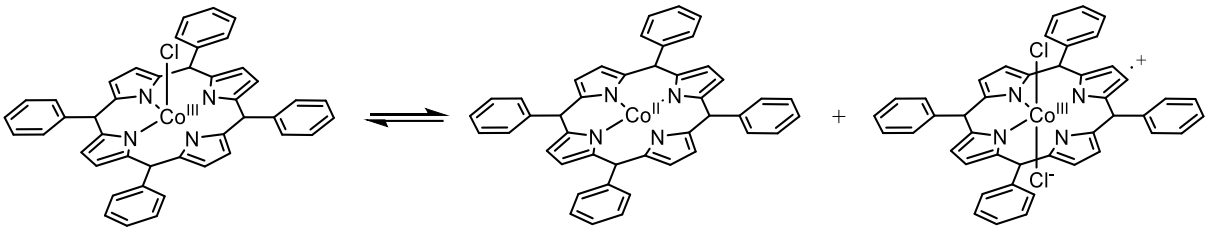

Scheme 25. The disproportionation of TPPCo(III)Cl.

The UV-Vis spectrum of TPPCoCl in DCM shows a Soret band at 406 nm and a broad Q band at 543 nm, which are similar to the literature (Figure A19).[94] Although broad signals are found within the range between 700 to 900 nm, which is a typical region for the appearance of the absorptions of porphyrin π-cation radicals, the intensities of these absorptions are too weak. As suggested by literature, the disproportionation of TPPCoCl in DCM may reach its equilibrium when only 0.12% TPPCoCl is converted to TPPCo(II) and the π-cation radical which may be an explanation for such weak absorptions.

Upon the addition of a coordinating solvent, such as THF, into the DCM solution of TPPCoCl, the UV-Vis spectrum shows a 20-nm red shift of the Soret band with an increase in its intensity. Meanwhile, the Q band becomes narrower with a shoulder appearing at 590 nm (Figure A19). This phenomena is explained by the transformation of a pentacoordinate TPPCoCl (in DCM) to a hexacoordinate one (in DCM+THF) (Scheme 26).

Aggregations in the DCM solution of TPPCoCl are initially suspected due to the observed increase of the intensity of the Soret band upon the addition of THF. The face-to-face (H-aggregation) stacking of the porphyrins exhibits a blue shift as suggested by literature, which is consistent with our observation.[95-97] Since π-π stacking is a weak intermolecular interaction, through the dilution of the concentration of TPPCoCl or the addition of extra aromatic solvents, such as toluene, the absorption of the monomeric TPPCoCl is expected to appear in the UV-Vis spectrum. However, no such change of the spectrum is observed. If the DCM solution of TPPCoCl is left for several weeks, a band at 436 nm is detected which is most probably due to a hexacoordinate TPPCoCl formed by the binding of water or oxygen.

ESI-Mass measurements are performed to further characterise TPPCoCl. In the cation mode, a signal at m/z 671 is detected in the spectrum (Figure A21) which has the same value as the molar mass of $TPPCo(III)^+$.

The single crystal of TPPCoCl which is suitable for X-ray diffraction is grown from a slow diffusion of hexane into a DCM solution. The resolved structure shows a hyperstoichiometric chlorine (1.3) binding on the metal (Figure A22). This can be explained either by a coordination of a compound having a chloride anion or the formation of a π-cation radical. Since no other cation has been detected by X-ray measurements and obvious precipitate, which is confirmed by UV-Vis spectroscopy to be TPPCo(II) (Soret band: 410 nm, Q-band: 525 nm), is noticed on the bottom of the vessel used to grow the crystal, the disproportionation of TPPCoCl most likely occurs.

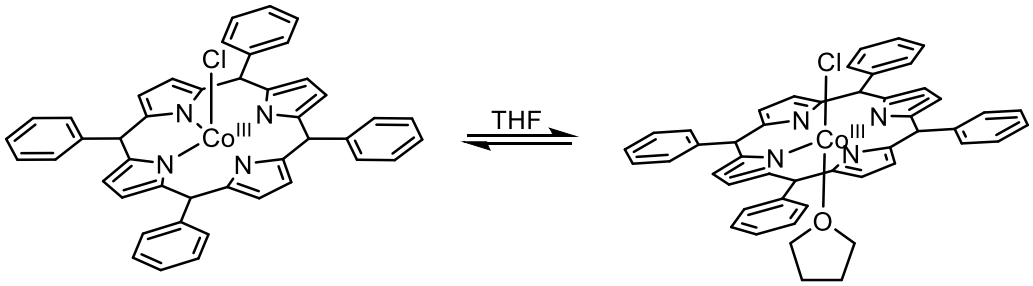

Scheme 26. The transformation of a pentacoordinate TPPCoCl to a hexacoordinate species upon the addition of THF.

On the other hand, the single crystal of TPPCoCl grown from a slow diffusion of hexane into an acetone solution shows a theoretical molar ratio between cobalt and chlorine (1:1) (Figure 36). The resolved structure exhibits a chlorine atom and an acetone molecule binding on each side of the metal with one more acetone co-crystalised in the unit cell.

Literature-known crystal structures of TPPCoCl include TPPCoCl (pentacoordinate),[98] TPPCoCl-H_2O[99] and TPPCoCl-pyridine.[100] The porphyrin core in the crystal structure of TPPCoCl is nearly flat whereas through *trans*-coordination of an acetone, the porphyrin core is ruffled. The bond lengths between cobalt and chloride in the above-mentioned three crystal structures are 2.145 Å, 2.216 Å and 2.251 Å respectively. In TPPCoCl-acetone, this value is 2.2026 Å. The theoretical bond length of cobalt and chlorine, calculated from the sum of the radii of the low-spin cobalt(III) and the chloride anion (68.5 pm and 167 pm, respectively) is 2.355 Å. Thereby,

the shorter Co-Cl bond length indicates a strong binding of the chlorine atom towards the cobalt centre.

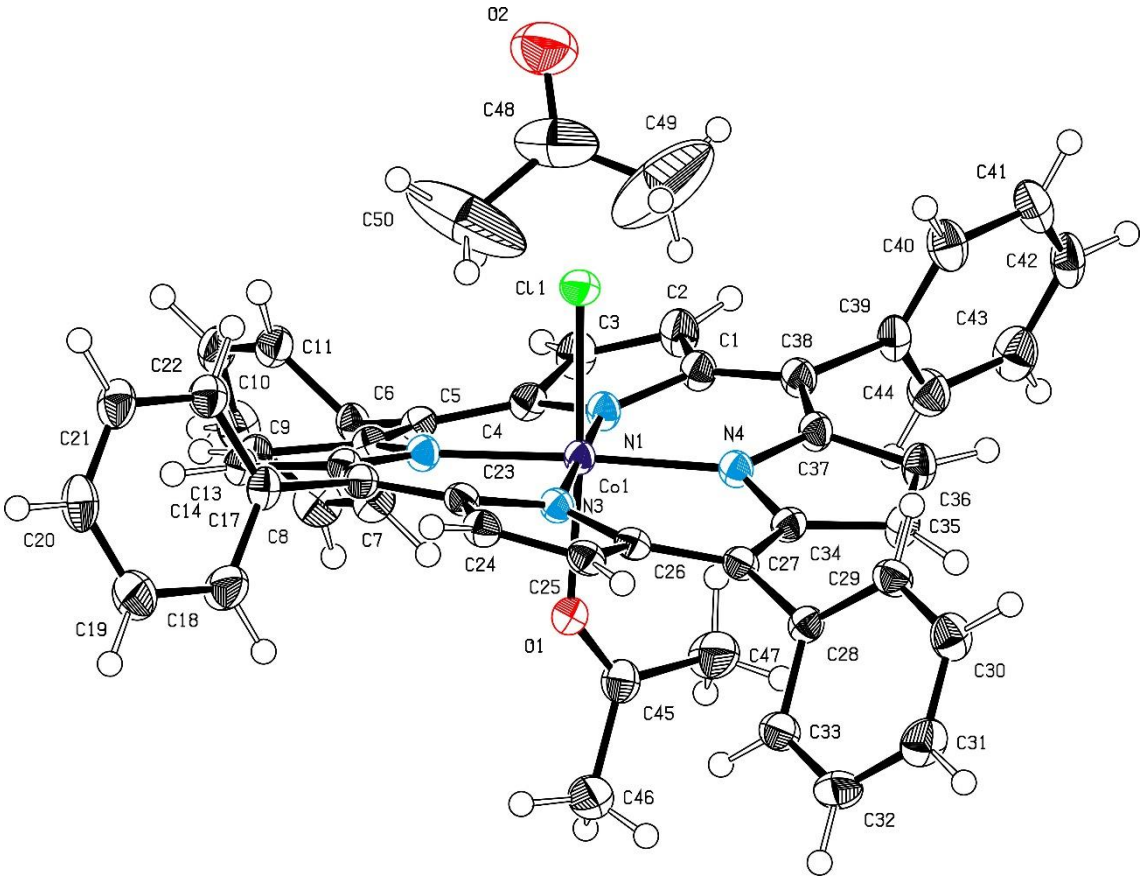

Figure 36. The resolved crystal structure of TPPCoCl-acetone.

5.3 Ring Opening of PO by TPPCoCl

The first question which is interesting to be answered is if the ring opening of the epoxide by the cobalt(III) porphyrin complex alone is feasible, since in the absence of a co-catalyst, no copolymer can be produced in PO/CO_2 copolymerisation,[30] the initiator may be the additional nucleophile. The copolymerisation of oxetane and CO_2 has been achieved by using a salenCr(III) catalyst with a co-catalyst of onium salts.[92] A crystal structure of salenCr(III)-oxetane is resolved, indicating the low possibility of the ring opening of oxetane by the salenCr(III) catalyst. As revealed by the crystal data of TPPCoCl-acetone, the rather strong binding of chlorine towards cobalt may induce a difficulty for PO ring opening.

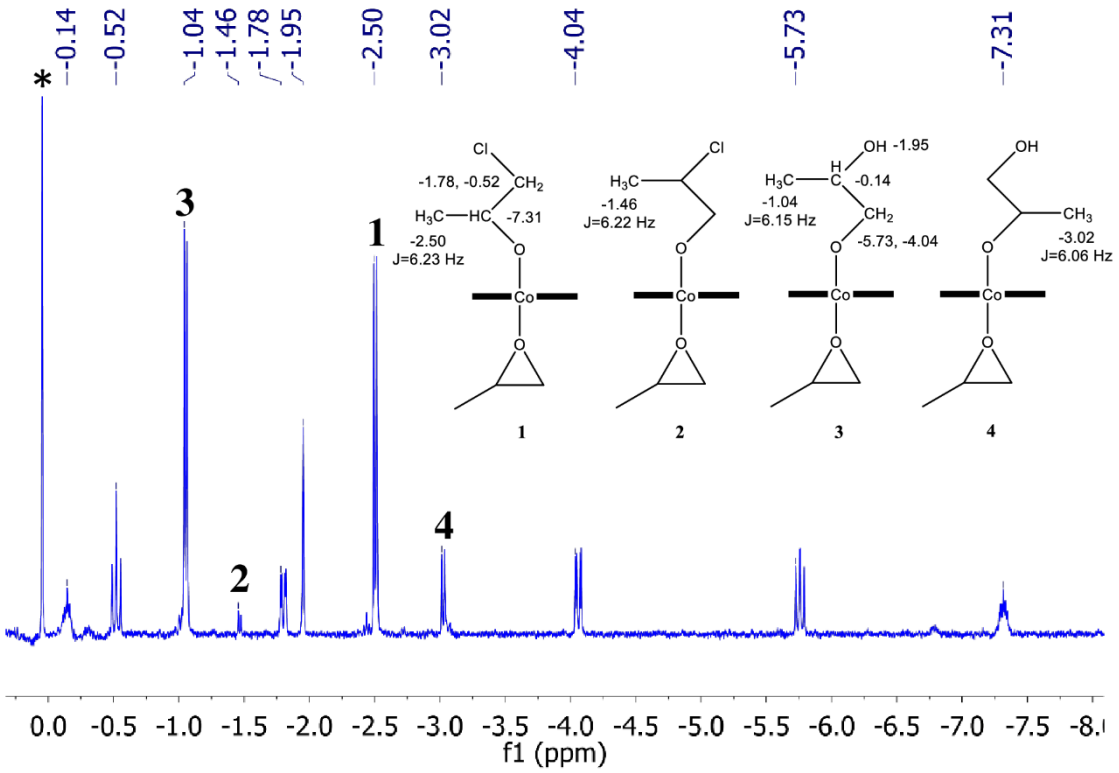

Figure 37. ^{1}H NMR spectrum collected at ring-opening time=30 min (CD_2Cl_2, 300 MHz, 25 ^{o}C).

To monitor the ring opening of PO by TPPCoCl, ^{1}H NMR spectroscopy is used, taking advantage of the ring-current effect of the porphyrin macrocycle. A series of ^{1}H NMR measurements is performed by mixing TPPCoCl (5 mg) and PO (0.3 mL) in CD_2Cl_2 (0.5 mL) at room temperature. The experiments are conducted without the protection of argon and both PO and CD_2Cl_2 are utilised as received. Hence, possible side reactions involving water or air need to be taken into consideration.

As shown in Figure 37, a series of high-field NMR signals is detected and after careful analyses of these peaks, four different cobalt alkoxides are identified, suggesting the feasibility of PO ring opening by TPPCoCl alone.

The first produced species is TPPCoOCH(CH_3)CH_2Cl (**1**). It is considered to be generated via the nucleophilic attack of Cl on the methylene carbon of PO (Scheme 27). The CH_3 signal shows a coupling constant of 6.23 Hz. Another doublet with a very low intensity grows simultaneously with the signals of **1**.Since it shows a very similar coupling constant (6.22 Hz) with the methyl group in **1**, it is assigned to the methyl group of TPPCoOCH_2CH(CH_3)Cl (**2**), which is afforded through the nucleophilic attack of Cl on the methine carbon of PO. The molar ratio between **1**

and **2** maintains constant throughout the reaction and is calculated to be 95:5, indicating a highly selective ring opening by Cl.

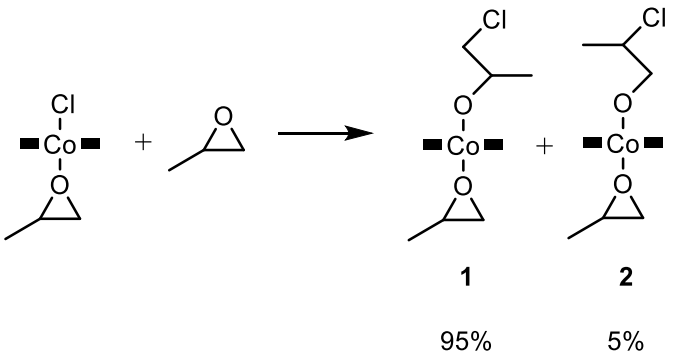

Scheme 27. The ring opening of PO by TPPCoCl.

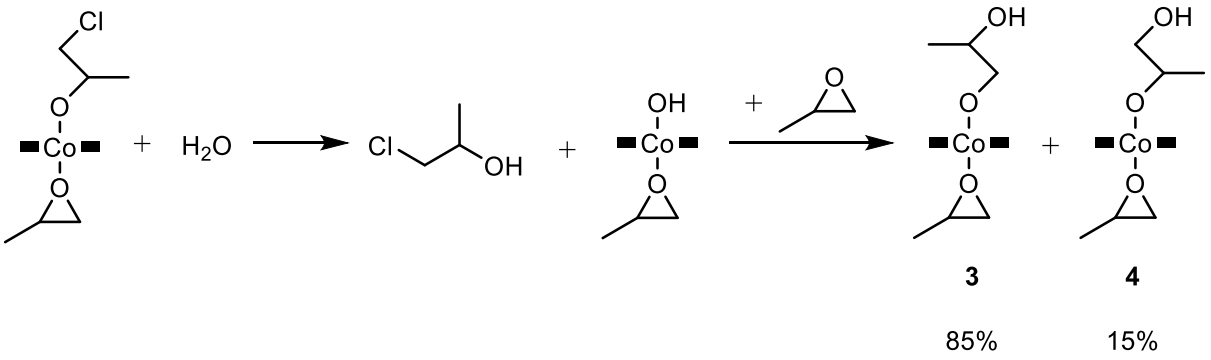

Scheme 28. The hydrolysis of complex **1** and subsequent ring opening of PO by TPPCoOH.

The hydrolysis of complex **1** takes place subsequently and produces 1-chloro-2propanol (Figure A23, A24) and TPPCoOH (Figure A25) which serves as a new nucleophile for PO ring opening (Scheme 28). Indeed, following the growth of the NMR signals of **1** and **2**, another series of peaks grows in the high field and is assigned to the complexes **3** and **4**. These two species are generated via the nucleophilic attack of OH on either the methylene or the methine carbon of PO (Scheme 28). The molar ratio between **3** and **4** maintains constant throughout the reaction and is calculated to be 85:15 which is in contrast to the ring opening by Cl.

The difference of the selectivity of the ring opening by Cl and OH is explained by a rearrangement of the hydroxypropoxide ligand. Since the alcoholysis of the initially formed cobalt alkoxides is demonstrated to be feasible by the formation of TPPCo(III)-methoxide via the addition of methanol (0.3 µL) into the ring-opening system as detected by ^{1}H NMR spectroscopy (Figure 38), the interconversion between complexes **3** and **4** should take place, yielding mainly the thermodynamically favoured structure, complex **3**.

The hydrolysis of **3** and **4** is proved by the detection of one of its products, propylene glycol, in the ^{1}H NMR spectrum (Figure A25, A26) (Scheme 29). TPPCoOH is considered as another product of the hydrolysis, however, this complex has not been well characterised in literature. During the ring opening, a singlet at -16.26 ppm is found which is attributed to the axial hydroxyl group (Figure A25). Since this proton resonance locates at such a high field, possible assignments are either a proton which is very close to the porphyrin core and is strongly shielded by the ring current or a metal hydride. As no signals of aldehyde or ketone is detected in the ^{1}H NMR spectrum, β-hydride elimination of metal alkoxides to afford metal hydrides is thus excluded. Therefore, the hypothesis of the formation of TPPCoOH is supported.

The ring opening of PO by TPPCoOH in DMSO-d_6 proceeds at a much slower rate compared with the reaction performed in CD_2Cl_2, and as a consequence, the high-field NMR resonance at -16.26 ppm for TPPCoOH is observable. The variation of the solvents has been proved to influence strongly on the ring-opening rate. If toluene-d_8 is used, the PO ring opening by TPPCoCl is at an extremely slow rate, that nearly no reaction takes place after more than one hour as proved by NMR spectroscopy.

The alcoholysis of TPPCo-hydroxypropoxide by 1-chloro-2-propanol may also take place and affords propylene glycol. In other words, the axial alkoxide groups on the cobalt centre are in equilibrium with the free alcohols and such a ligand exchange is slow with respect to the NMR time scale, as reflected in the well-separated NMR signals of different alkoxides in the high field. As proposed by Inoue by using TPPAlCl as a catalyst,[101] such a ligand exchange may also take place during the polymerisation of epoxides and CO_2.

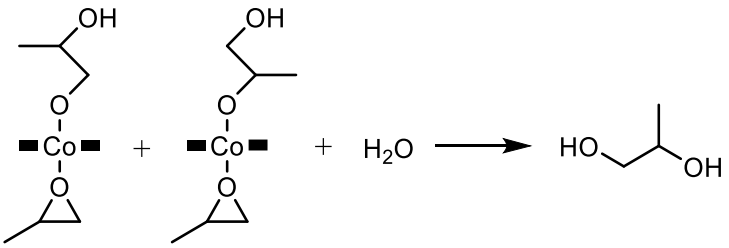

Scheme 29. The hydrolysis of **3** and **4** to afford propylene glycol.

The hydrolysis of complex **1** followed by the formation of species **3** and **4** demonstrated herein may be an explanation for the typically observed bimodal molecular weight distribution of PPC generated by TPPCoCl.[29] Two distinct initiators, Cl^- and OH^-, would produce copolymer chains with terminating groups allowing their propagation either at only one end (chloro-initiated) or simultaneously at both ends (hydroxy-initiated).[102] Such a mechanism of the polymer formation with the bimodal distribution implies a faster chain transfer caused by the presence of hydroxyl groups compared with the propagation rate.

The chemical shift of the porphyrin β-H signal is sensitive to the axial ligand. TPPCoCl shows a β-H signals at 9.06 ppm (Figure A18), during the ring opening, the intensity of this signal decreases and two other β-H signals appear at 9.03 ppm and 9.01 ppm (Figure A23), corresponding to complexes **1** and **3**. Molecular sieves (3 Å) are used in the ring-opening system to scavenge the residual water and an NMR spectrum is collected at 30 minutes. This shows complexes **1** and **2** as the exclusive ring-opening intermediates which supports the viewpoint that complexes **3** and **4** result from the hydrolysis of TPPCo-chloropropoxides (Figure A27).

As proved in our previous work, the homopolymerisation of propylene oxide by TPPCoCl/PPNCl to afford poly(propylene oxide) shows nearly no activity.[30] This is explained by an extremely slow ring opening of PO by TPPCo-alkoxides (Scheme 31). As shown by NMR measurements, no repeating insertion of PO are found in the high field which supports this explanation.

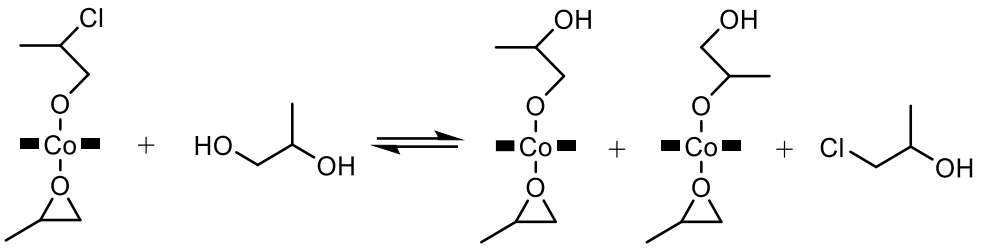

Scheme 30. The alcoholysis of **1**-**4** leading to an axial ligand exchange.

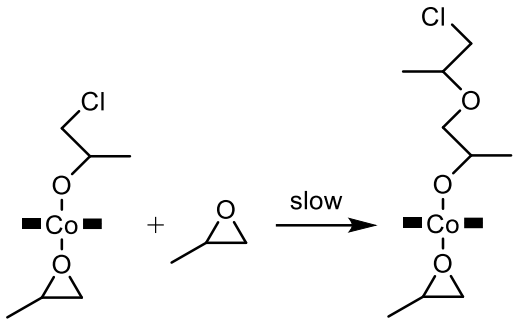

Scheme 31. Repeating insertion of PO for complex **1**.

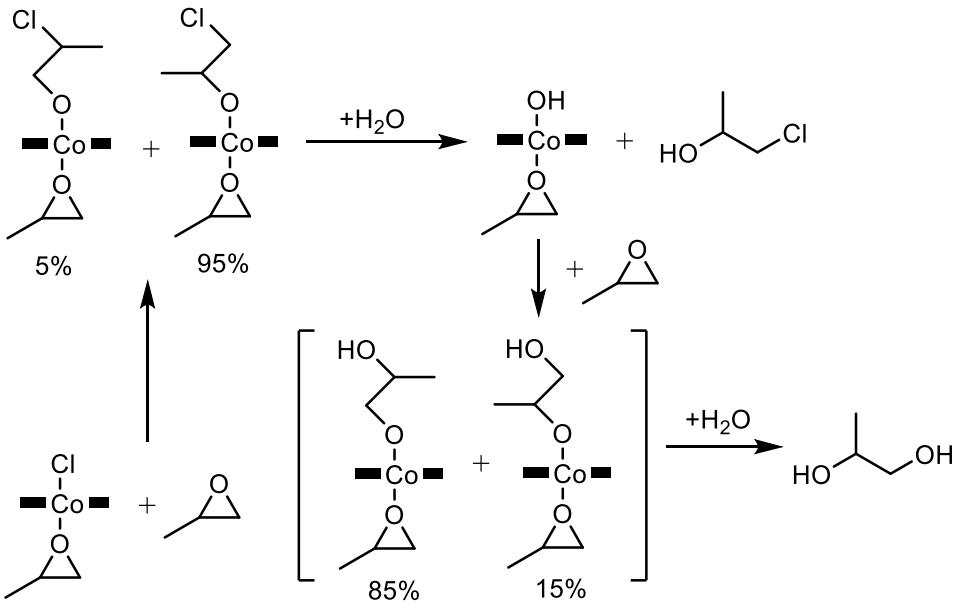

Scheme 32. The ring-opening pathway of PO by TPPCoCl.

In summary, the ring opening of propylene oxide by TPPCoCl undergoes a reaction pathway as shown in Scheme 32.

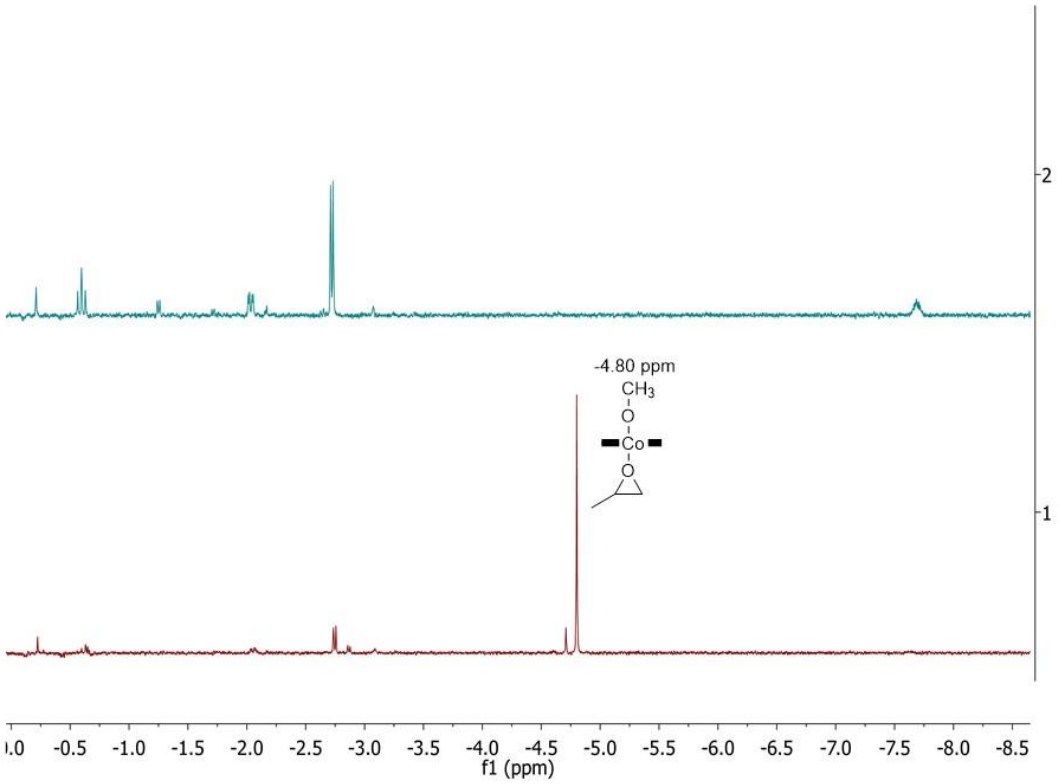

Figure 38. ^{1}H NMR spectrum (300 MHz, 25 ^{o}C) of TPPCoCl (5 mg), PO (0.3 mL) in $CDCl_3$ (0.5 mL) (Spectrum 2) and after the addition of 0.3 µL methanol (Spectrum 1).

The ^{1}H NMR spectrum of TPPCo-methoxide formed via the addition of methanol (1 equivalent) into the ring-opening system is shown in Figure 38. An obvious decrease of the proton resonances of the complexes **1**-**4** at high field is detected with a new signal appearing at -4.80 ppm (Figure 38). This axial methoxide is also able to conduct the ring opening. TPPCo-ethoxide and –isopropoxide have been produced as well, which show an order of the rate of ring opening as follow: methoxide>ethoxide>isopropoxide. This order shows a correspondence with the degree of the bulkiness of the nucleophiles. Therefore, the difficulty of the TPPCo-chloro/hydroxy propoxide to undergo a further ring opening of PO may result from the bulkiness of the axial nucleophile.

In addition, the aminolysis of the cobalt(III) porphyrin alkoxides has also been proved by ^{1}H NMR spectroscopy. As shown in Figure 39, the formations of two isomers of TPPCo-acetamides via the addition of acetamide to the ring-opening system are demonstrated by the appearances of four extra proton resonances in the high field.

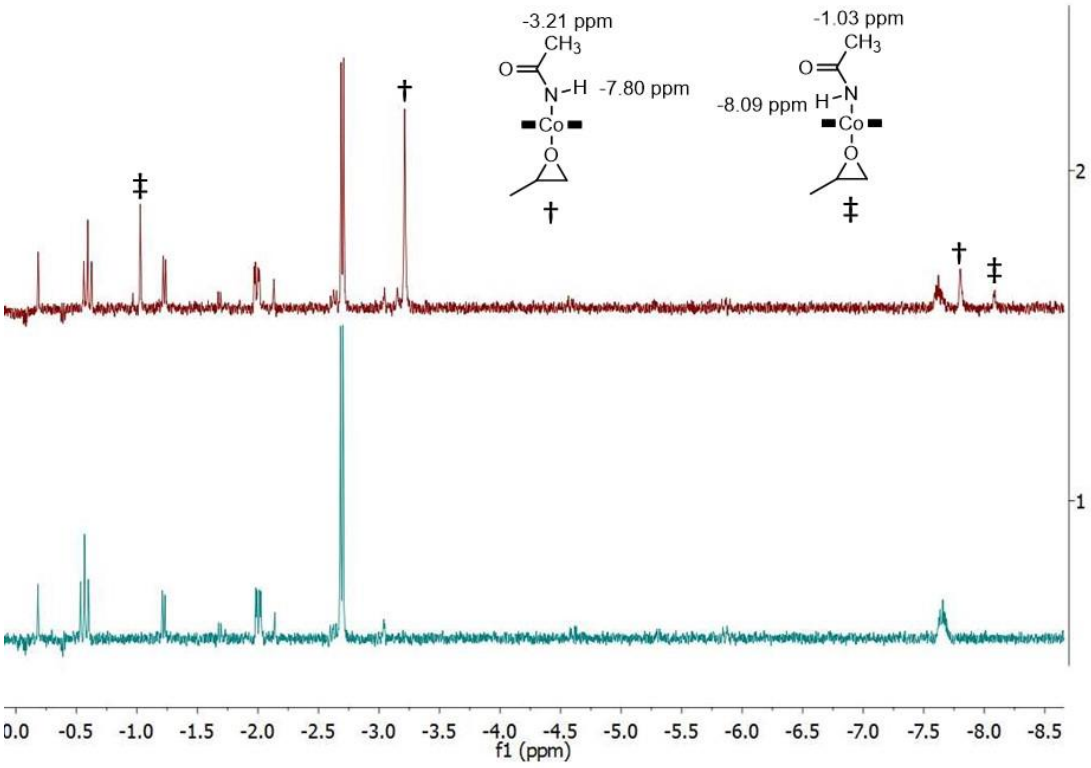

Figure 39. ^{1}H NMR spectrum (300 MHz, 25 ^{o}C) of TPPCoCl (5 mg), PO (0.3 mL) in $CDCl_3$ (0.5 mL) (Spectrum 1) and after the addition of acetamide (Spectrum 2).

The reaction order of TPPCoCl in the PO ring opening is successfully determined by monitoring the decrease of the TPPCoCl β-H signal. A pseudo-first order is established by the linear correlation between the reaction time and the logarithm of c_t/c_0 as shown in Figure 40 (Table A2).

However, this result is not able to distinguish if the ring opening takes place via a monometallic route or a bimetallic pathway. Therefore, further kinetic studies by varying the initial TPPCoCl concentrations are performed. Unexpectedly, the total time for the full conversion of TPPCoCl to cobalt alkoxides varies in each measurement from thirty minutes to one hour under exactly the same experimental conditions. The amount of water (or other small binding molecules, e.g. methanol) in the catalyst is suspected to be influential. After the exposure of the catalyst under air atmosphere for 3 days, the rate of PO ring opening shows a good reproducibility which enables the kinetic studies. A brief summary of the functionality of water in the PO ring opening is shown in Scheme 33. Water induces the hydrolysis of the initially formed metal

alkoxides and subsequently offers a new nucleophile, OH, which produces two additional ring-opening intermediates.

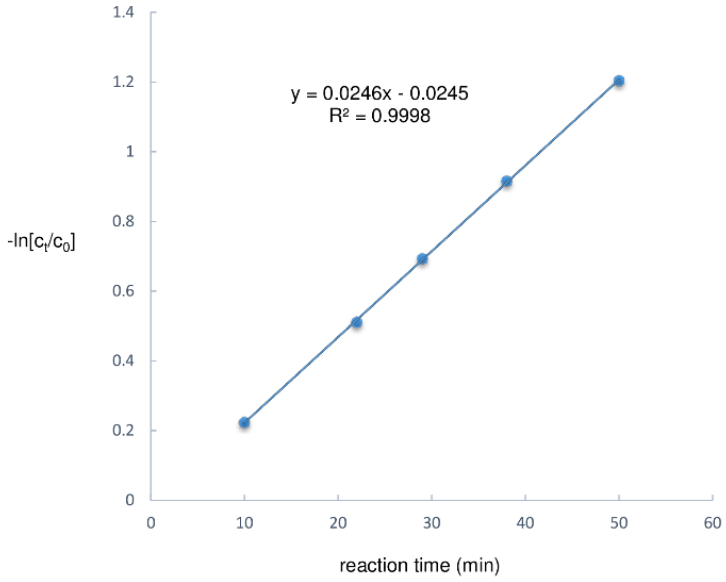

Figure 40. The plot of reaction time versus $-\ln(c_t/c_0)$.

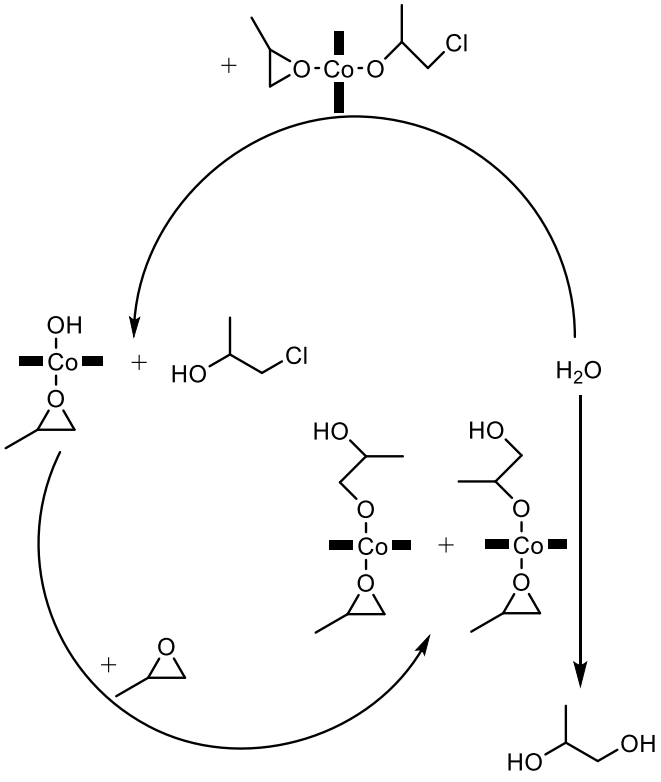

Scheme 33. The role of water in the ring opening of PO by TPPCoCl.

A series of ^{1}H NMR measurements is conducted by varying the initial TPPCoCl concentrations (2.5 mg, 1.25 mg, 0.65 mg, 0.25 mg) (Figure 41). The conversion of TPPCoCl is determined by the ratio of the integrations between the poprhyrin β-H peaks. As shown in Figure 41, the slopes of the fitting lines decrease upon the dilution of the TPPCoCl concentration. The double logarithmic plot of the catalyst concentration versus the reaction rate fits in a linearity with a slope of 1.5, indicating a combined ring-opening pathway by TPPCoCl.

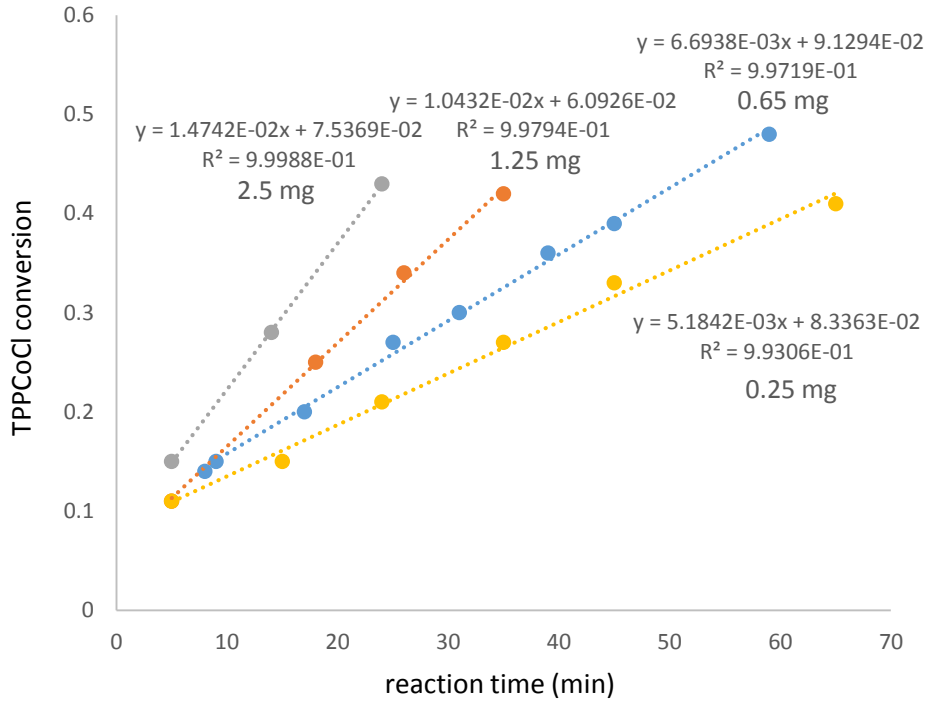

Figure 41. The graphic of the TPPCoCl conversion versus the reaction time.

Jacobsen discovered a bimetallic mechanism in a salenCr(III) catalysed ring opening of epoxides.[23] An exact second is obtained reflected in the kinetic results whereas in our case, a 1.5 order of TPPCoCl suggests a combined reaction pathway. Both monometallic and bimetallic routes involve in the ring-opening event (Scheme 34). Moreover, the exclusion of water via the addition of molecular sieve (3Å) shows a same order as 1.5, indicating no influence of trace amount of water on the rate equation.

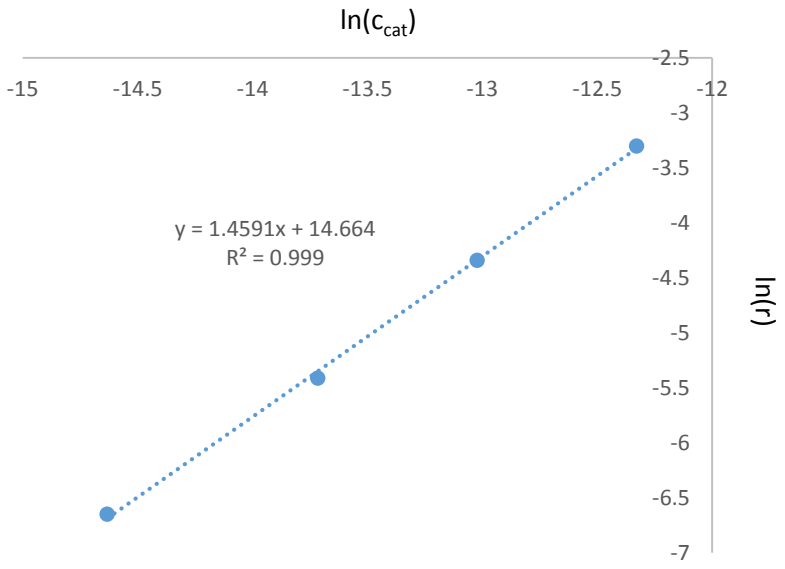

Figure 42. The kinetics data showing a 1.45 order of TPPCoCl.

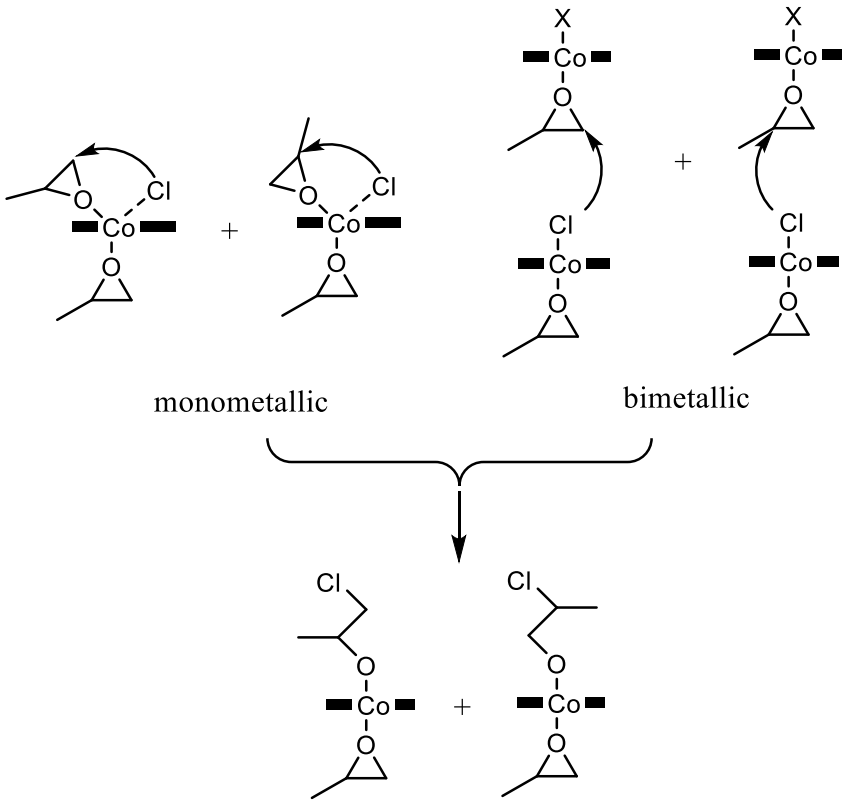

Scheme 34. Two ring-opening pathways.

5.4 Ring Opening of PO by TPPCoCl in the Presence of Onium Salts

Onium salts such as PPNCl are commonly used as co-catalysts in the copolymerisation of PO and CO_2 and they efficiently accelerate the reactions. Catalytic systems, such as cobalt(III) salen and porphyrin complexes show poor activities in the absence of a co-catalyst (TOF<100 h^{-1}) while the value of TOF is significantly enhanced in the presence of a co-catalyst.

Thereby, the PO ring opening catalysed by TPPCoCl is further explored in the presence of a series of onium salts to examine their influences on the ring-opening rate. The addition of 1 equivalent of PPNCl, $PPNN_3$ or NBu_4Br significantly accelerates the reaction. The first collected ^1H NMR spectrum (equal to the reaction time<five minutes) shows a nearly completed conversion of TPPCoCl to metal alkoxides. On the other hand, in the absence of onium salts, it takes approximately one hour to achieve such a full conversion.

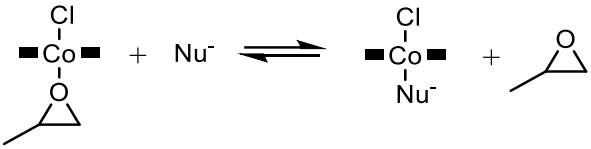

Scheme 35. Axial ligand exchange on the cobalt centre.

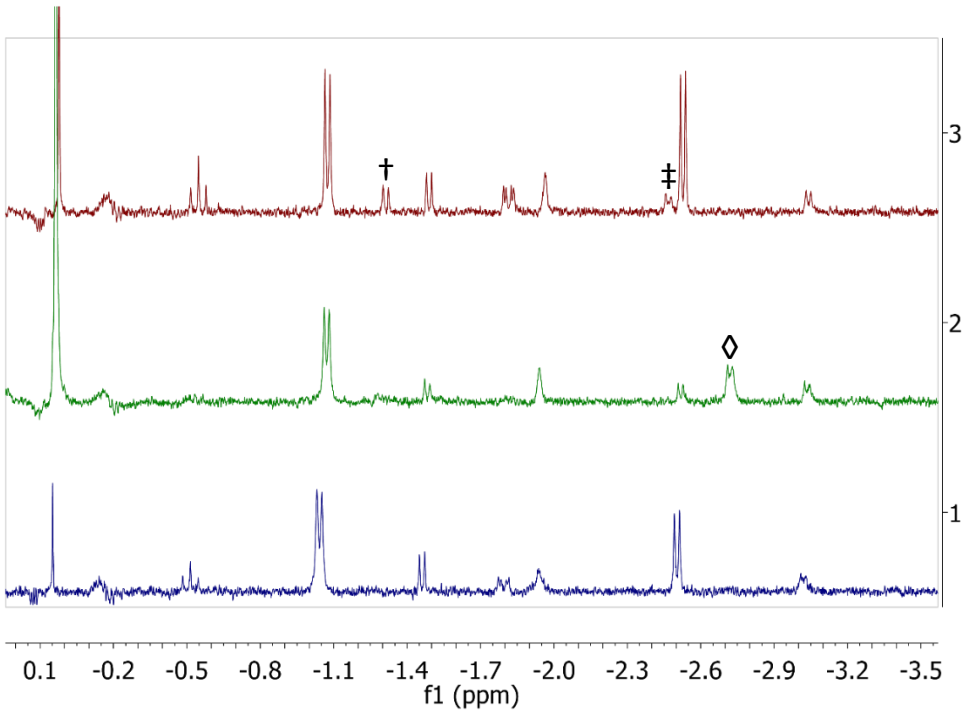

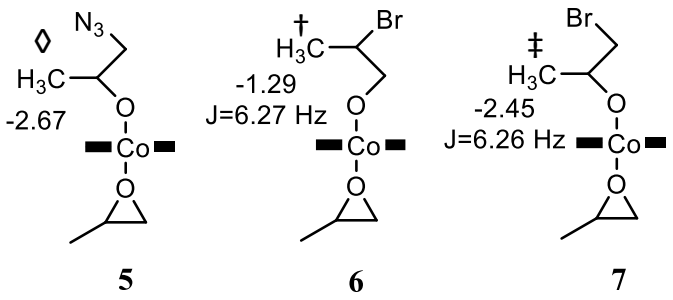

Figure 43. ^{1}H NMR spectrum showing ring-opening intermediates produced by additional nucleophiles.

A ligand exchange probably exists during the ring opening, if onium salts comprising nucleophilic anions are introduced as indicated by ^{1}H NMR spectroscopy. The addition of 1 equivalent of PPNCl into a TPPCoCl (5 mg) and PO (0.3 mL) mixture in CD_2Cl_2 (0.5 mL) causes obvious line broadenings of the proton signals of the porphyrin complex. A further addition to 10 equivalents of PPNCl intensifies this line broadenings and slightly shifts these proton resonances (Figure A28). Since the addition of 3 equivalents of PPNCl into a CD_2Cl_2 solution of TPPCoCl does not exhibit broad NMR signals in the absence of PO (Figure A29), paramagnetism of the cobalt centre induced by a *trans*-coordination of the chloride anion to form $[TPPCoCl_2^-]PPN^+$ is thus excluded. Thereby, most probably, there exists a ligand exchange on the cobalt porphyrin complex between the additional nucleophiles and PO (Scheme 35) which causes the observed line broadenings.

To further prove this viewpoint, a weakly coordinating anion, BF_4^-, is utilized for comparison. The addition of 1 equivalent to 10 equivalents of $PPNBF_4$ does not induce a noticeable change of the NMR signals of the porphyrin complex (Figure A30) which supports our hypothesis that the line broadening results from axial ligand exchange. Similar line broadenings of proton resonances upon the addition of $PPNN_3$ or NBu_4Br are also found in the NMR spectra (Figure A31, A32).

Since the additional nucleophiles may serve as extra initiators, upon the addition of PPNCl, $PPNN_3$ and NBu_4Br, additional alkoxide anions may be produced.

Indeed, the ring-opening intermediates produced by the additional nucleophiles are detected by using ^{1}H NMR spectroscopy (Figure 43). Through the addition of 1 eq. $PPNN_3$ into a TPPCoCl (5 mg) and PO (0.3 mL) mixture in CD_2Cl_2 (0.5 mL), the NMR signal of the methyl group of

complex **1** (-2.50 ppm) disappears completely. Meanwhile, a new proton resonance is found at -2.67 ppm and is assigned to the methyl group of $TPPCoOCH_2CH(CH_3)N_3$ (**5**) (Figure A32). If the amount of $PPNN_3$ is reduced to 0.3 equivalent, both **1** and **5** can be detected by NMR spectroscopy during the ring opening.

Similarly, if 10 equivalents of NBu_4Br is introduced, the ring-opening intermediates produced by Br (**6** and **7**) are detected by using ^1H NMR spectroscopy. The molar ratio between **6** and **7** is calculated to be nearly 1:1. On the other hand, the nucleophilic attack of N_3 takes place almost exclusively on the methine carbon of PO.

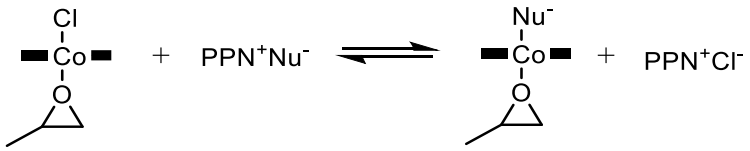

Scheme 36. Anion exchange between the axial ligand and the co-catalyst.

In addition, an anion exchange between the axial Cl and onium salts may presumably take place as shown in Scheme 36.

As demonstrated by Sugimoto, DMAP is also an effective co-catalyst if combined with TPPCoCl for poly(propylene carbonate) formation. The addition of 4 equivalents of DMAP to a TPPCoCl (5 mg), PO (0.3 mL) and CD_2Cl_2 (0.5 mL) solution shows a disappearance of the high-field signals of TPPCo-chloropropoxides with the formation of a di-DMAP coordinated species, $[TPPCo(DMAP)_2]^+$. On the other hand, the proton resonances of TPPCo-hydroxypropoxides can still be found in the spectrum (Figure A33). Possible explanation is that a five-membered ring is formed via the coordination of the OH group as shown in Figure 44, which increases the stability of TPPCo-hydroxypropoxides, although no further evidence at the moment can support such a hypothesis.

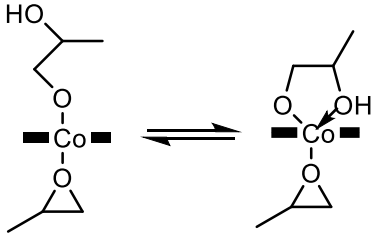

Figure 44. The possible formation of a five-membered ring from TPPCo-hydroxypropoxide.

The functionality of DMAP as an initiator has been proved by Lu by using mass spectrometry.[37] However, in the present work, no proof of the ring opening by DMAP can be found. The formed di-DMAP coordinated cobalt(III) porphyrin complex is relatively stable and is in slow ligand exchange as indicated by the well-resolved NMR signals of the coordinated DMAP.

The high affinity of DMAP towards the cobalt centre demonstrated here may be an indication that the functionality of DMAP in the TPPCoCl-catalysed PO/CO_2 copolymerisation is a coordinating ligand which binds to the metal altering its Lewis acidity. On the other hand, a highly excessive addition of DMAP may displace the growing chain as well, leading to the degradation of the polymer via the bacl-biting reaction and thus, shows a decrease in the polymerisation rate.

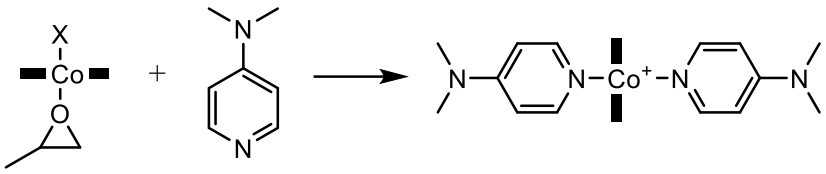

Scheme 37. The formation of a di-DMAP coordinated cobalt(III) porphyrin complex.

6. Reduction of Cobalt(III) Porphyrin Complexes in the Presence of Propylene Oxide

6.1 Introduction

Since the initial discovery of epoxide/CO_2 copolymerisation by Inoue in 1969, this reaction has attracted significant attention and cobalt(III)-based complexes, such as cobalt(III) salens and porphyrins, have become one of the most important classes of catalysts, owing to their high activities, good selectivity for copolymer as well as high regio-selectivity. However, Coates and co-workers noticed a reduction of cobalt(III) salen complexes during the copolymerisation of PO and CO_2, in that red precipitate is observed after the accomplishment of the reactions.[25] In 2013, Chisholm and co-workers reported a reduction reaction of cobalt(III) porphyrins to cobalt(II) complexes in propylene oxide.[24] The same deactivation of cobalt(III) porphyrins in propylene oxide is observed by us as well.[103]

The reduction of cobalt(III) porphyrins in the presence of certain ligands such as methylpiperidine[104] and hydroquinone dianions[105] has been reported in previous literature. In addition, similar reduction of TPPFe(III)Cl has also been observed in the presence of certain axial ligands such as CN^-, piperidine.[106-108] In this chapter, the reduction of TPPCo(III)Cl in propylene oxide is studied by using UV-Vis and ^1H NMR spectroscopies. The results are discussed in detail.

6.2 Reduction of Cobalt(III) Porphyrin Complexes in the Presence of Propylene Oxide

During the investigations of the literature-known catalyst, TPPCoCl, active for PO/CO_2 copolymerisation, the UV-Vis spectrum of TPPCoCl in PO shows noticeable changes with time.

A typical UV-Vis spectrum of TPPCoCl in DCM shows a Soret band at 406 nm and a broad Q band at 542.9 nm (Figure A19). Upon the addition of a coordinating solvent, such as THF or propylene oxide, the Soret band exhibits a 20-nm red shift with an increase in its intensity while the Q band becomes narrower with a shoulder appearing at 590 nm (Figure A19). On the other hand, TPPCo(II) shows a Soret band at 409 nm and a Q band at 528 nm in DCM

(Figure A34). Only a 1.1-nm red shift of the Soret band is observed upon the addition of a coordinating solvent such as methanol (Figure A34). Taking advantage of the readily distinguishable UV-Vis spectra of TPPCo(III) and TPPCo(II) complexes, the redox reaction between these two species is successfully monitored *in situ*.

A series of time-resolved UV-Vis spectra is collected for TPPCoCl in pure propylene oxide (10^{-6} M) at room temperature. As shown in Figure 45, a continuing shift of the Soret band of TPPCo(III) (436.9 nm) towards lower wavelengths is observed, indicating the reduction of TPPCo(III) to TPPCo(II) takes place (Scheme 38). No isosbestic point is found during the first three hours probably due to the PO ring opening by TPPCoCl to produce TPPCo-alkoxides (Scheme 39). Afterwards, an isosbestic point at 426 nm is observed. The initial reaction rate of TPPCo(III) reduction is calculated to be 10.3%/h (Figure A35).

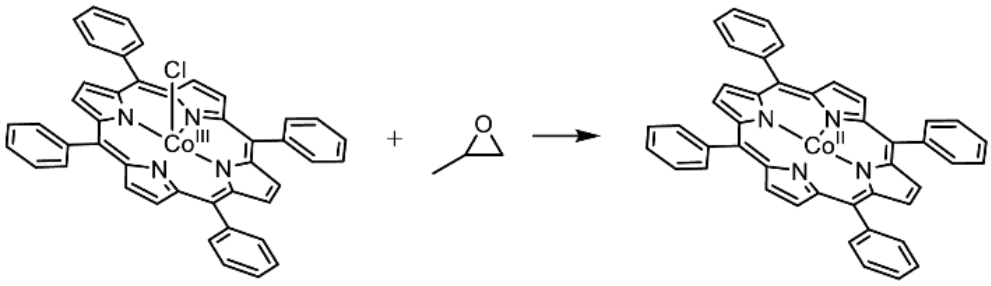

Scheme 38. The reduction of TPPCo(III)Cl in PO to TPPCo(II).

TPPCo(II) in a DCM solution shows no oxidation to TPPCo(III) under the air atmosphere after a 10-hour standing as indicated by UV-Vis spectrum (Scheme 40). Hence, the presence of air is expected to have nearly no influence towards such a reduction.

PPNCl is widely used as a co-catalyst for PO/CO_2 copolymerisation, it is considered to be able to stabilise the metal centre during the polymerisation.[25] Therefore, the influence of PPNCl is examined in the present work.

A series of time-resolved UV-Vis measurements is performed for TPPCo(III)Cl+PPNCl (1 equivalent) in pure propylene oxide (0.75 mM). As shown in Figure 46, a continuing shift of TPPCo(III) Q band (542.9 nm) towards lower wavelengths indicates that the reduction of TPPCo(III)Cl takes place and after an overnight reaction, the maximum absorption of the Q band is similar to that of pure TPPCo(II), suggesting a nearly completed reduction of

TPPCo(III)Cl to TPPCo(II). This result implies that the addition of PPNCl has nearly no influences on such a deactivation of the catalyst.

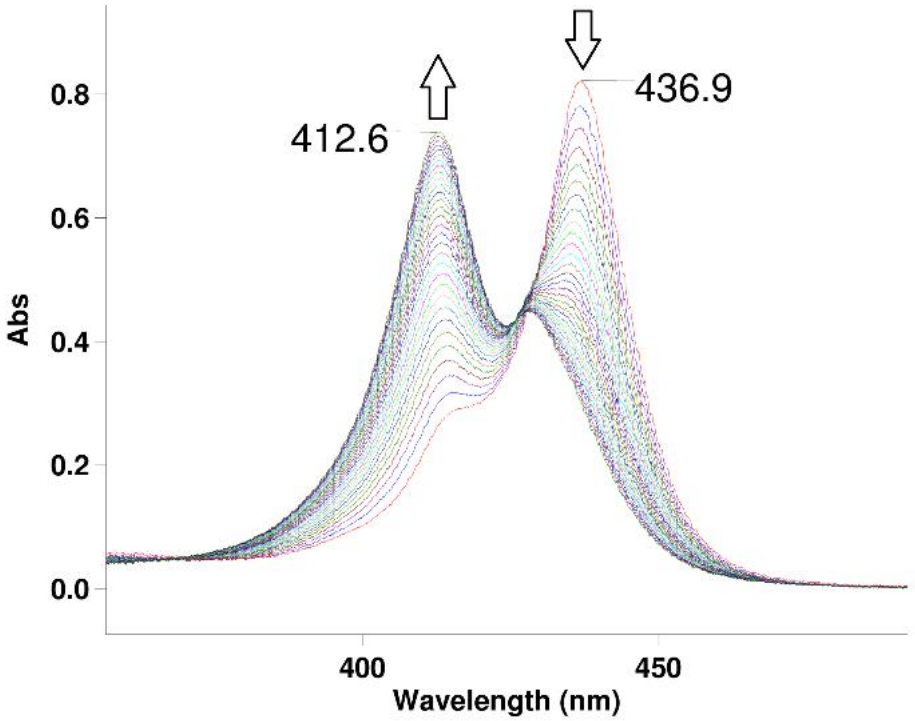

Figure 45. Time-resolved UV-Vis spectra of TPPCoCl in pure propylene oxide.

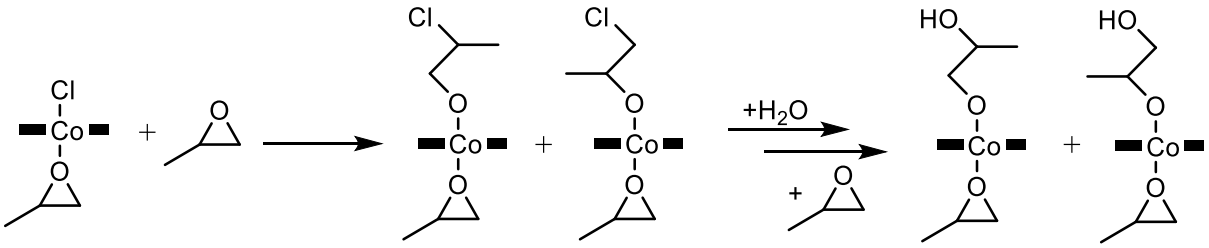

Scheme 39. PO ring opening catalysed by TPPCoCl.

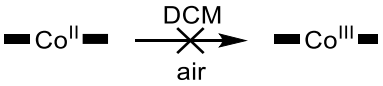

Scheme 40. TPPCo(II) shows no oxidation to TPPCo(III) in a DCM solution under air atmosphere.

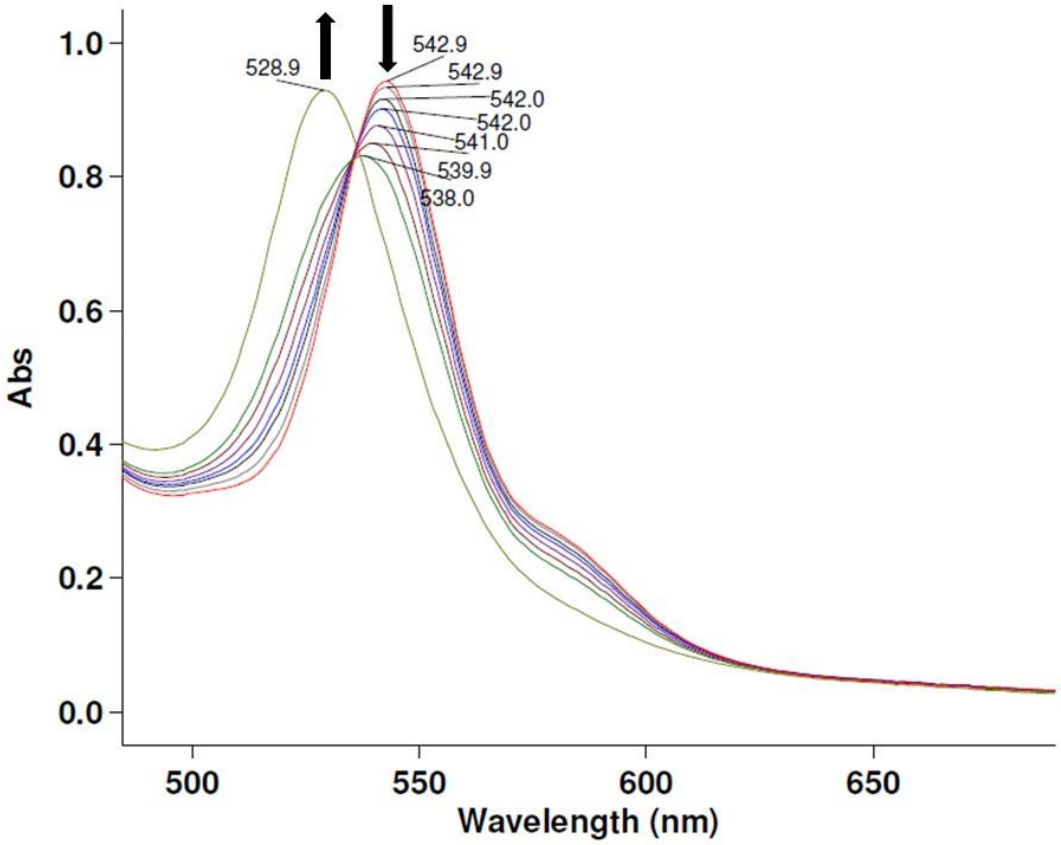

Figure 46. UV-Vis spectum of TPPCoCl+PPNCl (1 eq.) in pure PO (0.75 mM).

The reduction of TPPCo(III) to TPPCo(II) is also detected by ^{1}H NMR spectroscopy. Paramagnetic TPPCo(II) in a PO and CD_2Cl_2 solution shows two broad signals in the NMR spectrum of pyrrole-H and aromatic ortho-H at 13.48 and 10.37 ppm respectively and the aromatic meta, para-H peaks locate at 8.87 and 8.59 ppm (Figure A36). Slight shifts of these proton resonances, compared with literature[93] are found probably due to PO coordination.

A series of ^{1}H NMR measurements is carried out at room temperature for TPPCoCl (5 mg) and PO (0.3 mL) in CD_2Cl_2 (0.5 mL). As shown in Figure 47, the reduction of TPPCo(III) to TPPCo(II) takes place and the initial reaction rate is calculated to be 0.98 mM/h in CD_2Cl_2.

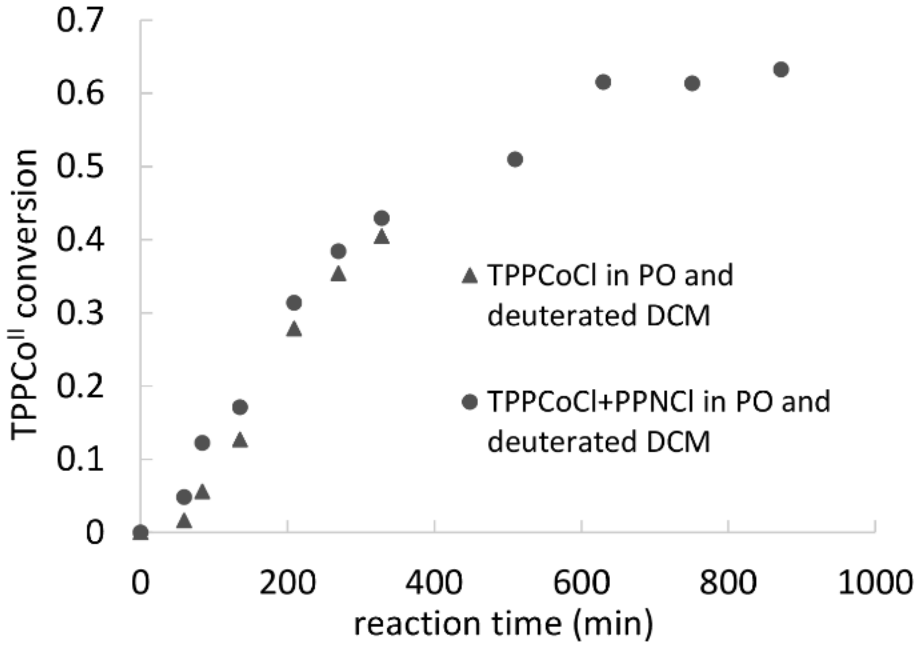

Figure 47. The reduction of TPPCoCl in PO and CD_2Cl_2 mixture in the absence and presence of PPNCl as detected by ^1H NMR spectroscopy.

Upon the addition of 0.3 equivalent of PPNCl (TPPCoCl (5 mg), PPNCl (0.3 eq.), PO (0.15 mL) in CD_2Cl_2), the reduction rate is not influenced as shown in Figure 47 (dots). A significant decrease in the rate of reduction is observed after the formation of TPPCo(II) reaches 60%. This phenomenon is explained by a saturation of the TPPCo(II) concentration and the further reaction leads to the precipitation of the product, which is not detectable by the solution NMR spectroscopy. Indeed, quantities of TPPCo(II) precipitate are found on the bottom of the NMR tube by performing an overnight reduction.

6.3 Reduction of Cobalt(III) Porphyrin Methoxide

Due to the fact that TPPCoCl is able to conduct the ring opening of PO, the reduction of TPPCo(III) to TPPCo(II) may take place via a cobalt(III) alkoxide intermediate. To prove this viewpoint, TPPCo(III)Cl (0.046 mg) is mixed with NaOMe (3000 eq.) in a DCM/MeOH solution (9/1) and as shown in Figure 48, the reduction of TPPCo(III) to TPPCo(II) takes place in the absence of PO (Scheme 41). The initial reaction rate is calculated to be 5.1×10^{-7} M/h (Figure A37, A38).

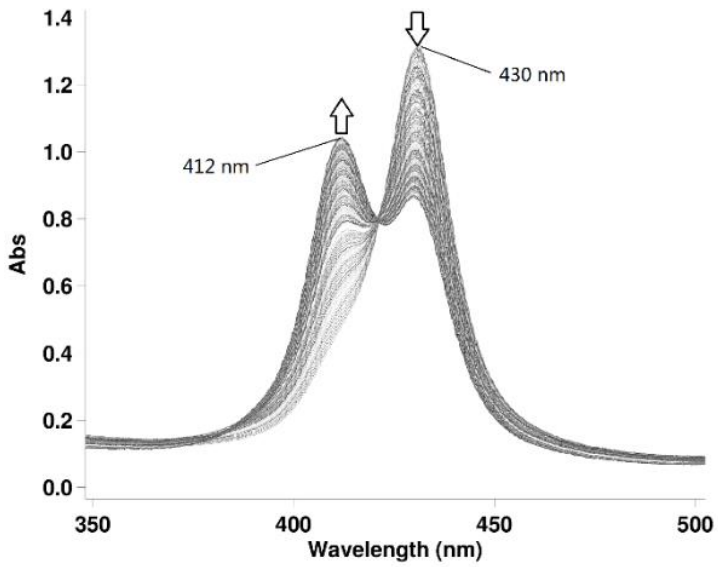

Figure 48. UV-Vis spectrum of TPPCoCl (1eq.)+NaOMe (3000 eq.) in DCM/MeOH (9 mL/1mL).

Therefore, the reduction of TPPCo(III)Cl in propylene oxide to TPPCo(II) presumably proceeds via the ring opening of PO by TPPCoCl to afford cobalt(III) porphyrin alkoxides. These species undergo a slow autoreduction to produce TPPCo(II) as illustrated in Scheme 42. Although cobalt(III) porphyrin complexes are known to be reduced to cobalt(II) species in the presence of certain ligands such as hydroquinone dianions[105] and methyl-piperidine,[104] the reduction of cobalt(III) porphyrin alkoxides has not been reported before.

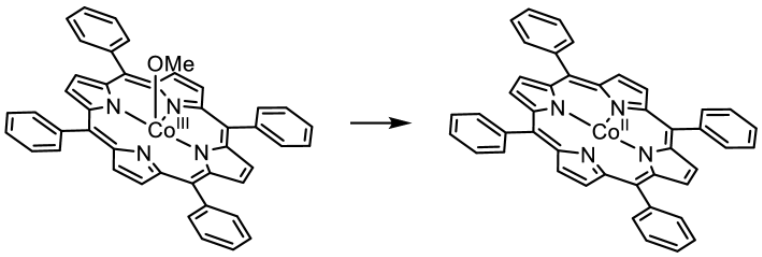

Scheme 41. The reduction of TPPCo(III) to TPPCo(II) in the presence of the methoxide anion.

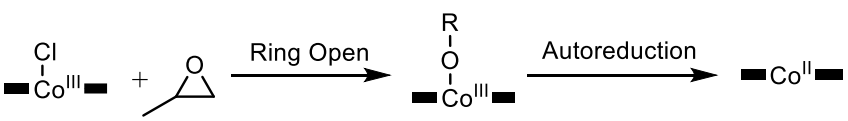

Scheme 42. A proposed pathway of TPPCo(III)Cl reduction in PO.

Further, the reaction order in the cobalt(III) porphyrin complex is explored by varying the initial TPPCoCl concentration monitored by UV-Vis spectroscopy. Prior to the reduction, an induction period with a continuous decrease of the intensity of TPPCo(III) Soret band (430 nm) is observed (Figure 49). This is probably due to the axial ligand exchange on the cobalt(III) porphyrin species. The duration of such an induction has a correlation with the concentration of TPPCoCl. The double logarithmic plot of the TPPCoCl concentration versus the initial reduction rate shows a good linear fit with a slope of 0.95 (Figure 50), suggesting a pseudo-first order in TPPCoCl. This value supports the view that the reduction may proceed via an electron transfer from the methoxide anion to the TPPCo(III) cation.

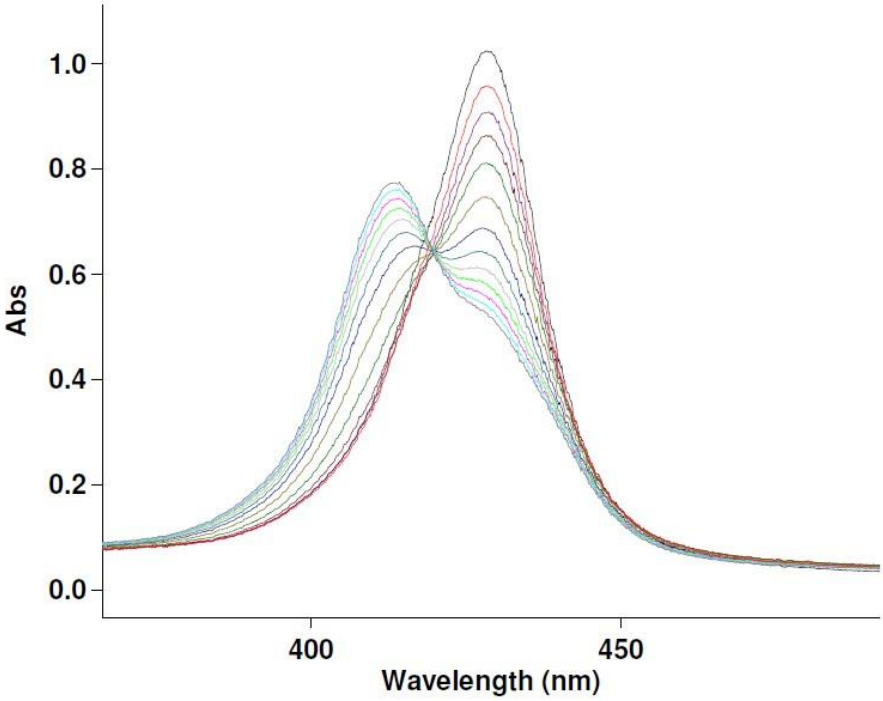

Figure 49. Time-resolved UV-Vis spectra of TPPCoCl (2.5×10^{-6} M) with NaOMe (3000 eq.) in a DCM/methanol (9/1) solution (interval: 1 h).

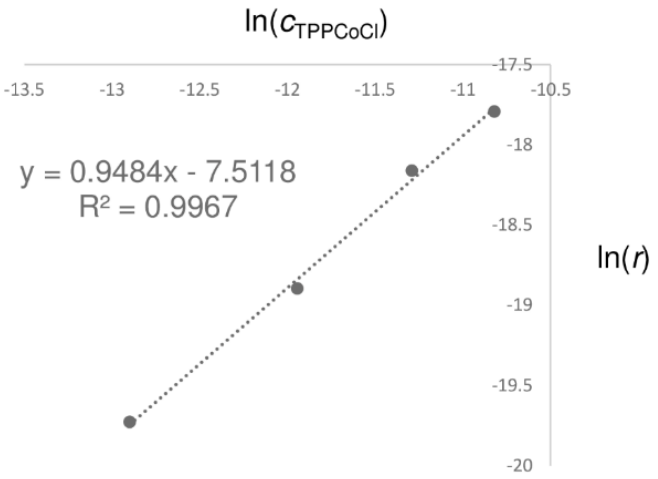

Figure 50. The double logarithmic plot of the TPPCoCl concentration versus the initial rate in its reduction with sodium methoxide.

In addition, such a reduction reaction is found to be reversible and the reaction direction is successfully switched by the presence or absence of light with the TPPCo(III) reduction under dark conditions (Figure A42). A possible explanation for such a phenomenon is that the reduction of TPPCoCl with sodium methoxide produces a methoxy radical which combines with each other to form a peroxide and the light induces the decomposition of this peroxide species to again form alkoxy radicals which react with TPPCo(II) to produce TPPCo(III)-OMe. Due to the lack of more evidences at the moment, this hypothesis remains disputable.

Interestingly, in the reaction system of TPPCoCl and PO, the formation of acetaldehyde is detected by ^{1}H NMR spectroscopy along with the catalyst reduction (Figure A40, A41). This unexpected side product is considered to be produced via a β-fragmentation of the alkoxy radicals.[109-113]

6.4 Reduction of cobalt(III) porphyrin complexes in the presence of propylene oxide and CO_2

The reduction of cobalt(III) porphyrin catalysts in propylene oxide is subsequently tested in the presence of CO_2. Since the TPPCo(III)Cl-catalysed copolymerisation of PO and CO_2 requires the presence of a co-catalyst, the capability of the CO_2 insertion into the initially formed

cobalt(III) alkoxide species in the absence of a co-catalyst is thus questioned. A series of IR measurements is conducted for TPPCoCl in pure propylene oxide (PO:TPPCoCl=2000:1) under 10 bar CO_2 pressure by using a self-made pressure cuvette and the C=O-stretching band of poly(propylene carbonate) at 1748 cm^{-1} increases with time, indicating the CO_2 insertion into TPPCo-alkoxides is feasible in the absence of a co-catalyst (Figure 51). After a 17-hour reaction, a C=O-stretching band at 1810 cm^{-1} is found in the spectrum which is attributed to the formation of cyclic carbonate.

A calibration is carried out with pure poly(propylene carbonate) in propylene oxide and the rate for the CO_2 insertion under 10 bar CO_2 pressure is then calculated to be 0.15 mole/(mole catalyst·h) which is extremely slow.

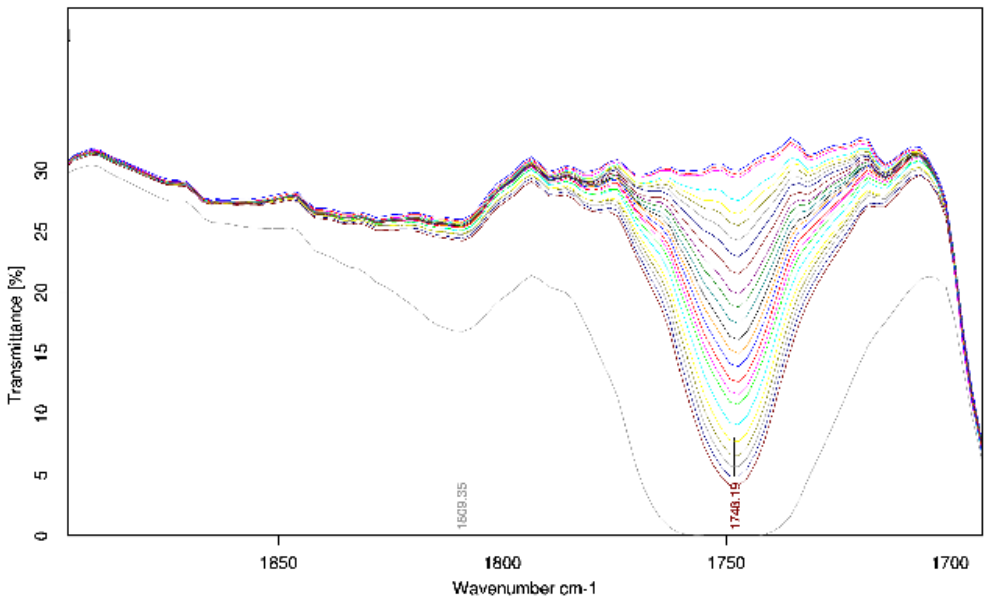

Figure 51. The IR spectrum collected *in situ* for the copolymerisation of PO/CO_2 catalysed by TPPCoCl (PO:TPPCoCl=2000:1, 10 bar CO_2, 25 ^oC).

If the copolymerisation of PO and CO_2 by using TPPCoCl as the catalyst in the presence of PPNCl is performed and monitored by *in-situ* IR spectroscopy, the obtained graphic of the poly(propylene carbonate) formation versus the reaction time shows only a very slight decrease in the polymerisation rate even after a 16-hour reaction as illustrated in Figure A39. This observation indicates that the reduction of TPPCo(III)Cl is efficiently inhibited under such

conditions. The formation of the carbonate chain end may account for such a protection of the catalyst during polymerisation (Scheme 43).

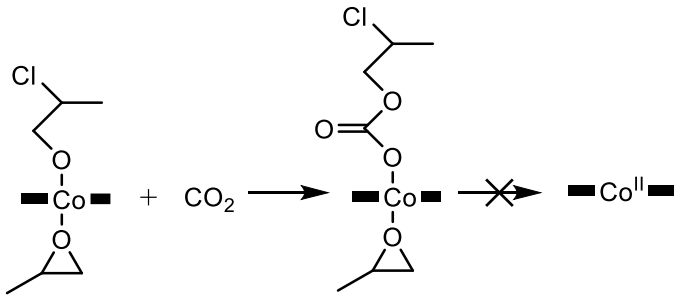

Scheme 43. CO_2 insertion into the Co-alkoxide bond prevents the catalyst from deactivation.

7. Experimental Section

Methods and Materials. Most of the experiments were carried out under Argon protection using standard Schlenk techniques unless otherwise stated. All commercially available chemicals were handled as received without further purification unless otherwise stated. Propylene oxide and triethylamine were distilled from calcium hydride prior to use and stored under Argon protection.

Solution NMR spectra were recorded using a Bruker AVIII-300 spectrometer. The reference for NMR spectra was determined by the solvent residue peaks. Mass spectra were collected on a Varian LC-MS 500 (50−2000 Da). GPC measurements were performed using a PolymerLaboratoriesGPC50 Plus chromatograph (carlibrated with polystyrene standards) at 35 °C with THF as eluent. UV-visible spectra were collected from a Varian 50 Scan UV−visible spectrophotometer. Elemental analysis was carried out at the microanalytic laboratory of the Department of Inorganic Chemistry at the Technical University of Munich. Single crystal X-ray diffraction was performed at Department of Inorganic Chemistry at TUM.

Synthesis of 5-(4-nitrophenyl)-10,15,20-triphenyl-21H,23H-Porphine (TPP-NO_2). This procedure is modified from the literature route.[114] 4-nitrobenzaldehyde (1 g, 6.617 mmol, 1 eq.), benzaldehyde (2 mL, 19.676 mmol, 3 eq.) and pyrrole (1.9 mL, 26.469 mmol, 4 eq.) were dissolved in 500 mL dry dichloromethane in a 1 L Schlenk flask, and the solution was stirred under Argon protection for ca. 5 min. Small amount of boron trifluoride diethyl etherate (0.1 mL, 0.796 mmol) was then added and the color of the reaction system gradually became dark purple. The mixture was continuously stirred at room temperature for 1 h. After the addition of DDQ (4.4 g, 19.38 mmol), the black purple mixture was stirred for another 1 h and then filtered under vacuum. The filter cake was washed three times wash with DCM, and the collected filtration solution was dried under vacuum. Column chromatography (dcm/hexane=1/1), and the desired product came out as the second eluate. (yield 12%).

^{1}H NMR ($CDCl_3$, 300 MHz, 25 ^{o}C, δ (ppm)): 8.87 (d, 2H, pyrrole-β-H), 8.85 (s, 4H, pyrrole-β-H), 8.72 (d, 2H, pyrrole-β-H), 8.60 (d, 2H, nitrophenyl-H), 8.37 (d, 2H, nitrophenyl-H), 8.19 (d, 6H, phenyl-o-H), 7.76 (m, 9H, phenyl-m, p-H), -2.80 (s, 2H, NH).

Mass (ESI$^+$) *m/z* 659.8 $[M]^+$, 681.7 $[M+Na]^+$.

UV-Vis (DCM+THF, nm): 418.0, 449.1, 515.0, 551.0, 591.1, 661.0.

Synthesis of 5-(4-aminophenyl)-10,15,20-triphenyl-21H,23H-Porphine (TPP-NH_2).[114] In a 500 ml flask were added TPP-NO_2 (0.97 g, 1.470 mmol, 1 eq.) and 100 mL concentrated hydrochloric acid aqueous solution, and the green suspension was heated up to 70 ^oC. After the addition of tin(II) chloride dihydrate (1.33 g, 5.879 mmol, 4 eq.), the mixture was stirred at 70 ^oC for 0.5 h. Ice bath was used to cool down the reaction system to 0 ^oC, followed by slow addition of ammonium aqueous solution until neutral. As long as the suspension turned purple, the solid crude product was isolated through filtration and washed with water (5×20 mL), air dry. After redissolved in DCM, The purple solution was washed again with water three times in a separation funnel and dried over sodium sulfate. The desired product was obtained as a purple solid (yield: 86%).

^1H NMR ($CDCl_3$, 300 MHz, 25 ^oC, δ (ppm)): 8.92 (d, 2H, pyrrole-β-H), 8.82 (s, 6H, pyrrole-β-H), 8.19 (d, 6H, phenyl-o-H), 7.97 (d, 2H, aminophenyl-H), 7.75 (m, 9H, phenyl-m, p-H), 7.04 (d, 2H, aminophenyl-H), 4.01 (s, 2H, NH_2), -2.77 (s, 2H, NH).

Mass (ESI^+) *m/z* 629.9 $[M]^+$.

UV-Vis (DCM+THF, nm): 418.9, 454.0, 515.0, 553.0, 593.0, 684.9.

General procedure for the preparation of amide side group porphyrin ligands of 1-3.[81] To 50 mL dry dichloromethane in a 100 mL Schlenk flask were added TPP-NH_2, carbonyl chloride substituted benzene and 0.2 mL triethylamine. The solution was kept stirring at room temperature overnight. After removing all the volatiles under vacuum, column chromatography and recrystallization, the catalyst ligands were obtained as a purple solid.

N-[4-(10,15,20-triphenyl-21H,23H-porphin-5-yl)phenyl]-Benzamide. TPP-NH_2, 0.2 g, 0.318 mmol; benzoyl chloride, 0.11 mL, 0.954 mmol. Yield: 50%.

^1H NMR (DMSO-d_6, 300 MHz, 25 ^oC, δ (ppm)): 10.73 (s, 1H, CO-NH), 8.92 (d, 2H, pyrrole-β-H), 8.83 (m, 6H, pyrrole-β-H), 8.10-8.29 (m, 12H, porphyrin-phenyl-o-H, porphyrin-benzamidophenyl-o, m-H, *N*-phenylcarbamoylphenyl-o-H), 7.85 (m, 9H, porphyrin-phenyl-m, p-H), 7.66 (m, 3H, N-phenylcarbamoylphenyl-m, p-H), -2.92 (s, 2H, pyrrole-NH).

^{13}C NMR (DMSO- d_6, 75.5 MHz, 25 ^oC, δ (ppm)): 166.1, 141.3, 139.3, 136.4, 135.2, 134.7, 134.3, 128.6, 128.2, 127.9, 127.1, 120.1, 120.0, 118.7.

UV-Vis (DCM+DMSO, nm): 419.1, 515.0, 551.0, 592.0, 648.0.

Anal. Calcd for $C_{51}H_{35}N_5O$: C, 83.47; H, 4.81; N, 9.54. Found: C, 83.47; H, 4.97; N, 9.51.

N,N′-bis[4-(10,15,20-triphenyl-21H,23H-porphin-5-yl)phenyl]-1,3-Benzenedicarboxamide. TPP-NH_2, 0.2 g, 0.318 mmol; 1,3-Benzenedicarbonyl dichloride, 32.3 mg, 0.159 mmol. Yield: 48%.

^{1}H NMR (DMSO-d_6, 300 MHz, 25 ^{o}C, δ (ppm)): 10.99 (s, 2H, CO-NH), 8.95 (d, 4H, pyrrole-β-H), 8.84 (m, 13H, pyrrole-β-H, 1, 3-di-(*N*-phenylcarbamoyl)-phenyl-2-H), 8.23-8.41 (m, 22H, porphyrin-phenyl-o-H, porphyrin-benzamidophenyl-o, m-H, 1, 3-di-(*N*-phenylcarbamoyl)-phenyl-4, 6-H), 7.85 (m, 19H, porphyrin-phenyl-m, p-H, 1, 3-di-(N-phenylcarbamoyl)-phenyl-5-H), -2.90 (s, 4H, pyrrole-NH).

UV-Vis (DCM+DMSO, nm): 419.1, 515.0, 551.0, 590.9, 647.0.

Anal. Calcd for $C_{96}H_{64}N_{10}O_2$: C, 82.98; H, 4.64; N, 10.08. Calcd for $C_{96}H_{64}N_{10}O_2$+H_2O: C, 81.91; H, 4.73; N, 9.95. Found: C, 81.72; H, 4.75; N, 9.99.

N,N′,N′′-tris[4-[10,15,20-triphenyl-21H,23H-porphin-5-yl]phenyl]-1,3,5 Benzenetricarboxamide. TPP-NH_2, 0.2 g, 0.318 mmol; 1,3,5-Benzenetricarbonyl trichloride, 28.1 mg, 0.106 mmol. Yield: 31%.

^{1}H NMR (DMSO-d_6, 300 MHz, 25 ^{o}C, δ (ppm)): 11.27 (s, 3H, CO-NH), 9.14 (s, 3H, 1,3,5-tri-(N-phenylcarbamoyl)-phenyl-H), 8.98(d, 6H, pyrrole-β-H), 8.85 (m, 18H, pyrrole-β-H), 8.23-8.45 (m, 30H, porphyrin-phenyl-o-H, porphyrin-benzamidophenyl-o, m-H), 7.85 (m, 27H, porphyrin-phenyl-m, p-H), -2.89 (s, 6H, pyrrole-NH).

^{13}C NMR (DMSO- d_6, 75.5 MHz, 25 ^{o}C, δ (ppm)): 165.2, 141.3, 141.2, 136.8, 135.9, 134.9, 134.3, 128.2, 127.1, 120.1, 120.0, 119.9, 118.8.

UV-Vis (DCM+DMSO, nm): 419.1, 515.9, 551.0, 590.9, 648.0.

Anal. Calcd for $C_{141}H_{93}N_{15}O_3$: C, 82.80; H, 4.58; N, 10.27. Calcd for $C_{141}H_{93}N_{15}O_3$+$3H_2O$: C, 80.67; H, 4.75; N, 10.01. Found: C, 80.95; H, 4.81; N, 9.76.

General procedure for the metallation and oxidation of porphyrin ligands.

Preparation of Co(II) porphyrin.[115] Porphyrin ligand was dissolved in 30 mL DMF in a 250 mL flask, and heated up to 110 ^{o}C. Cobalt (II) acetate tetrahydrate was then added as a solid, and

the reaction system was stirred under 110 °C for half an hour (the transformation from free porphyrin to Co(II) porphyrin was monitored by UV-Vis spectroscopy).

Oxidation of Co(II) porphyrin to Co(III) chloride porphyrin. After the metalation, DMF was removed under vacuum and the solid was allowed to cool down to room temperature and used directly for the oxidation reaction. 200 mL MeOH was then added together with 5 mL concentrated hydrochloric acid aqueous solution, and the reaction mixture was stirred under room temperature overnight. After the remove of the MeOH under vacuum, the remaining aqueous suspension was filtered under vacuum and the filter cake was washed with water (2×20mL), saturated sodium hydrogen carbonate aqueous solution (2×20mL), and again water (5×20mL). The filter cake was dissolved in DCM, and dried over sodium sulfate anhydrous powder. After recrystallization, the desired product was obtained as a purple solid. The yield was calculated as an overall value for both metallation and oxidation reaction.

Amide side chain monoporphyrin cobalt(II). Porphyrin ligand, 200 mg, 0.273 mmol, $Co(OAc)_2 \cdot 4H_2O$, 101.8 mg, 0.409 mmol.

Amide side chain monoporphyrin cobalt(III) chloride (1). Yield: 75%.

^1H NMR (THF-d_8, 300 MHz, 25 °C, δ (ppm)): 9.76 (s, 1H, CO-NH), 9.11 (d, 2H, pyrrole-β-H), 9.02 (m, 6H, pyrrole-β-H), 8.05-8.22 (m, 12H, porphyrin-phenyl-o-H, porphyrin-benzamidophenyl-o, m-H, *N*-phenylcarbamoylphenyl-o-H), 7.76 (m, 9H, porphyrin-phenyl-m, p-H), 7.56 (m, 3H, N-phenylcarbamoylphenyl-m, p-H).

^{13}C NMR (THF- d_8, 75.5 MHz, 25 °C, δ (ppm)): 166.6, 145.9, 145.7, 143.4, 140.8, 138.3, 137.1, 135.2, 135.0, 134.7, 134.5, 132.3, 129.3, 128.7, 128.6, 127.8, 121.3, 119.1.

UV-Vis (DCM+DMSO, nm): 435.1, 550.0.

Anal. Calcd for $C_{51}H_{33}N_5OCoCl$: C, 74.14; H, 4.03; N, 8.48. Calcd for $C_{51}H_{33}N_5OCoCl+2H_2O$: C, 71.04; H, 4.33; N, 8.12. Found: C, 71.58; H, 4.21; N, 7.85.

Amide side chain bisporphyrin cobalt(II). Porphyrin ligand, 200 mg, 0.144 mmol, $Co(OAc)_2 \cdot 4H_2O$, 107.6 mg, 0.432 mmol.

Amide side chain bisporphyrin cobalt(III) chloride (2). Yield: 72%.

UV-Vis (DCM+DMSO, nm): 436.0, 550.0, 685.0 (broad).

Anal. Calcd for $C_{96}H_{60}N_{10}O_2Co_2Cl_2$: C, 73.24; H, 3.84; N, 8.90. Calcd for $C_{96}H_{60}N_{10}O_2Co_2Cl_2$+4$H_2O$: C, 70.03; H, 4.16; N, 8.51. Found: C, 69.90; H, 3.99; N, 8.26.

Amide side chain trisporphyrin cobalt(II). Porphyrin ligand, 200 mg, 0.098 mmol, $Co(OAc)_2 \cdot 4H_2O$, 109.6 mg, 0.440 mmol.

Amide side chain trisporphyrin cobalt(III) chloride (3). Yield: 70%.

UV-Vis (DCM+DMSO, nm): 434.0, 550.0.

Anal. Calcd for $C_{141}H_{87}N_{15}O_3Co_3Cl_3$: C, 72.92; H, 3.78; N, 9.05. Calcd for $C_{141}H_{87}N_{15}O_3Co_3Cl_3$+6$H_2O$: C, 69.68; H, 4.11; N, 8.64. Found: C, 67.50; H, 4.03; N, 8.33.

5,10,15,20-Tetraphenylporphyrin cobalt(II). 5,10,15,20-Tetraphenyl-21H,23H-porphine, 100 mg, 0.163 mmol, $Co(OAc)_2 \cdot 4H_2O$, 61.0 mg, 0.245 mmol.

5,10,15,20-Tetraphenylporphyrin cobalt(III) chloride. Yield: 82%.

^{1}H NMR (THF-d_8, 300 MHz, 25 ^{o}C, δ (ppm)): 9.02 (s, pyrrole-β-H, 8H), 8.20 (m, phenyl-o-H, 8H), 7.76 (m, phenyl-m, p-H, 12H).

^{13}C NMR (THF-d_8, 75.5 MHz, 25 ^{0}C, δ (ppm)): 135.1, 126.6, 125.4, 118.4, 115.6, 114.1, 113.8.

ESI-Mass m/z: 671.5 ($TPPCo^+$).

UV-Vis (DCM+DMSO, nm): 433.1, 548.0.

Anal. Calcd for $C_{44}H_{28}N_4CoCl$: C, 74.74; H, 3.99; N, 7.92. Found: C, 74.21; H, 4.04; N, 7.93.

Gerneral procedure for the copolymerisation reaction. The prepared catalyst and PPNCl were weighed and added into a dry 200 mL stainless steel autoclave followed by the addition of propylene oxide and dichloromethane using syringe under the protection of argon flow. The autoclave was then pressurized with CO_2 (and heated up to the required temperature in an oil bath if necessary). After the reaction was finished, the pressure was released slowly out of the autoclave. A small amount of reaction mixture was taken out for ^{1}H NMR spectroscopy analysis and the rest mixture dissolved in dichlorimethane followed by slow addition of hydrochloric acid methanolic solution (0.5 mol/L). The polymer precipitated out by adding excess of methanol, and the remaining impurity was removed by refluxing in chloroform solution with activated charchoal. After hot filtration, the colorless solution was dried under vacuum to obtain the pure poly(propylene carbonate).

8. Appendix

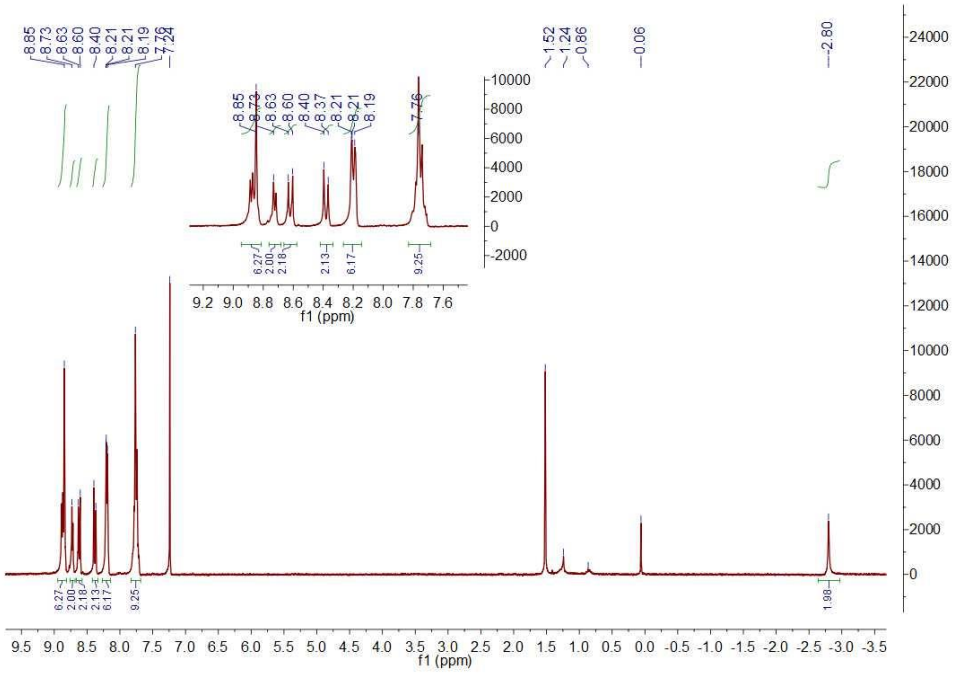

Figure A1. ^{1}H NMR spectrum of TPP-NO_2 ($CDCl_3$, 300 MHz, 25^{o}C).

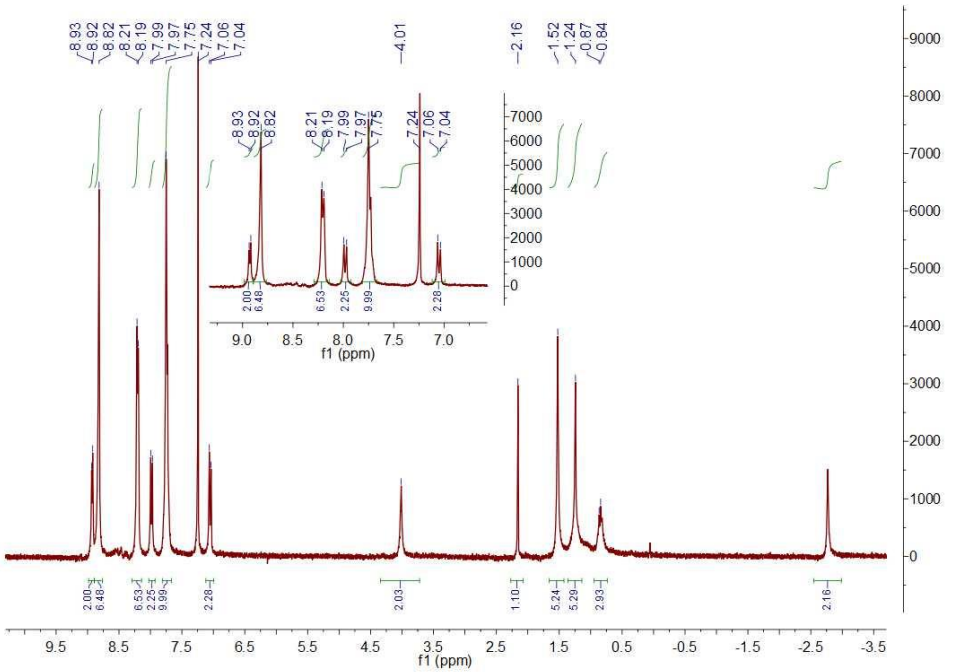

Figure A2. ^{1}H NMR spectrum of TPP-NH_2 ($CDCl_3$, 300 MHz, 25^{o}C).

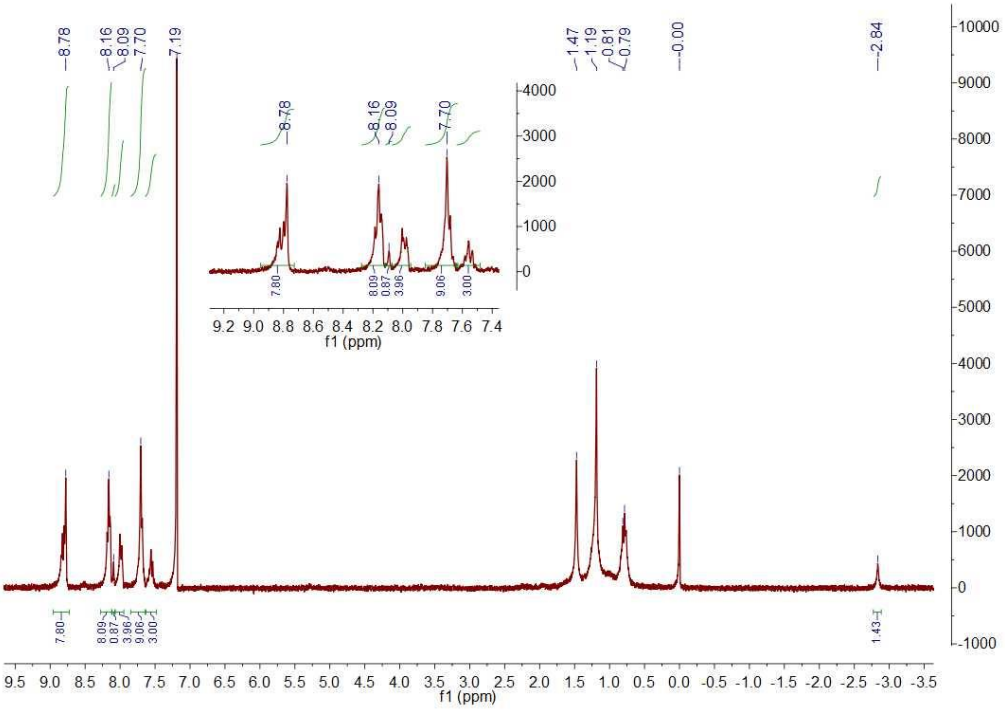

Figure A3. ^{1}H NMR spectrum of ligand of **1** ($CDCl_3$, 300 MHz, 25^{o}C).

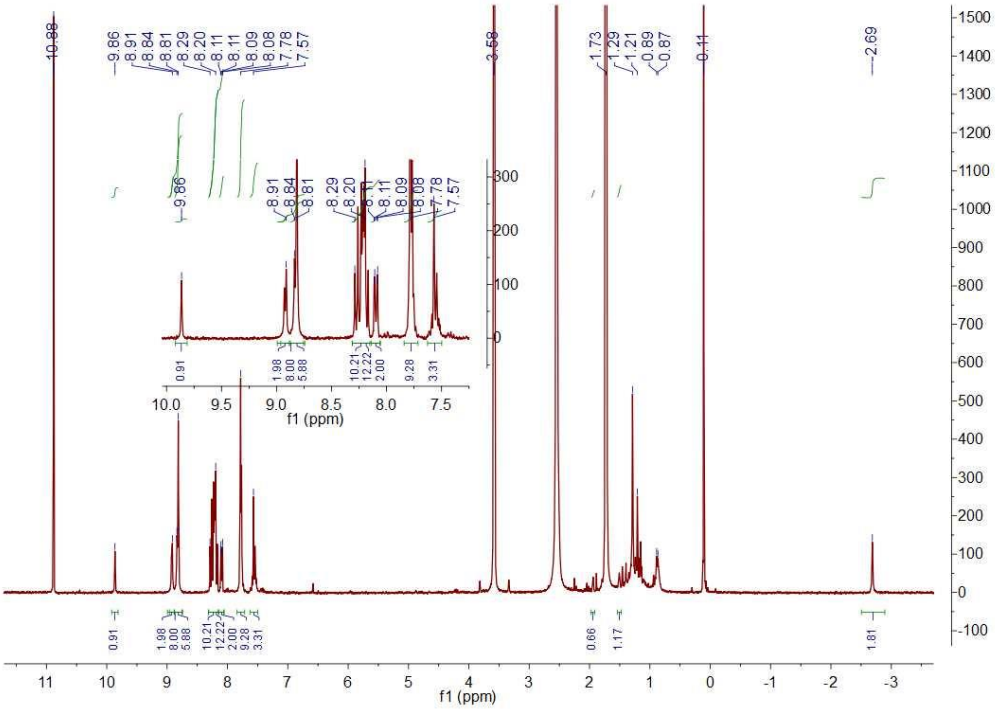

Figure A4. ^{1}H NMR spectrum of ligand of **1** (THF-d_8, 300 MHz, 25^{o}C).

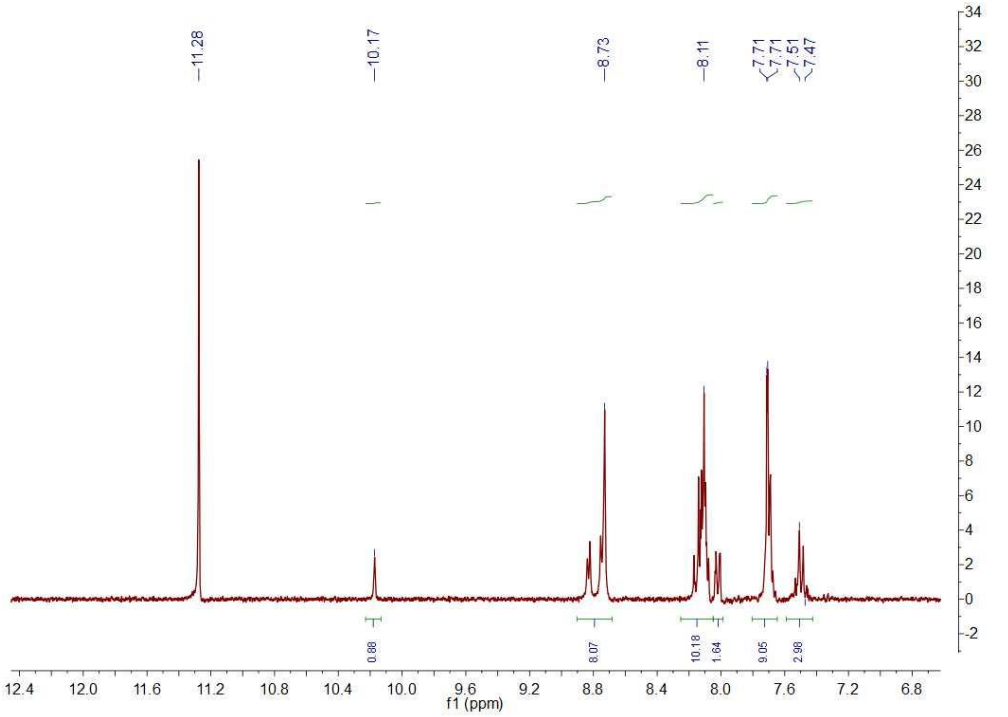

Figure A5. ^{1}H NMR spectrum of ligand of **1** (THF-d_8+MeOH, 300 MHz, 25^{o}C).

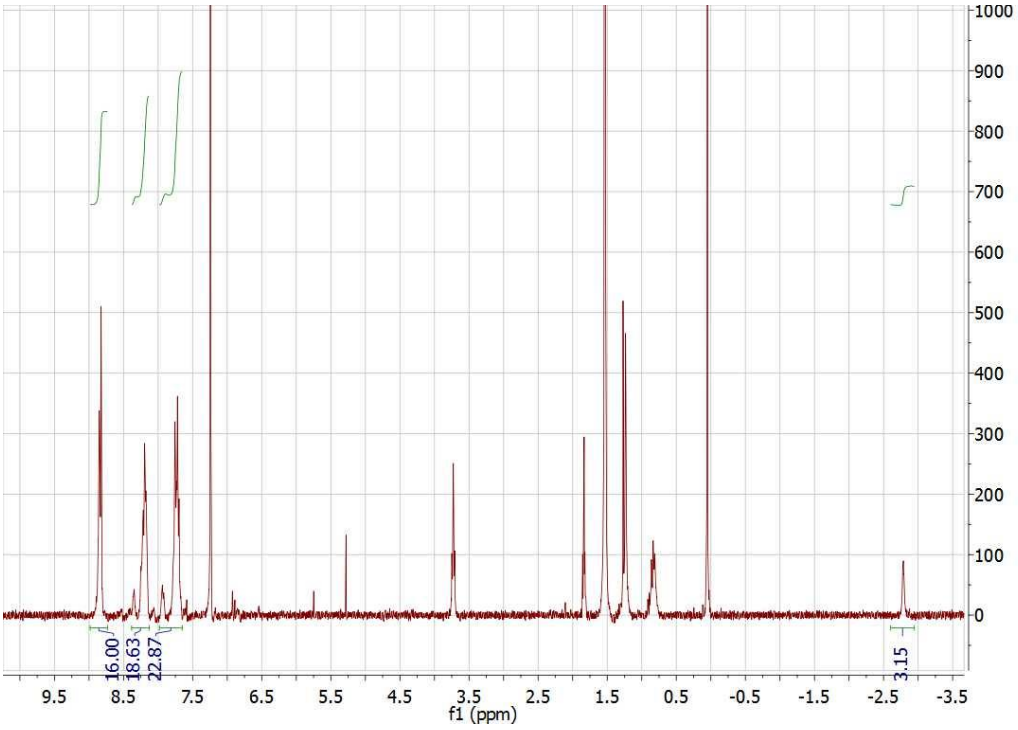

Figure A6. ^{1}H NMR spectrum of ligand of **2** ($CDCl_3$, 300 MHz, 25^{o}C).

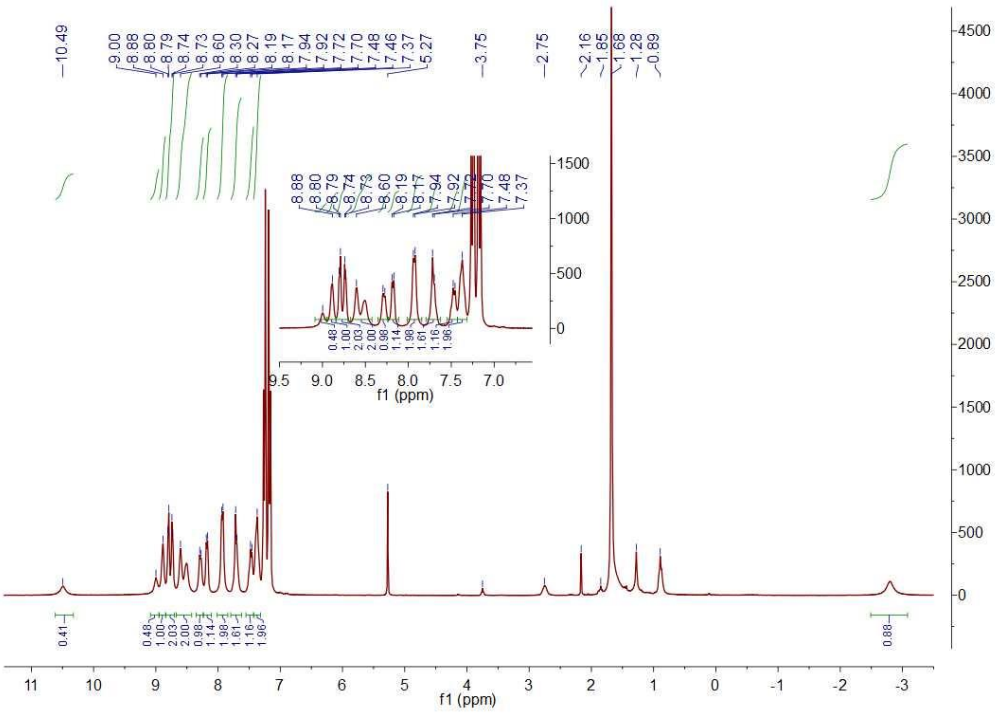

Figure A7. ^{1}H NMR spectrum of ligand of **3** ($CDCl_3$, 300 MHz, 25°C).

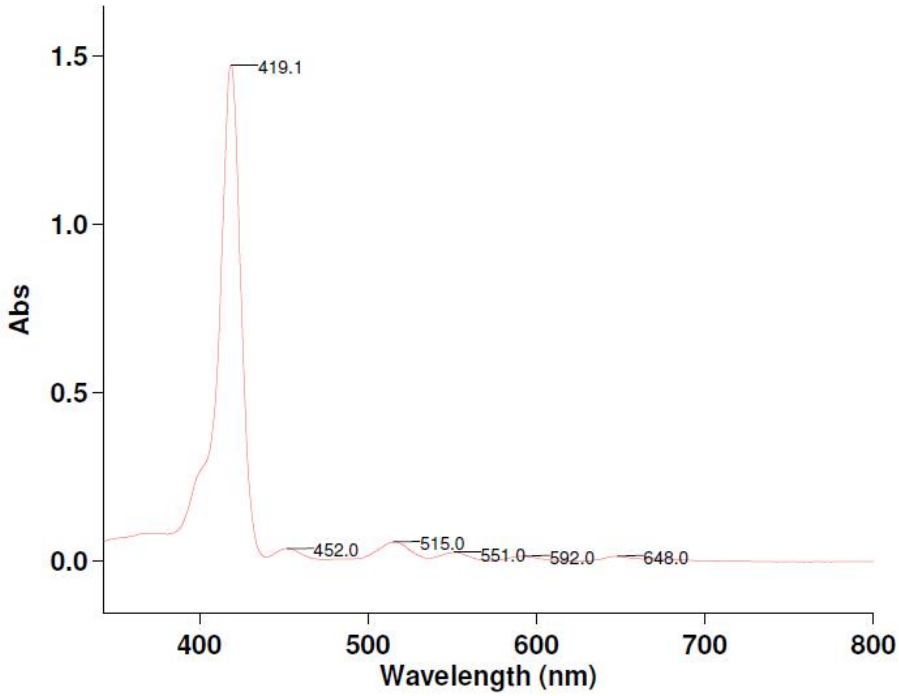

Figure A8. UV-Vis spectrum of ligand of **1** (DCM+DMSO).

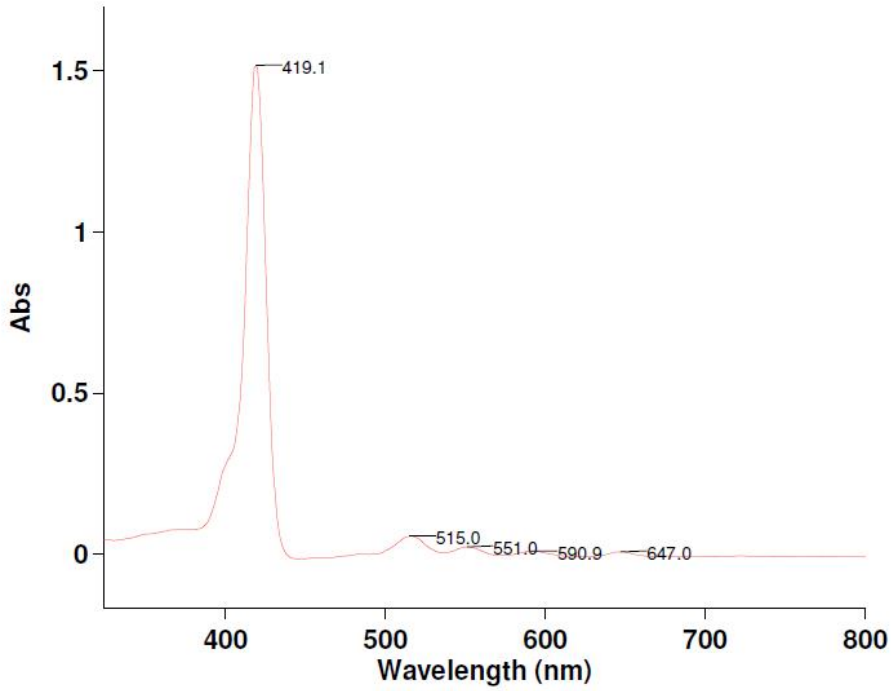

Figure A9. UV-Vis spectrum of ligand of **2** (DCM+DMSO).

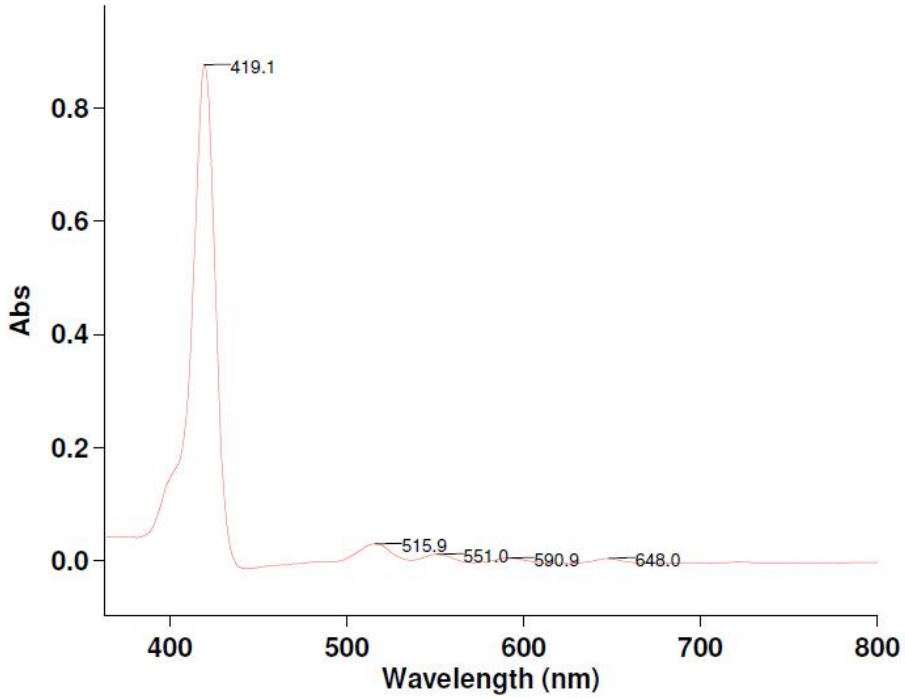

Figure A10. UV-Vis spectrum of ligand of **3** (DCM+DMSO).

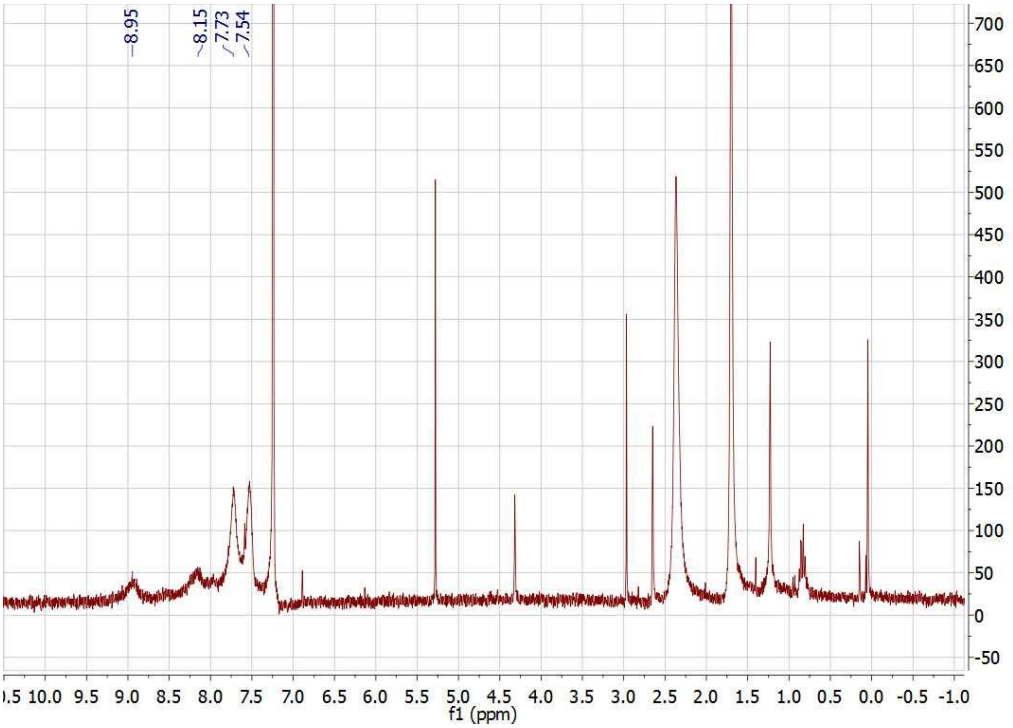

Figure A11. ^{1}H NMR spectrum of **1** ($CDCl_3$, 300 MHz, 25°C).

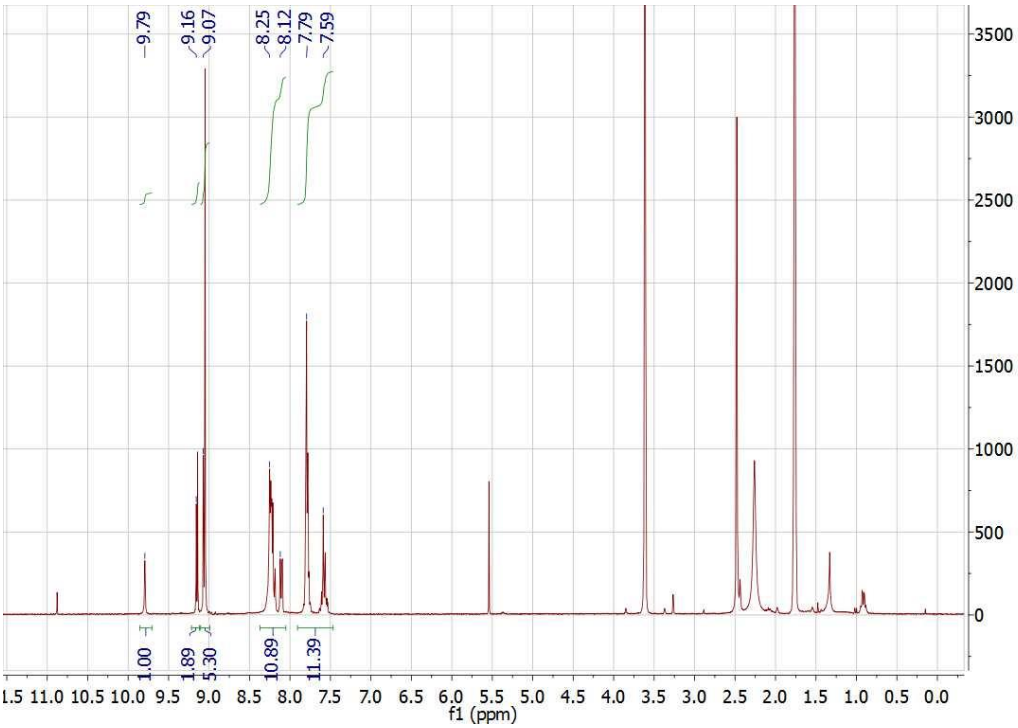

Figure A12. ^{1}H NMR spectrum of **1** (THF-d_8, 300 MHz, 25°C).

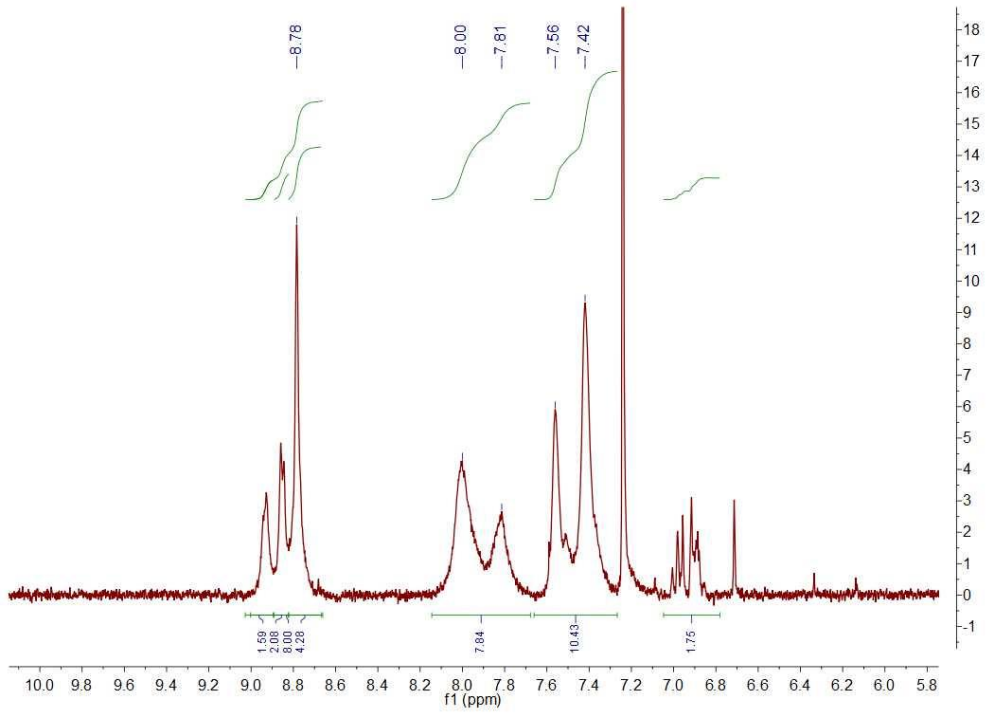

Figure A13. ^{1}H NMR spectrum of **2** ($CDCl_3$+THF, 300 MHz, 25^{o}C).

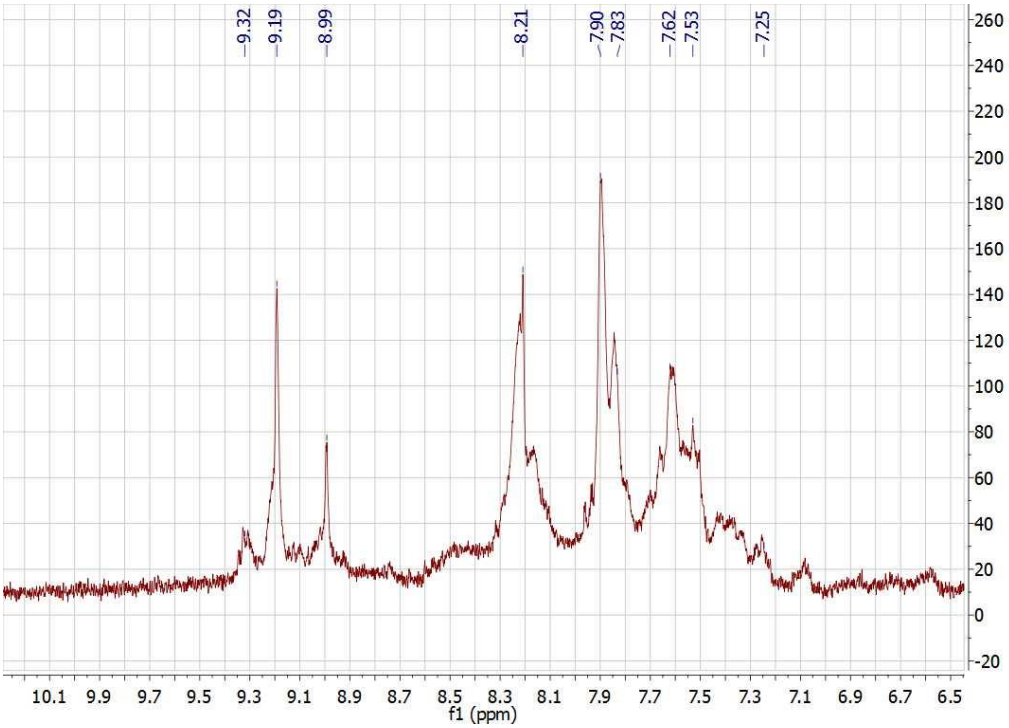

Figure A14. ^{1}H NMR spectrum of **3** (DMSO-d_6, 300 MHz, 25^{o}C).

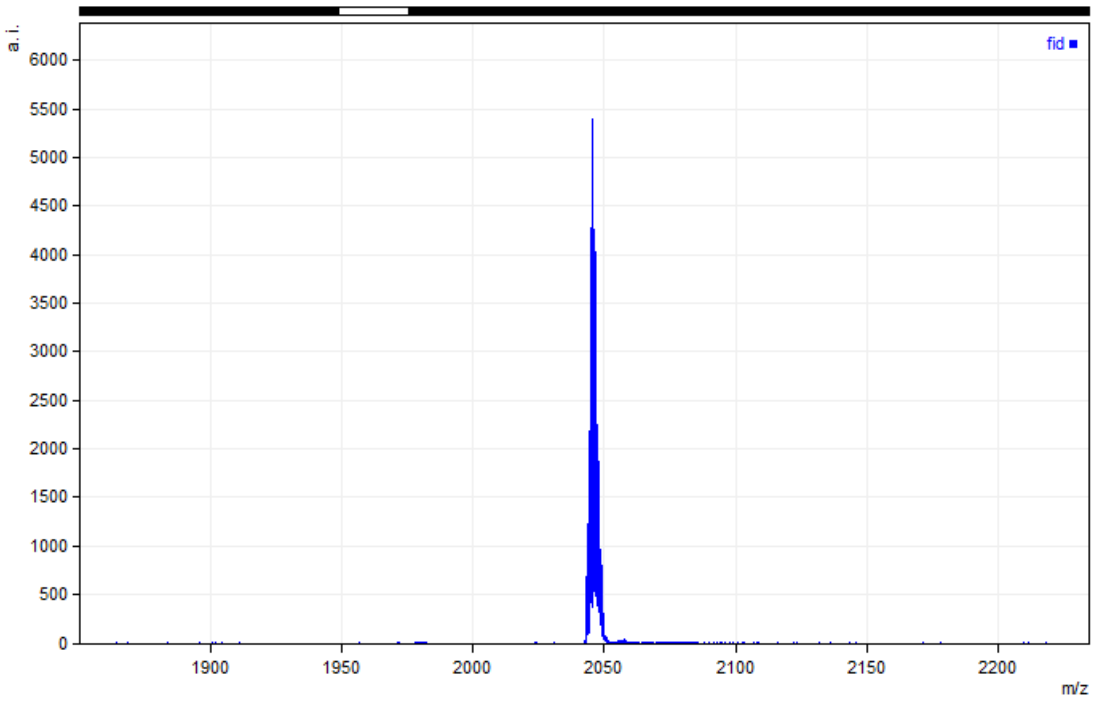

Figure A15. MALDI-TOF Mass spectrum of **3.**

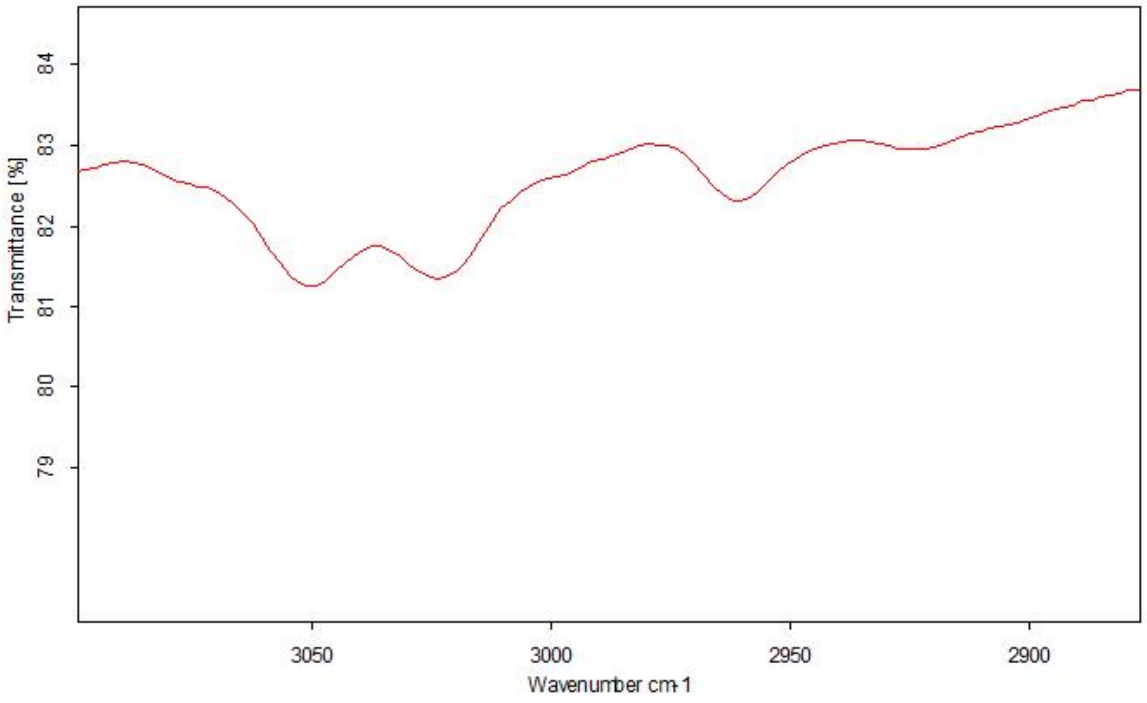

Figure A16. IR spectrum of **2** in solid state.

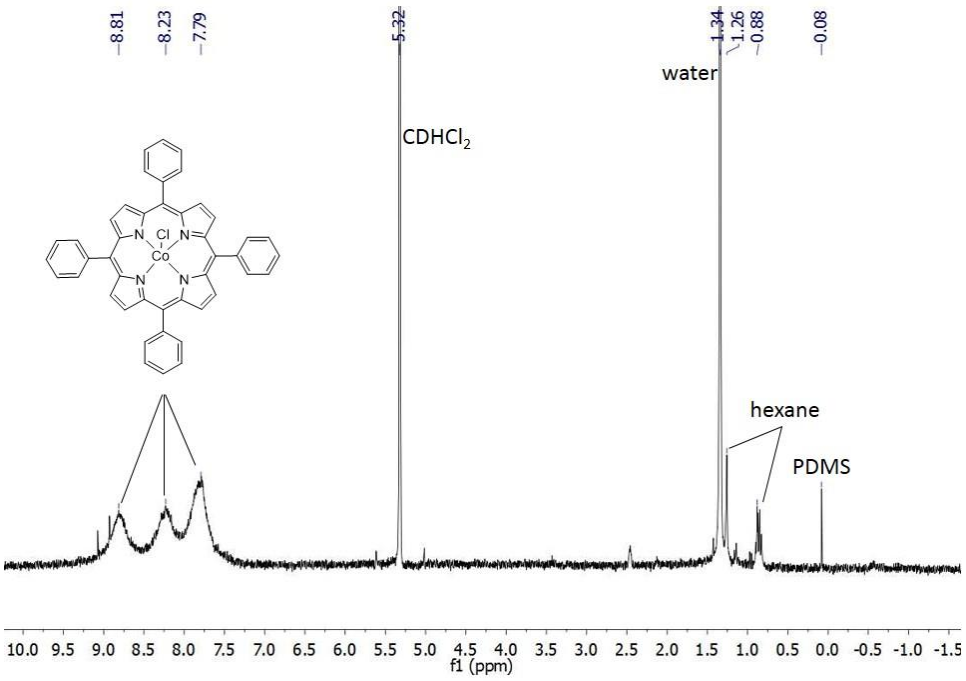

Figure A17. ^{1}H NMR spectrum of TPPCoCl (CD_2Cl_2, 300 MHz, 25 ^{0}C).

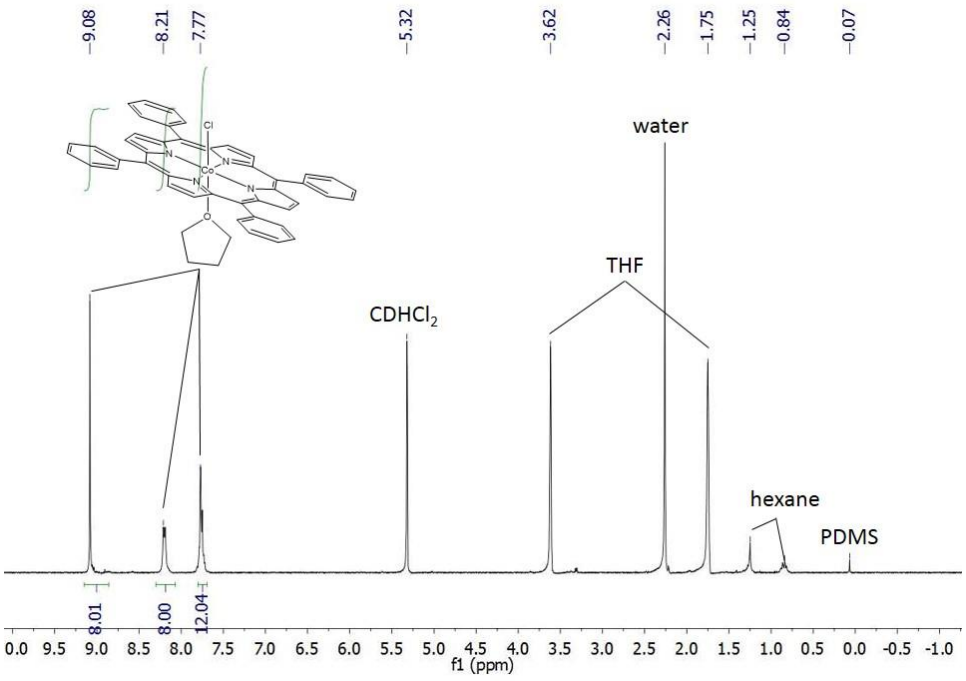

Figure A18. ^{1}H NMR spectrum of TPPCoCl (CD_2Cl_2+THF-d_8, 300 MHz, 25 ^{0}C).

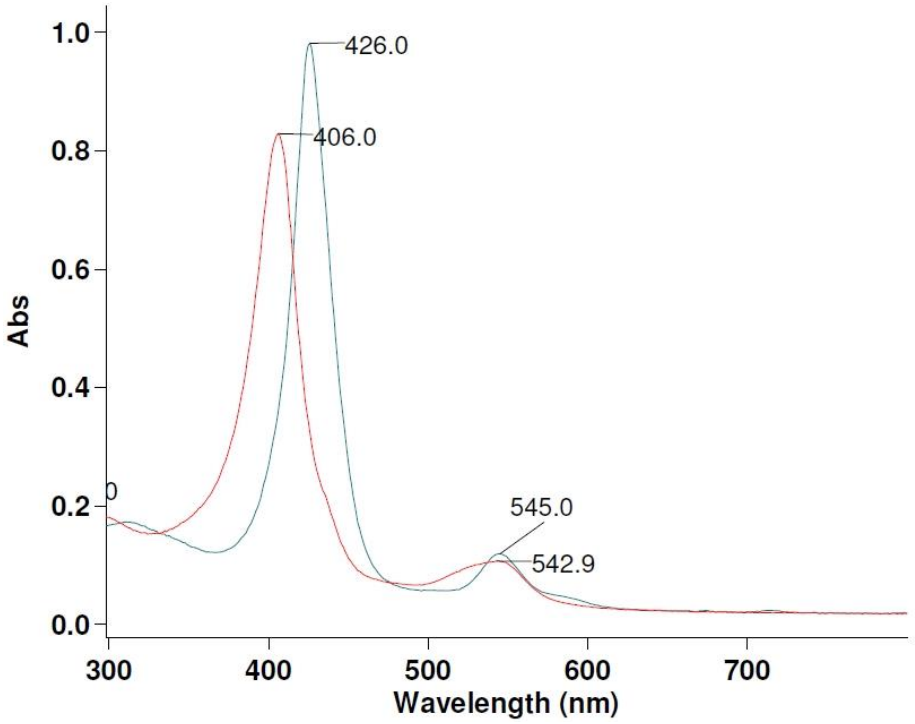

Figure A19. UV-Vis spectrum of TPPCoCl (300-800 nm, red curve: in DCM, blue curve: in DCM+THF).

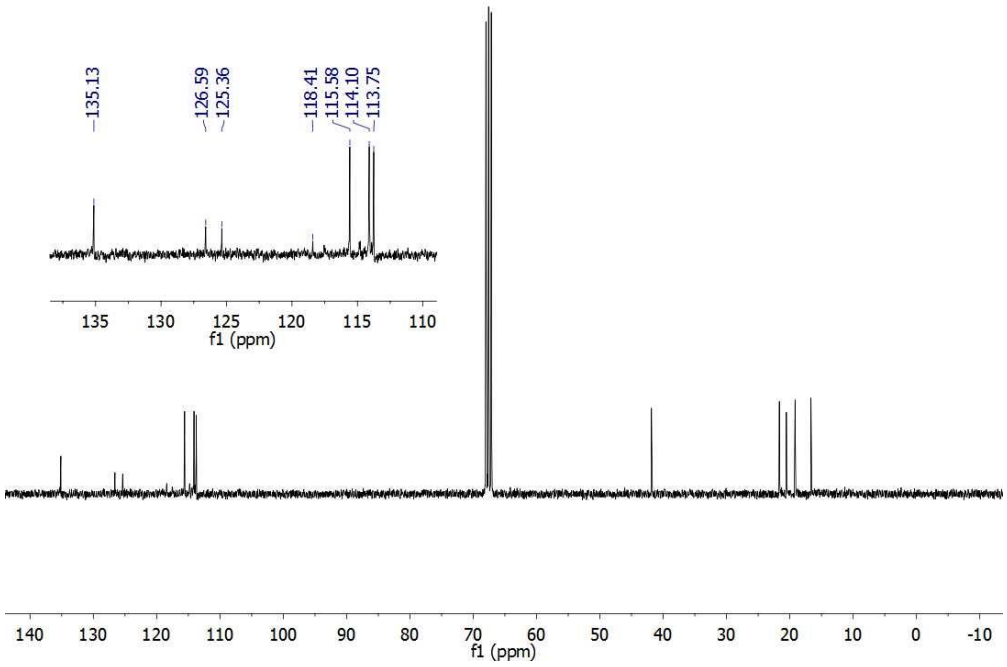

Figure A20. ^{13}C NMR spectrum of TPPCoCl (THF-d_8, 300 MHz, 25 ^{0}C).

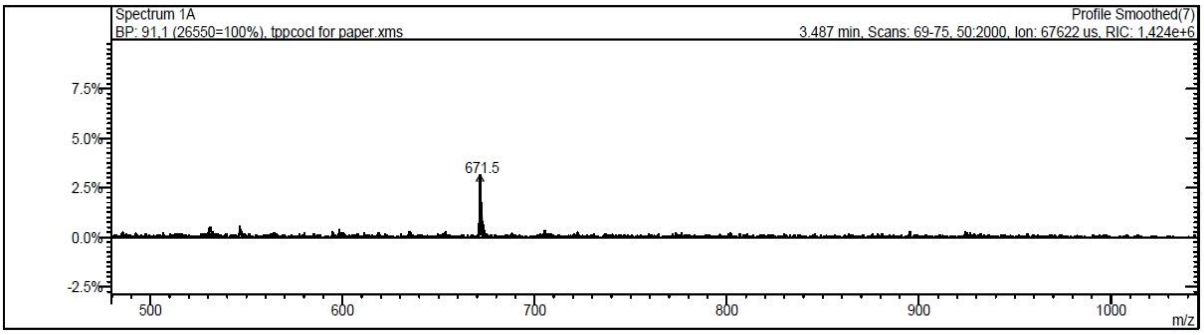

Figure A21. Mass spectrum of TPPCoCl.

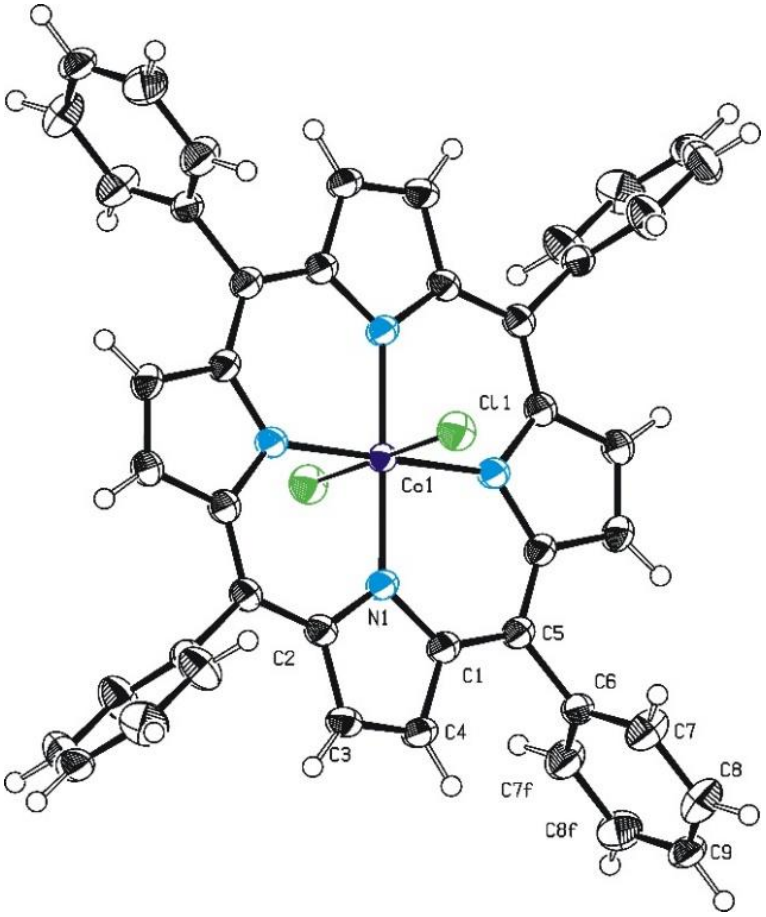

Figure A22. Unexpected TPPCoCl crystal structure showing extra chlorine binding on the cobalt centre (C_{44} H_{28} $Cl_{1.28}$Co N_4).

Table A1. Full crystal data of $TPPCoClC_3H_6O \cdot C_3H_6O$.

Formula	$C_{47}\ H_{34}\ Cl\ Co\ N_4\ O,\ C_3\ H_6\ O$
Formula Weight	823.24
Crystal System	Orthorhombic
Space group	Pbca (No. 61)
a, b, c [Angstrom]	11.7326(4) 23.1594(9) 29.3278(10)
alpha, beta, gamma [deg]	90 90 90
V [Ang**3]	7969.0(5)
Z	8
D(calc) [g/cm**3]	1.372
Mu(MoKa) [/mm]	0.545
F(000)	3424
Crystal Size [mm] 0.09 x 0.15 x 0.19	Crystal Size [mm] 0.09 x 0.15 x 0.19

Data Collection

Temperature (K)	123
Radiation [Angstrom]	0.71073
Theta Min-Max [Deg]	1.4, 25.4
Dataset	-14: 14 ; -27: 27 ; -35: 35
Tot., Uniq. Data, R(int)	151924, 7299, 0.055
Observed data [I > 2.0 sigma(I)]	5978

Refinement

Nref, Npar	7299, 527
R, wR2, S	0.0318, 0.0803, 1.04
w = 1/[\s^2^(Fo^2^)+(0.0268P)^2^+8.3257P] where P=(Fo^2^+2Fc^2^)/3	
Max. and Av. Shift/Error	0.00, 0.00
Min. and Max. Resd. Dens. [e/Ang^3]	-0.32, 0.33

Bond Length (Å)

Co1 -Cl1 2.2026(5)	C38 -C39 1.497(3)
Co1 -O1 2.0276(13)	C39 -C40 1.383(3)
Co1 -N1 1.9549(16)	C39 -C44 1.393(3)
Co1 -N2 1.9689(15)	C40 -C41 1.396(3)

Co1 -N3 1.9642(16)	C41 -C42 1.371(4)
Co1 -N4 1.9624(15)	C42 -C43 1.387(3)
O1 -C45 1.211(2)	C43 -C44 1.389(3)
N1 -C4 1.372(3)	C45 -C46 1.491(3)
N1 -C1 1.384(3)	C45 -C47 1.491(3)
N2 -C12 1.376(3)	
N2 -C15 1.376(3)	O2 -C48 1.196(4)
N3 -C26 1.371(2)	C48 -C49 1.479(6)
N3 -C23 1.380(3)	C48 -C50 1.479(6)
N4 -C34 1.383(2)	
N4 -C37 1.377(3)	C2 -H21 0.95
C1 -C38 1.383(3)	C3 -H31 0.95
C1 -C2 1.436(3)	C7 -H71 0.95
C2 -C3 1.340(3)	C8 -H81 0.95
C3 -C4 1.433(3)	C9 -H91 0.95
C4 -C5 1.391(3)	C10 -H101 0.95
C5 -C6 1.494(3)	C11 -H111 0.95
C5 -C12 1.391(3)	C13 -H131 0.95
C6 -C11 1.391(3)	C14 -H141 0.95
C6 -C7 1.399(3)	C18 -H181 0.95
C7 -C8 1.384(3)	C19 -H191 0.95
C8 -C9 1.386(3)	C20 -H201 0.95
C9 -C10 1.377(3)	C21 -H211 0.95
C10 -C11 1.391(3)	C22 -H221 0.95
C12 -C13 1.440(3)	C24 -H241 0.95
C13 -C14 1.349(3)	C25 -H251 0.95
C14 -C15 1.435(3)	C29 -H291 0.95
C15 -C16 1.391(3)	C30 -H301 0.95
C16 -C17 1.501(3)	C31 -H311 0.95
C16 -C23 1.385(3)	C32 -H321 0.95
C17 -C18 1.391(3)	C33 -H331 0.95
C17 -C22 1.384(3)	C35 -H351 0.95

C18 -C19 1.390(3)	C36 -H361 0.95
C19 -C20 1.375(3)	C40 -H401 0.95
C20 -C21 1.380(3)	C41 -H411 0.95
C21 -C22 1.394(3)	C42 -H421 0.95
C23 -C24 1.437(3)	C43 -H431 0.95
C24 -C25 1.347(3)	C44 -H441 0.95
C25 -C26 1.433(3)	C46 -H462 0.98
C26 -C27 1.396(3)	C46 -H463 0.98
C27 -C28 1.493(3)	C46 -H461 0.98
C27 -C34 1.389(3)	C47 -H472 0.98
C28 -C33 1.395(3)	C47 -H473 0.98
C28 -C29 1.393(3)	C47 -H471 0.98
C29 -C30 1.389(3)	
C30 -C31 1.379(3)	C49 -H491 0.98
C31 -C32 1.382(3)	C49 -H492 0.98
C32 -C33 1.386(3)	C49 -H493 0.98
C34 -C35 1.435(3)	C50 -H501 0.98
C35 -C36 1.343(3)	C50 -H502 0.98
C36 -C37 1.434(3)	C50 -H503 0.98
C37 -C38 1.391(3)	

Bond Angle (º)

Cl1 -Co1 -O1 174.94(4)	C15 -C16 -C23 122.75(18)
Cl1 -Co1 -N1 89.93(5)	C17 -C16 -C23 118.91(17)
Cl1 -Co1 -N2 91.18(5)	C16 -C17 -C18 120.56(19)
Cl1 -Co1 -N3 90.79(5)	C16 -C17 -C22 120.71(18)
Cl1 -Co1 -N4 91.76(5)	C18 -C17 -C22 118.7(2)
O1 -Co1 -N1 94.28(6)	C17 -C18 -C19 120.9(2)
O1 -Co1 -N2 86.02(6)	C18 -C19 -C20 119.8(2)
O1 -Co1 -N3 85.01(6)	C19 -C20 -C21 120.0(2)
O1 -Co1 -N4 91.06(6)	C20 -C21 -C22 120.3(2)
N1 -Co1 -N2 90.06(7)	C17 -C22 -C21 120.3(2)
N1 -Co1 -N3 179.21(7)	N3 -C23 -C16 125.17(17)

N1 -Co1 -N4 89.88(7)

N2 -Co1 -N3 90.24(6)

N2 -Co1 -N4 177.06(7)

N3 -Co1 -N4 89.79(6)

Co1 -O1 -C45 137.71(13)

Co1 -N1 -C1 126.58(13)

Co1 -N1 -C4 127.37(13)

C1 -N1 -C4 105.74(16)

Co1 -N2 -C12 127.37(13)

Co1 -N2 -C15 126.51(13)

C12 -N2 -C15 106.03(15)

Co1 -N3 -C23 126.71(13)

Co1 -N3 -C26 127.23(12)

C23 -N3 -C26 105.88(15)

Co1 -N4 -C34 127.04(13)

Co1 -N4 -C37 127.08(13)

C34 -N4 -C37 105.67(16)

N1 -C1 -C2 109.55(17)

N1 -C1 -C38 125.24(18)

C2 -C1 -C38 124.73(19)

C1 -C2 -C3 107.22(19)

C2 -C3 -C4 107.51(19)

N1 -C4 -C3 109.90(17)

N1 -C4 -C5 126.01(18)

C3 -C4 -C5 123.82(19)

C4 -C5 -C6 117.25(17)

C4 -C5 -C12 122.43(18)

C6 -C5 -C12 120.31(18)

C5 -C6 -C7 118.59(18)

C5 -C6 -C11 122.98(18)

C7 -C6 -C11 118.42(19)

C6 -C7 -C8 121.1(2)

N3 -C23 -C24 109.49(17)

C16 -C23 -C24 124.90(18)

C23 -C24 -C25 107.29(18)

C24 -C25 -C26 107.08(17)

N3 -C26 -C25 110.13(16)

N3 -C26 -C27 125.75(17)

C25 -C26 -C27 124.09(17)

C26 -C27 -C28 117.77(17)

C26 -C27 -C34 122.18(18)

C28 -C27 -C34 120.00(18)

C27 -C28 -C29 122.08(18)

C27 -C28 -C33 119.37(18)

C29 -C28 -C33 118.55(19)

C28 -C29 -C30 120.6(2)

C29 -C30 -C31 120.2(2)

C30 -C31 -C32 120.0(2)

C31 -C32 -C33 120.0(2)

C28 -C33 -C32 120.68(19)

N4 -C34 -C27 125.00(18)

N4 -C34 -C35 109.59(17)

C27 -C34 -C35 125.10(18)

C34 -C35 -C36 107.38(18)

C35 -C36 -C37 107.32(18)

N4 -C37 -C36 109.91(17)

N4 -C37 -C38 125.44(18)

C36 -C37 -C38 124.31(19)

C1 -C38 -C37 122.63(19)

C1 -C38 -C39 118.29(18)

C37 -C38 -C39 118.64(18)

C38 -C39 -C40 120.51(19)

C38 -C39 -C44 120.23(19)

C40 -C39 -C44 119.2(2)

C7 -C8 -C9 119.8(2)	C39 -C40 -C41 120.2(2)
C8 -C9 -C10 119.7(2)	C40 -C41 -C42 120.4(2)
C9 -C10 -C11 120.7(2)	C41 -C42 -C43 119.9(2)
C6 -C11 -C10 120.3(2)	C42 -C43 -C44 120.0(2)
N2 -C12 -C5 125.18(18)	C39 -C44 -C43 120.3(2)
N2 -C12 -C13 109.77(16)	O1 -C45 -C46 118.60(19)
C5 -C12 -C13 125.02(18)	O1 -C45 -C47 125.08(19)
C12 -C13 -C14 107.02(18)	C46 -C45 -C47 116.32(19)
C13 -C14 -C15 107.30(18)	
N2 -C15 -C14 109.85(16)	O2 -C48 -C49 120.1(3)
N2 -C15 -C16 126.23(18)	O2 -C48 -C50 120.5(4)
C14 -C15 -C16 123.85(18)	C49 -C48 -C50 119.4(4)
C15 -C16 -C17 118.11(18)	
C1 -C2 -H21 126.00	C36 -C35 -H351 126.00
C3 -C2 -H21 126.00	C34 -C35 -H351 126.00
C2 -C3 -H31 126.00	C32 -C33 -H331 120.00
C4 -C3 -H31 126.00	C35 -C36 -H361 126.00
C6 -C7 -H71 119.00	C37 -C36 -H361 126.00
C8 -C7 -H71 120.00	C39 -C40 -H401 120.00
C7 -C8 -H81 120.00	C41 -C40 -H401 120.00
C9 -C8 -H81 120.00	C40 -C41 -H411 120.00
C8 -C9 -H91 120.00	C42 -C41 -H411 120.00
C10 -C9 -H91 120.00	C41 -C42 -H421 120.00
C9 -C10 -H101 120.00	C43 -C42 -H421 120.00
C11 -C10 -H101 120.00	C42 -C43 -H431 120.00
C6 -C11 -H111 120.00	C44 -C43 -H431 120.00
C10 -C11 -H111 120.00	C39 -C44 -H441 120.00
C12 -C13 -H131 126.00	C43 -C44 -H441 120.00
C14 -C13 -H131 126.00	C45 -C46 -H461 109.00
C13 -C14 -H141 126.00	C45 -C46 -H462 109.00
C15 -C14 -H141 126.00	C45 -C46 -H463 109.00
C17 -C18 -H181 120.00	H461 -C46 -H462 109.00

C19 -C18 -H181 120.00
C18 -C19 -H191 120.00
C20 -C19 -H191 120.00
C19 -C20 -H201 120.00
C21 -C20 -H201 120.00
C20 -C21 -H211 120.00
C22 -C21 -H211 120.00
C17 -C22 -H221 120.00
C21 -C22 -H221 120.00
C23 -C24 -H241 126.00
C25 -C24 -H241 126.00
C24 -C25 -H251 127.00
C26 -C25 -H251 126.00
C28 -C29 -H291 120.00
C30 -C29 -H291 120.00
C29 -C30 -H301 120.00
C31 -C30 -H301 120.00
C30 -C31 -H311 120.00
C32 -C31 -H311 120.00
C31 -C32 -H321 120.00
C33 -C32 -H321 120.00
C28 -C33 -H331 120.00

H461 -C46 -H463 110.00
H462 -C46 -H463 109.00
C45 -C47 -H471 109.00
C45 -C47 -H472 110.00
C45 -C47 -H473 109.00
H471 -C47 -H472 109.00
H471 -C47 -H473 109.00
H472 -C47 -H473 109.00

C48 -C49 -H491 109.00
C48 -C49 -H492 110.00
C48 -C49 -H493 109.00
H491 -C49 -H492 110.00
H491 -C49 -H493 109.00
H492 -C49 -H493 110.00
C48 -C50 -H501 109.00
C48 -C50 -H502 109.00
C48 -C50 -H503 109.00
H501 -C50 -H502 109.00
H501 -C50 -H503 110.00
H502 -C50 -H503 109.00

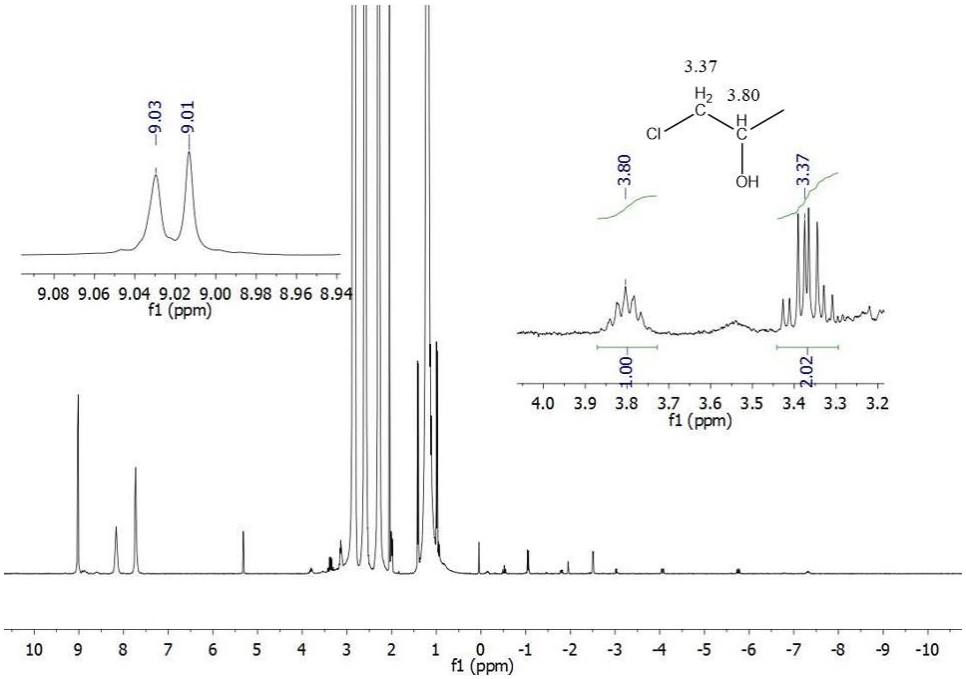

Figure A23. ^{1}H NMR spectrum of TPPCoCl (5 mg)+PO (0.3 mL) (CD_2Cl_2, 300 MHz, 25 ^{0}C).

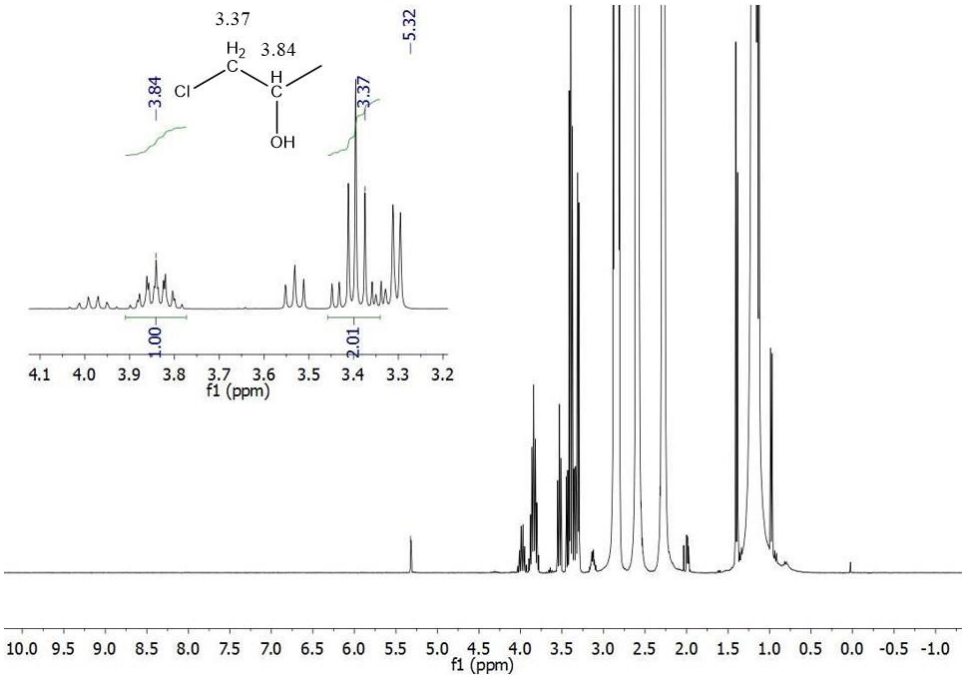

Figure A24. ^{1}H NMR spectrum of 1-chloro-2-propanol+2-chloro-1-propanol (75%:25%)+PO (0.3 mL) for comparison with Figure A23 (CD_2Cl_2, 300 MHz, 25 ^{0}C).

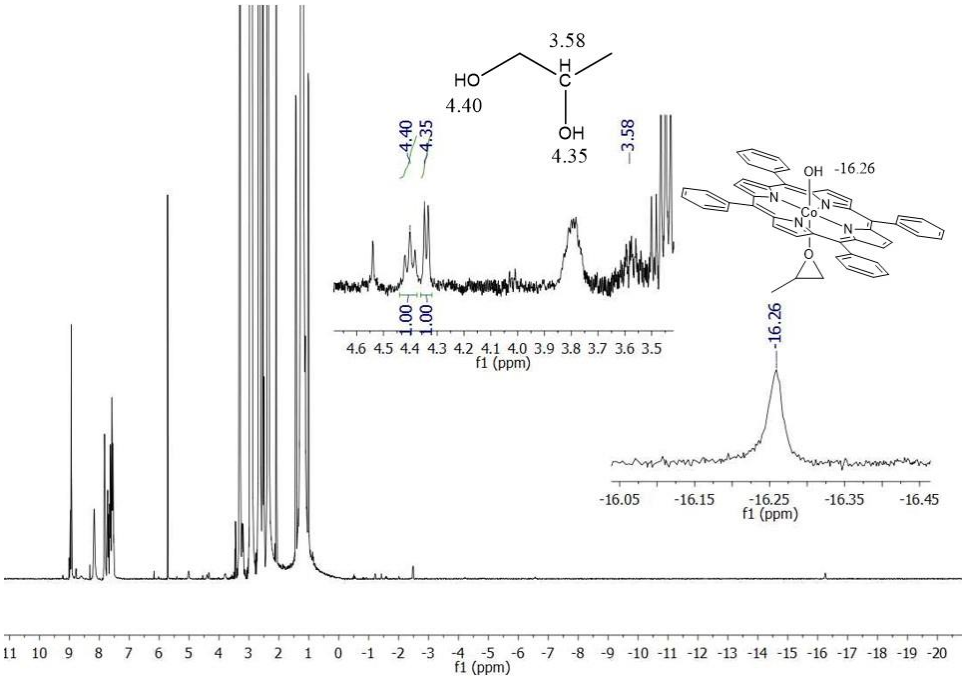

Figure A25. ^{1}H NMR spectrum of TPPCoCl (5 mg)+PO (0.3 mL)+PPNCl (1eq.) (DMSO-d_6, 300 MHz, 25 ^{0}C).

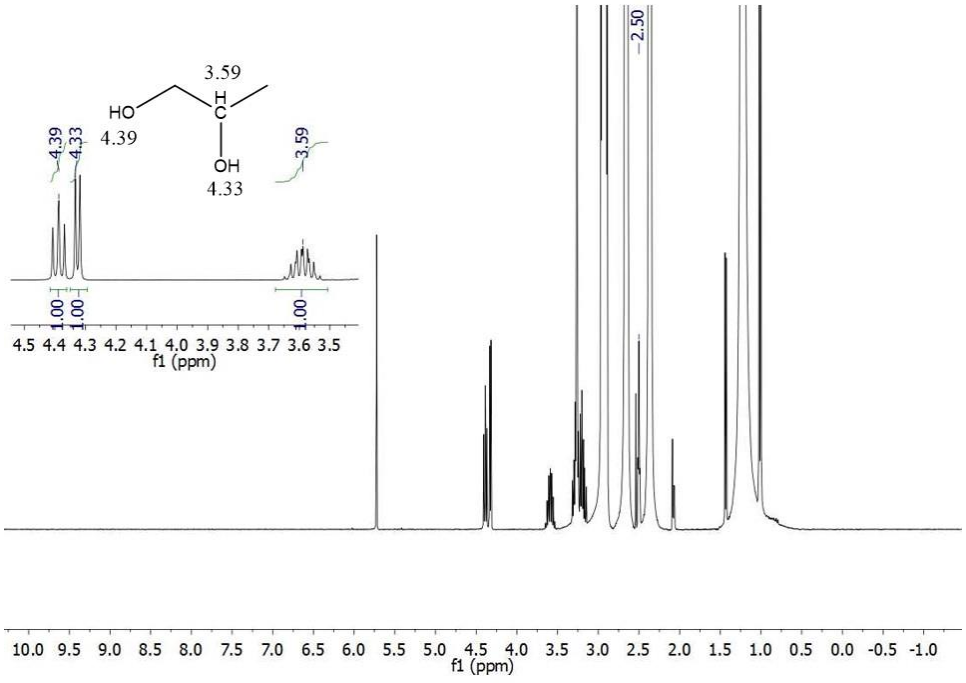

Figure A26. ^{1}H NMR spectrum of propylene glycol+PO (0.3 mL) for comparison with Figure A25 (DMSO-d_6, 300 MHz, 25 ^{0}C).

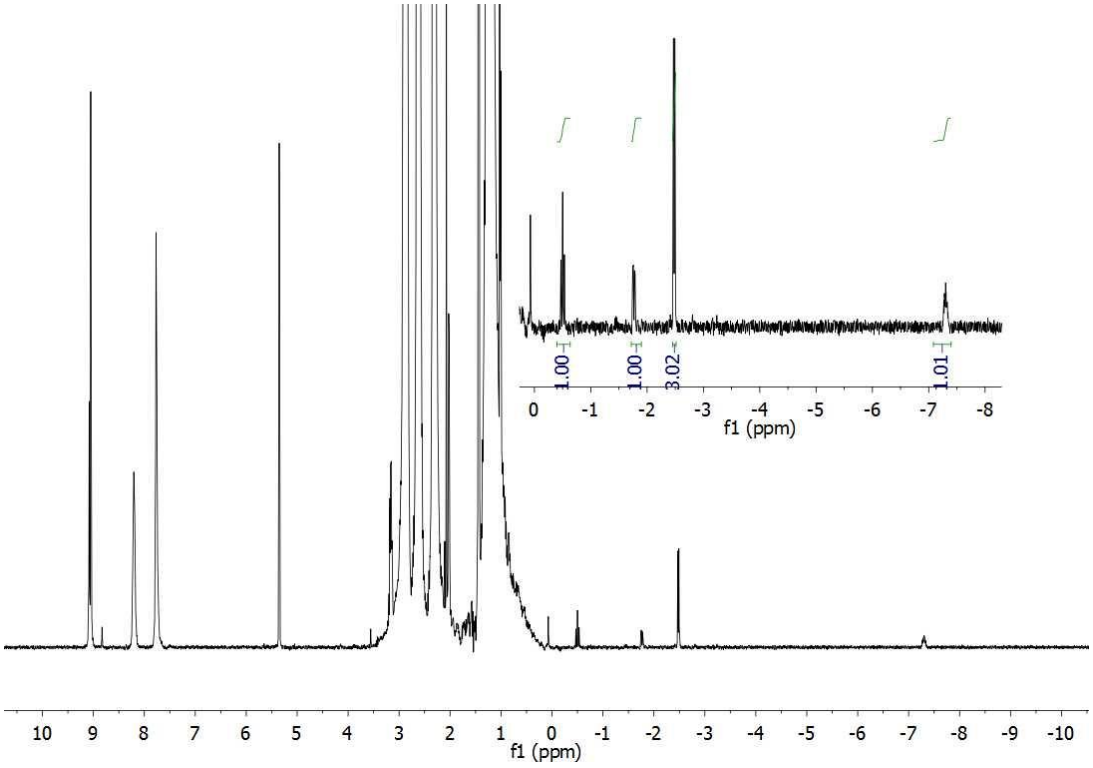

Figure A27. ^{1}H NMR spectrum of TPPCoCl (4 mg)+PO (0.3 mL)+molecular sieve 3Å, t=30 min (CD_2Cl_2 (0.5 mL), 300 MHz, 25 ^{0}C).

reaction time (min)	c_t/c_o	$-\ln(c_t/c_o)$	$1/(c_t/c_0)$
10	0.8	0.223144	1.25
22	0.6	0.510826	1.666667
29	0.5	0.693147	2
38	0.4	0.916291	2.5
50	0.3	1.203973	3.333333

Table A2. Kinetics Data for Determining TPPCoCl Order in the Ring Opening Reaction of PO.

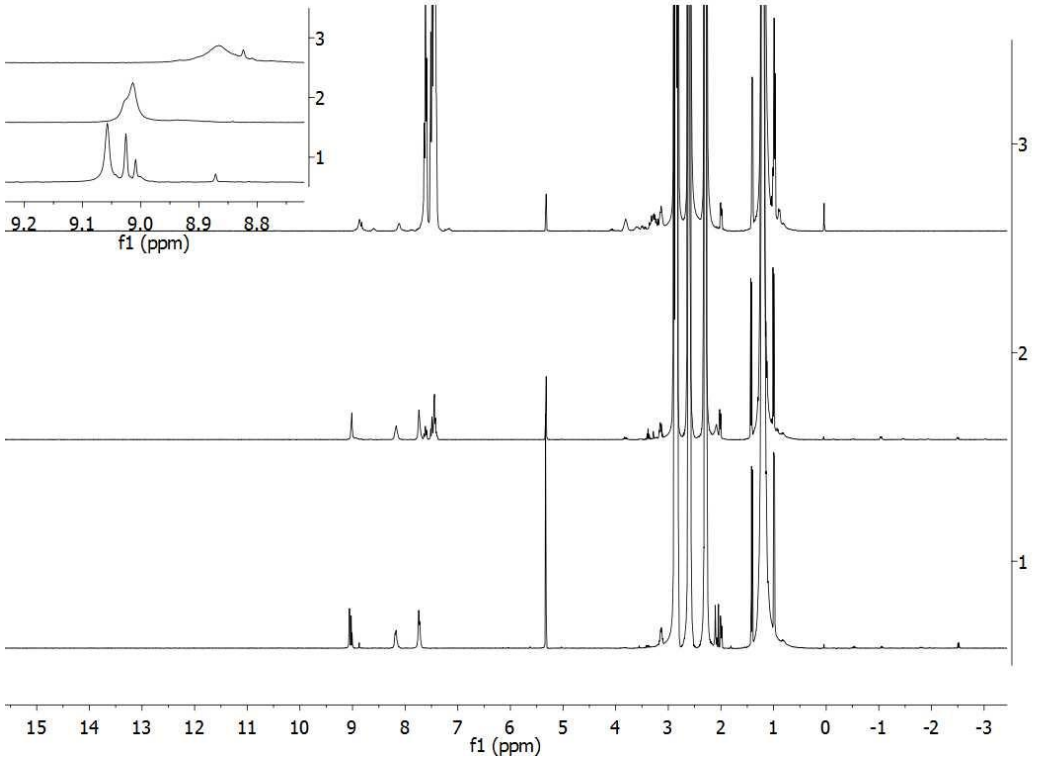

Figure A28. ^{1}H NMR spectra of TPPCoCl (5 mg)+PO (0.3 mL)+0 eq. (Spectrum 1); 1 eq.(Spectrum 2); 10 eq. (Spectrum 3) PPNCl (CD_2Cl_2, 300 MHz, 25 ^{0}C).

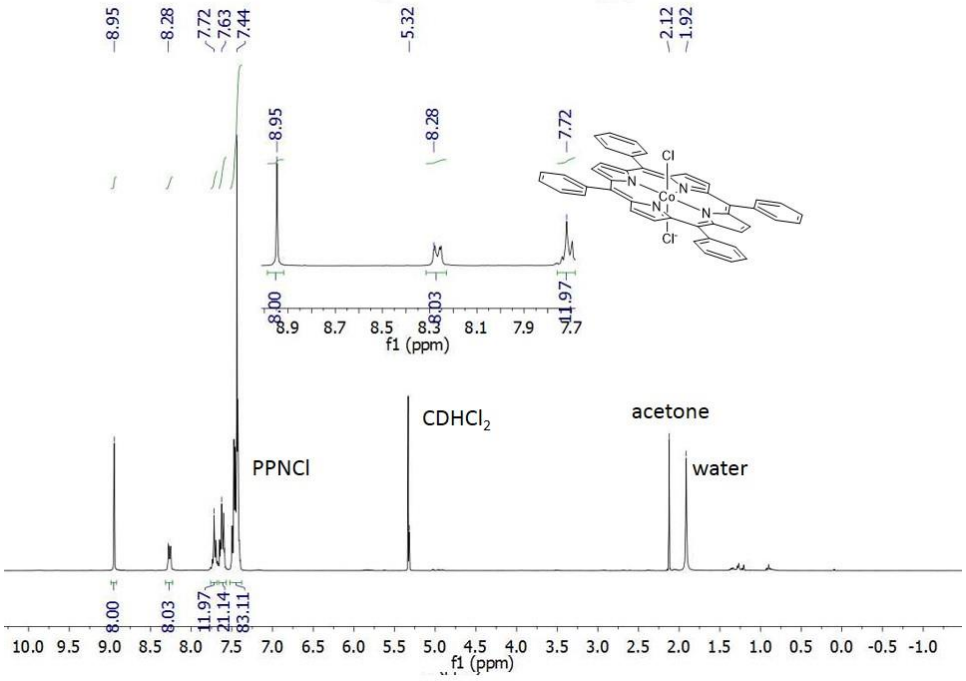

Figure A29. ^{1}H NMR spectrum of TPPCoCl (5 mg) +3 eq. PPNCl (CD_2Cl_2, 300 MHz, 25 ^{0}C).

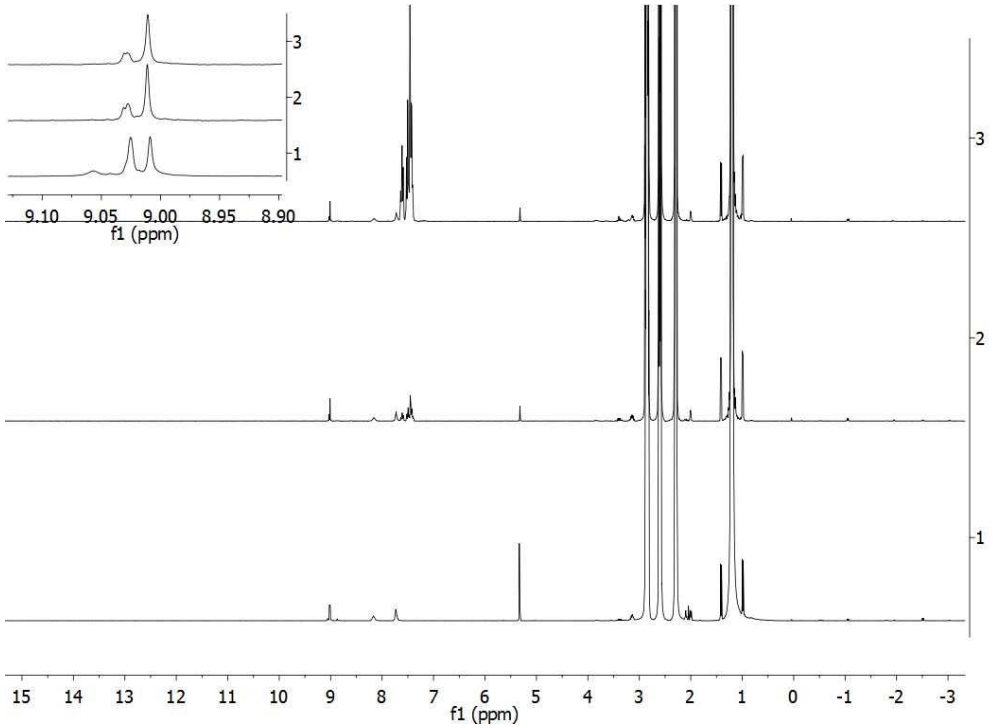

Figure A30. ^{1}H NMR spectrum of TPPCoCl (5 mg)+PO (0.3 mL)+0 eq. (Spectrum 1); 1 eq.(Spectrum 2); 10 eq. (Spectrum 3) $PPNBF_4$ (CD_2Cl_2, 300 MHz, 25 ^{0}C).

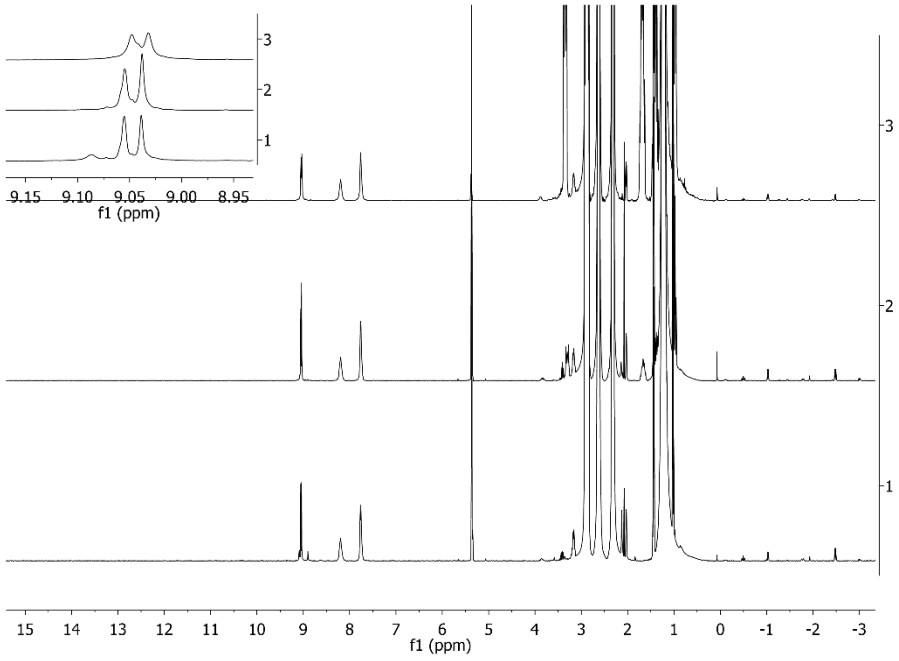

Figure A31. ^{1}H NMR spectrum of TPPCoCl (5 mg)+PO (0.3 mL)+0 eq. (Spectrum 1); 1 eq.(Spectrum 2); 10 eq. (Spectrum 3) NBu_4Br (CD_2Cl_2, 300 MHz, 25 ^{o}C).

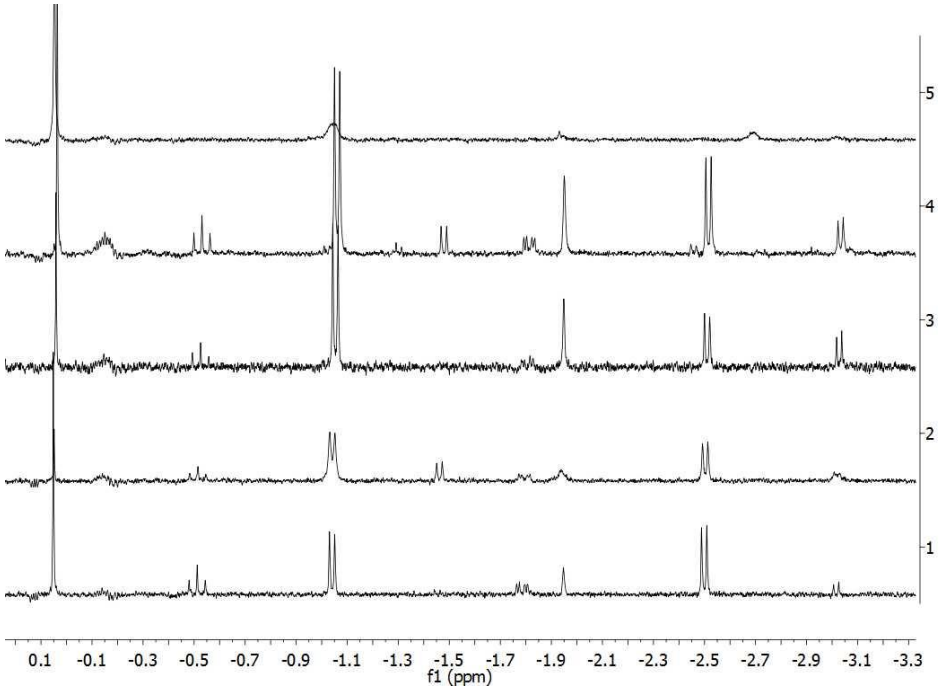

Figure A32. Comparison spectra (-3.2 ppm to 0.2 ppm) of TPPCoCl (5 mg)+PO (0.3 mL) (Spectrum 1); +1 eq. PPNCl (Spectrum 2); +1 eq. $PPNBF_4$ (Spectrum 3); +1 eq. NBu_4Br (Spectrum 4); +1 eq. $PPNN_3$ (Spectrum 5) (CD_2Cl_2, 300 MHz, 25 ^{0}C).

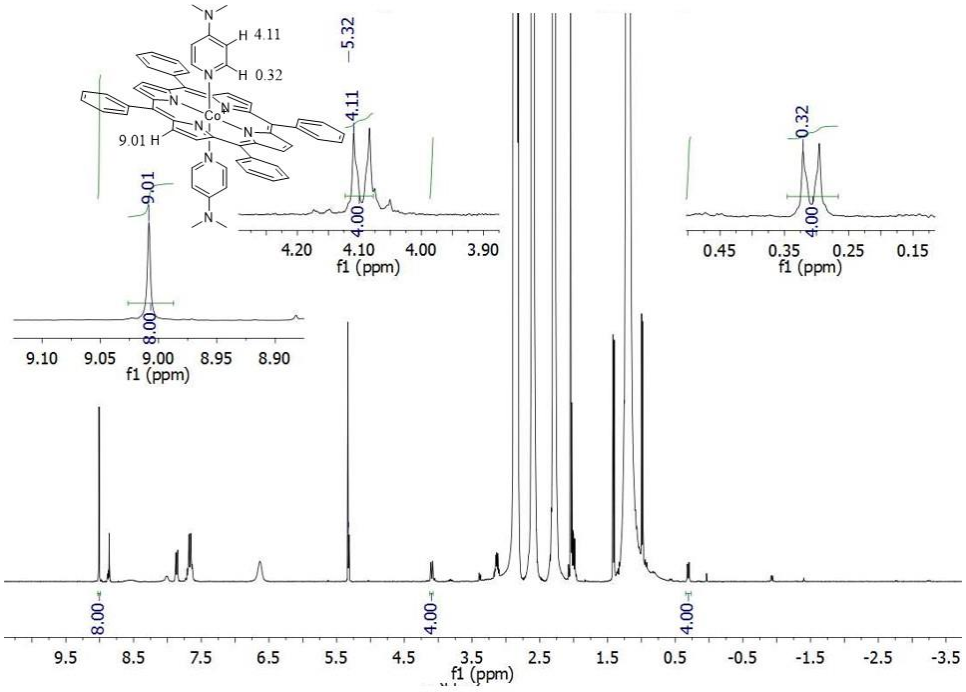

Figure A33. ^{1}H NMR spectrum of TPPCoCl (5 mg)+1200eq. PO+10 eq. DMAP (CD_2Cl_2, 300 MHz, 25 ^{0}C).

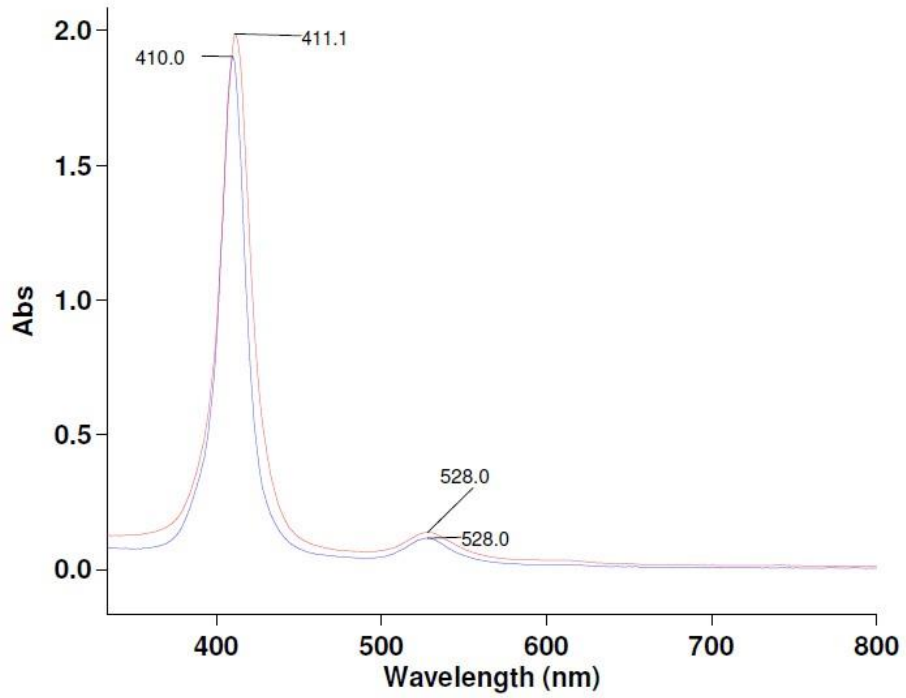

Figure A34. UV-Vis spectrum of TPPCo(II) in DCM (blue curve) and in DCM+MeOH (red curve).

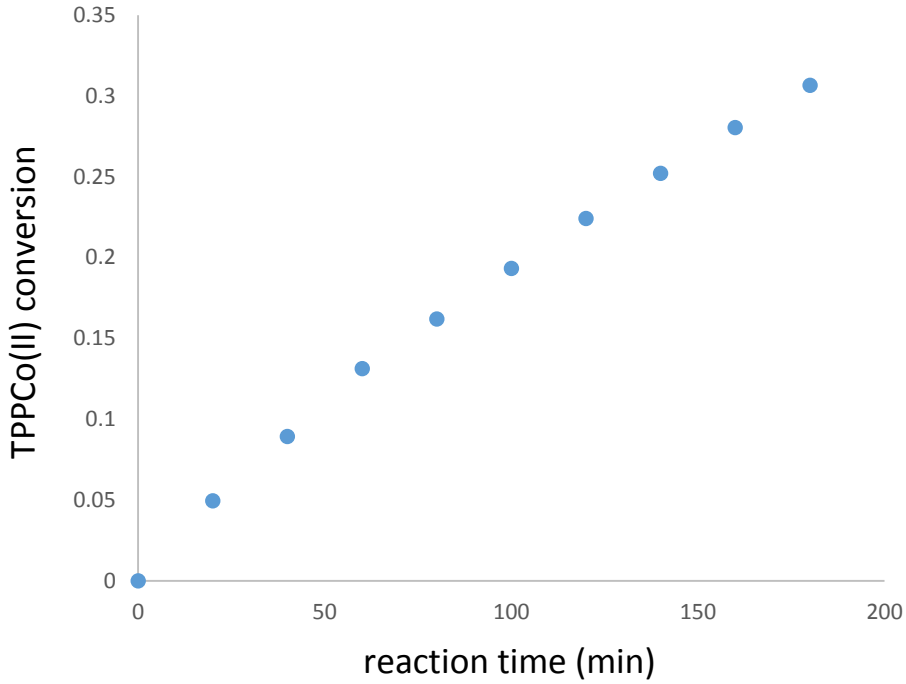

Figure A35. Plot of reaction time versus TPPCo(II) conversion using data in Table A3.

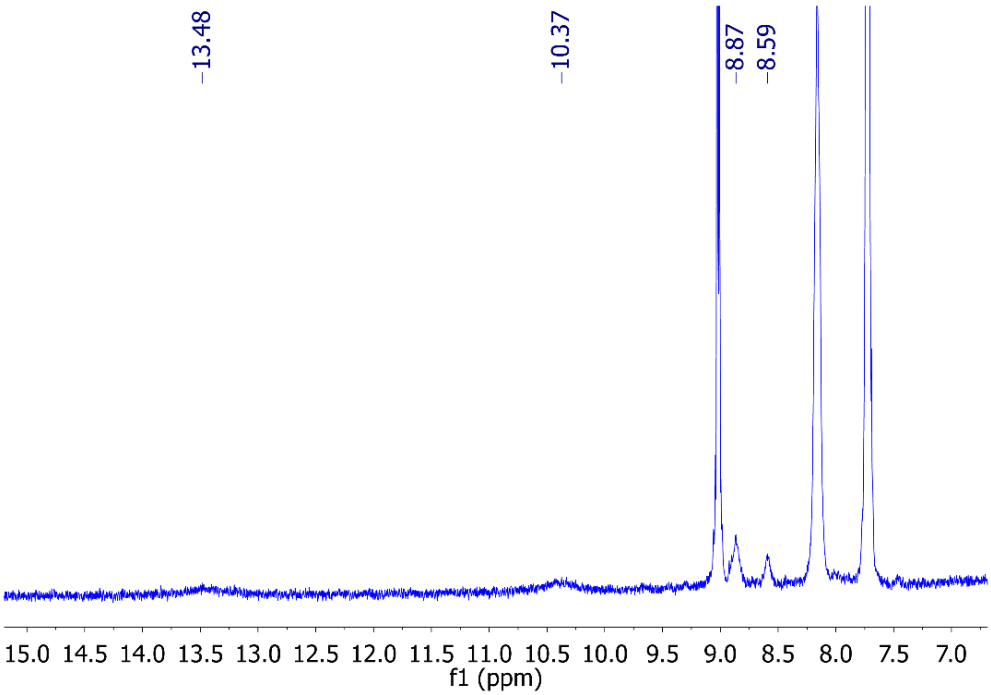

Figure A36. ^{1}H NMR spectrum (CD_2Cl_2, 300MHz, 25 ^{o}C) of TPPCoCl (5 mg), PO (0.3 mL) in CD_2Cl_2 (0.5 mL)) showing the formation of TPPCo(II).

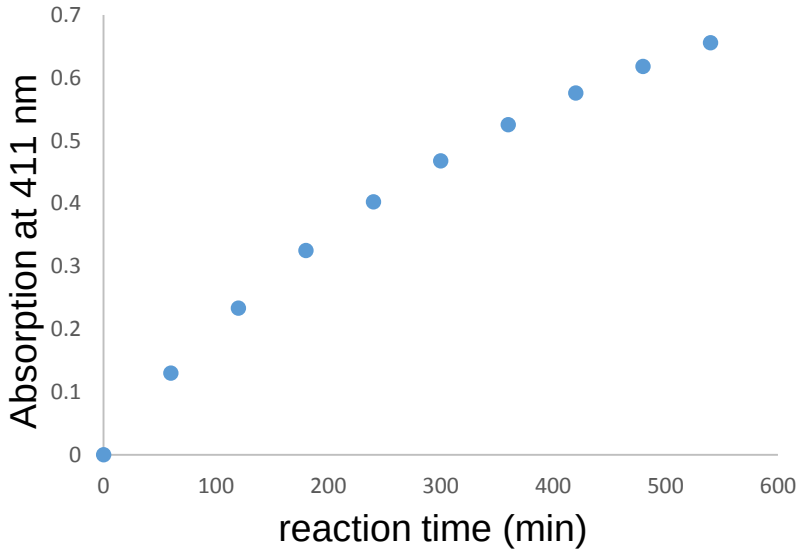

Figure A37. TPPCo(II) conversion versus time for TPPCo(III)OMe autoreduction.

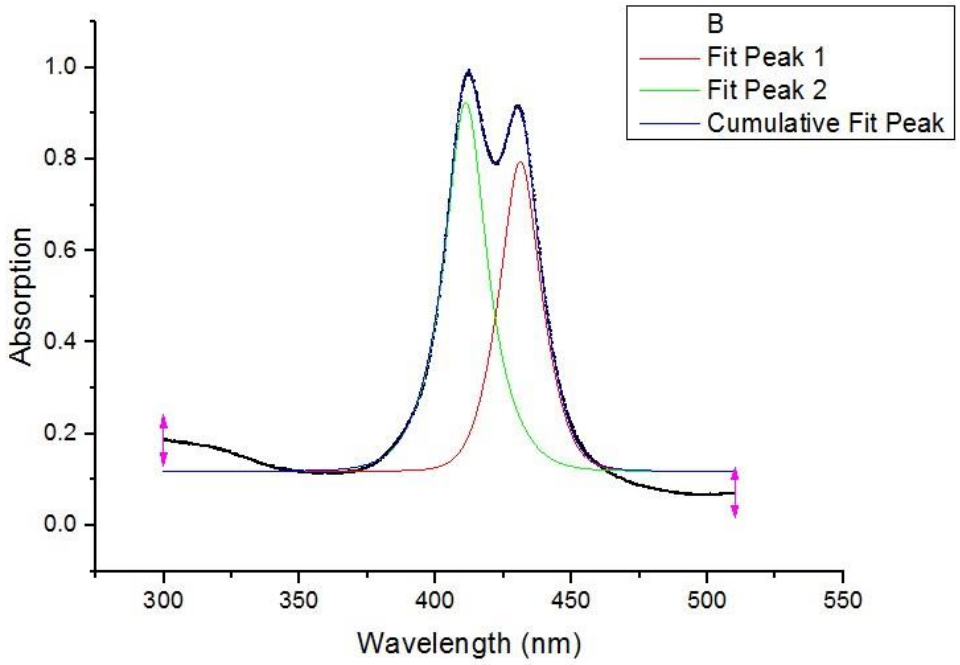

Figure A38. An example of multiple peak fit by using InvsPoly method processed in Origin.

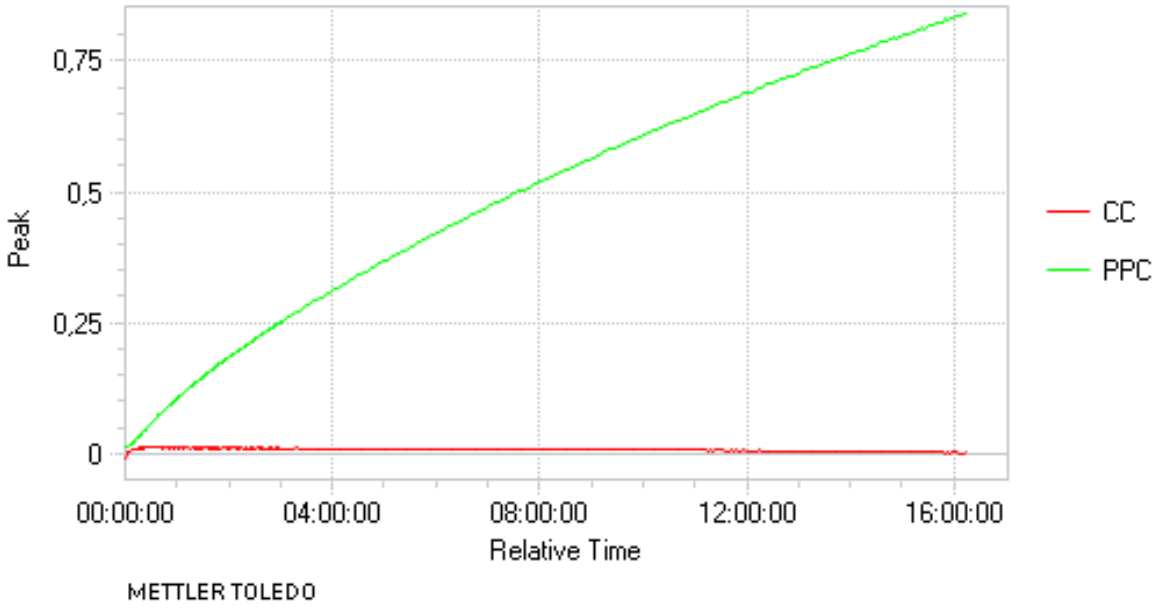

Figure A39. Poly(propylene carbonate) and cyclic carbonate formation curves obtained from in situ IR spectrometer (polymerisation conditions: PO:TPPCoCl:PPNCl=5600:1:1, PO=7 mL, DCM=3 mL, 20 Bar CO_2, 25 ^oC).

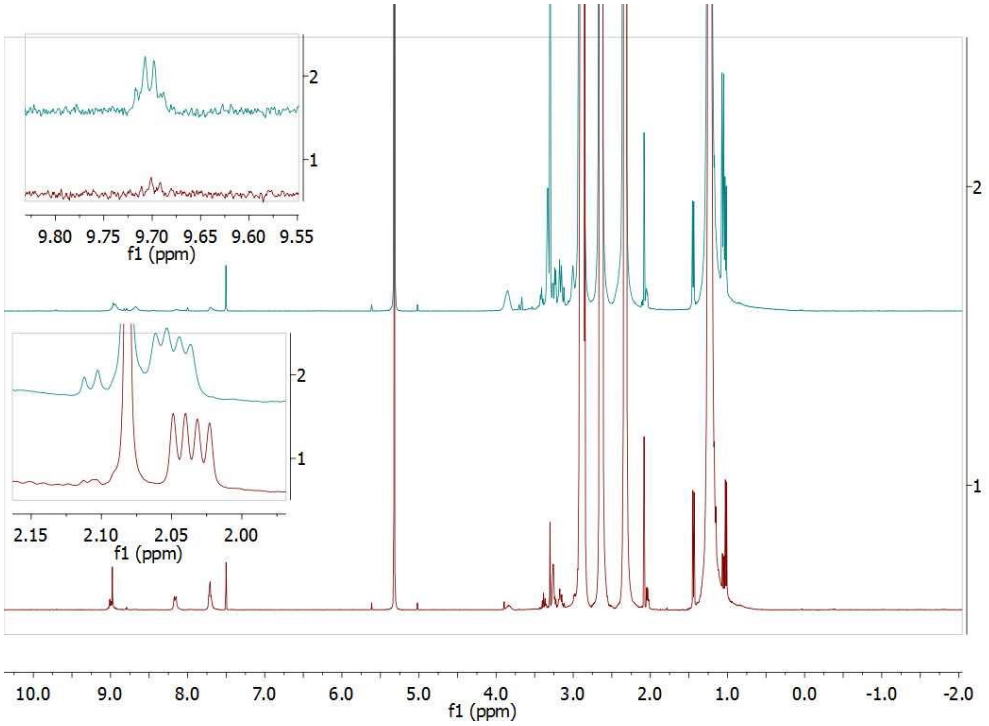

Figure A40. ^{1}H NMR spectra of TPPCoCl (5 mg), PO (0.3 mL) in CD_2Cl_2 (0.5 mL), spectrum 1: t=0; spectrum 2: t=overnight (300 MHz, 25 ^{o}C).

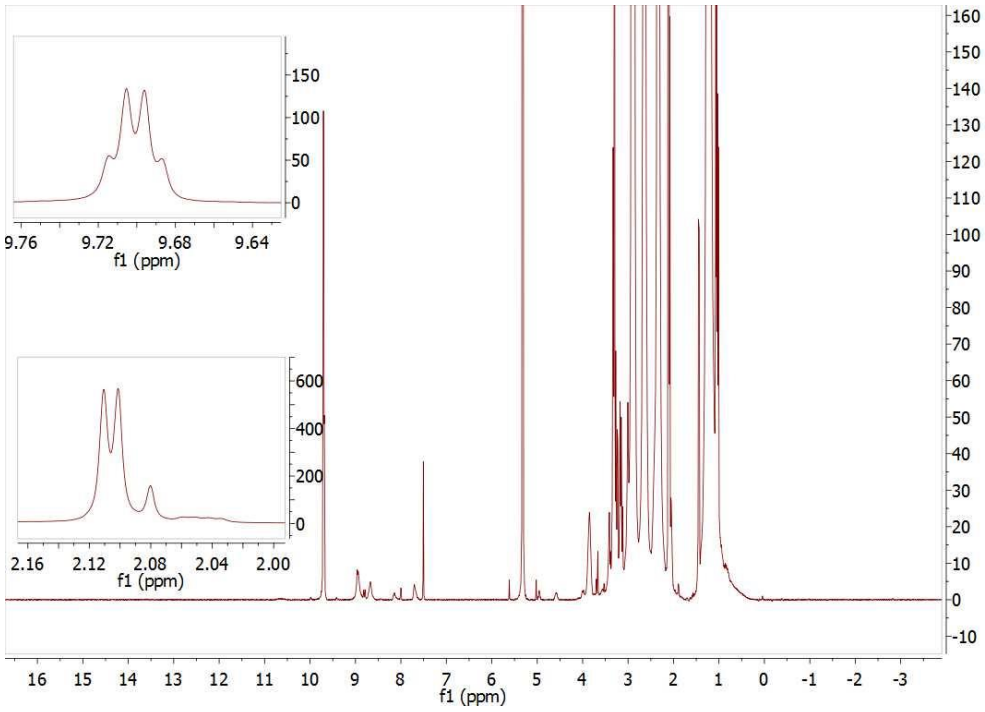

Figure A41. ^{1}H NMR spectrum of TPPCoCl (5 mg), PO (0.3 mL) and acetaldehyde in CD_2Cl_2 (0.5 mL), t=overnight, for comparison with Figure A40 (300 MHz, 25 ^{o}C).

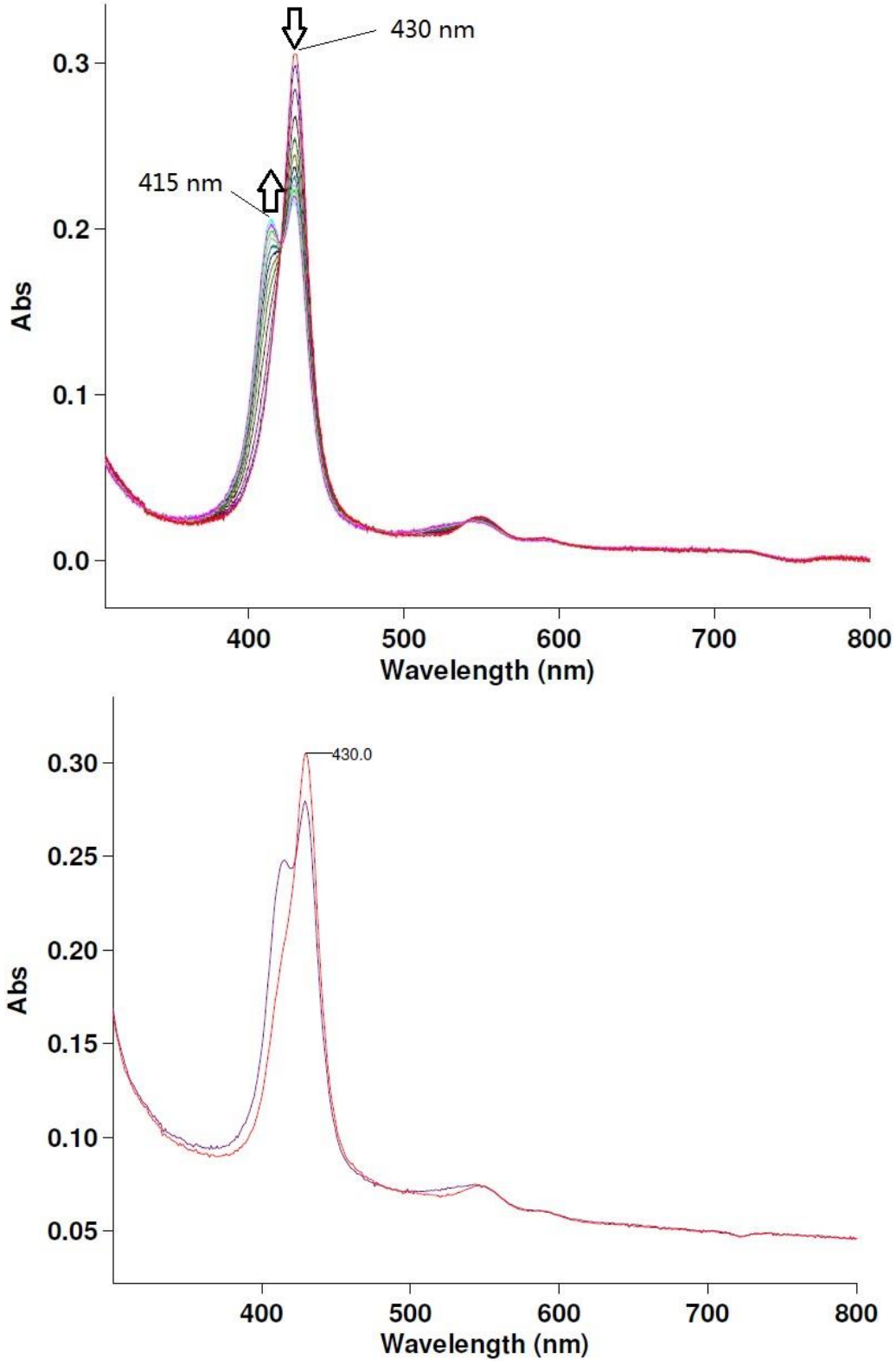

Figure A42. UV-Vis spectra of TPPCoCl with NaOMe (3000 eq.) in DCM/methanol (9/1) (upper spectrum: time-resolved spectra with 1 h interval; lower spectrum: after exposure to light for six hours (red curve) showing re-oxidation to $TPPCo^{III}$, hidden in dark again for 2 hours (purple curve) showing re-reduction to $TPPCo^{II}$).

9. References

(1) Cokoja, M.; Bruckmeier, C.; Rieger, B.; Herrmann, W. A.; Kuehn, F. E. *Angew. Chem. Int. Ed.* **2011**, *50*, 8510.

(2) Hoberg, H.; Schaefer, D. *J. Organomet. Chem.* **1982**, *236*, C28.

(3) Schubert, G.; Papai, I. *J. Am. Chem. Soc.* **2003**, *125*, 14847.

(4) Galindo, A.; Pastor, A.; Perez, P. J.; Carmona, E. *Organometallics* **1993**, *12*, 4443.

(5) Hoberg, H.; Peres, Y.; Krueger, C.; Tsay, Y. H. *Angew. Chem.* **1987**, *99*, 799.

(6) Alvarez, R.; Carmona, E.; Cole-Hamilton, D. J.; Galindo, A.; Gutierrez-Puebla, E.; Monge, A.; Poveda, M. L.; Ruiz, C. *J. Am. Chem. Soc.* **1985**, *107*, 5529.

(7) Yamamoto, T.; Igarashi, K.; Komiya, S.; Yamamoto, A. *J. Am. Chem. Soc.* **1980**, *102*, 7448.

(8) Inoue, Y.; Hibi, T.; Satake, M.; Hashimoto, H. *J. Chem. Soc., Chem. Commun.* **1979**, 982.

(9) Binger, P.; Weintz, H. J. *Chem. Ber.* **1984**, *117*, 654.

(10) Braunstein, P.; Matt, D.; Nobel, D. *Chem. Rev.* **1988**, *88*, 747.

(11) Hoberg, H.; Gross, S.; Milchereit, A. *Angew. Chem.* **1987**, *99*, 567.

(12) Inoue, S.; Koinuma, H.; Tsuruta, T. *Makromol. Chem.* **1969**, *130*, 210.

(13) Kuran, W. *Prog. Polym. Sci.* **1998**, *23*, 919.

(14) Darensbourg, D. J.; Holtcamp, M. W. *Coord. Chem. Rev.* **1996**, *153*, 155.

(15) Coates, G. W.; Moore, D. R. *Angew. Chem., Int. Ed.* **2004**, *43*, 6618.

(16) Darensbourg, D. J. *Chem. Rev. (Washington, DC, U. S.)* **2007**, *107*, 2388.

(17) Sugimoto, H.; Inoue, S. *J. Polym. Sci., Part A: Polym. Chem.* **2004**, *42*, 5561.

(18) Darensbourg, D. J.; Mackiewicz, R. M.; Phelps, A. L.; Billodeaux, D. R. *Acc. Chem. Res.* **2004**, *37*, 836.

(19) Nozaki, K. *Pure Appl. Chem.* **2004**, *76*, 541.

(20) Aida, T.; Ishikawa, M.; Inoue, S. *Macromolecules* **1986**, *19*, 8.

(21) Darensbourg, D. J.; Holtcamp, M. W. *Macromolecules* **1995**, *28*, 7577.

(22) Cheng, M.; Lobkovsky, E. B.; Coates, G. W. *J. Am. Chem. Soc.* **1998**, *120*, 11018.

(23) Jacobsen, E. N. *Acc. Chem. Res.* **2000**, *33*, 421.

(24) Chatterjee, C.; Chisholm, M. H.; El-Khaldy, A.; McIntosh, R. D.; Miller, J. T.; Wu, T. *Inorg. Chem.* **2013**, *52*, 4547.

(25) Cohen, C. T.; Chu, T.; Coates, G. W. *J. Am. Chem. Soc.* **2005**, *127*, 10869.

(26) Lehenmeier, M. W.; Kissling, S.; Altenbuchner, P. T.; Bruckmeier, C.; Deglmann, P.; Brym, A.-K.; Rieger, B. *Angew. Chem., Int. Ed.* **2013**, *52*, 9821.

(27) Chen, P.; Chisholm, M. H.; Gallucci, J. C.; Zhang, X.; Zhou, Z. *Inorg. Chem.* **2005**, *44*, 2588.

(28) Sugimoto, H.; Kuroda, K. *Macromolecules* **2008**, *41*, 312.

(29) Qin, Y.; Wang, X.; Zhang, S.; Zhao, X.; Wang, F. *J. Polym. Sci., Part A: Polym. Chem.* **2008**, *46*, 5959.

(30) Anderson, C. E.; Vagin, S. I.; Xia, W.; Jin, H.; Rieger, B. *Macromolecules* **2012**, *45*, 6840.

(31) Jin, L.; Jing, H.; Chang, T.; Bu, X.; Wang, L.; Liu, Z. *J. Mol. Catal. A: Chem.* **2007**, *261*, 262.

(32) Allmendinger, M.; Molnar, F.; Zintl, M.; Luinstra, G. A.; Preishuber-Pfluegl, P.; Rieger, B. *Chem. - Eur. J.* **2005**, *11*, 5327.

(33) Nielsen, L. P. C.; Stevenson, C. P.; Blackmond, D. G.; Jacobsen, E. N. *J. Am. Chem. Soc.* **2004**, *126*, 1360.

(34) Hansen, K. B.; Leighton, J. L.; Jacobsen, E. N. *J. Am. Chem. Soc.* **1996**, *118*, 10924.

(35) Wu, W.; Qin, Y.; Wang, X.; Wang, F. *J. Polym. Sci., Part A: Polym. Chem.* **2013**, *51*, 493.

(36) Chisholm, M. H.; Zhou, Z. *J. Am. Chem. Soc.* **2004**, *126*, 11030.

(37) Rao, D.-Y.; Li, B.; Zhang, R.; Wang, H.; Lu, X.-B. *Inorg. Chem.* **2009**, *48*, 2830.

(38) Lu, X.-B.; Wang, Y. *Angew. Chem., Int. Ed.* **2004**, *43*, 3574.

(39) Lu, X.-B.; Shi, L.; Wang, Y.-M.; Zhang, R.; Zhang, Y.-J.; Peng, X.-J.; Zhang, Z.-C.; Li, B. *J. Am. Chem. Soc.* **2006**, *128*, 1664.

(40) Shi, L.; Lu, X.-B.; Zhang, R.; Peng, X.-J.; Zhang, C.-Q.; Li, J.-F.; Peng, X.-M. *Macromolecules* **2006**, *39*, 5679.

(41) Cohen, C. T.; Coates, G. W. *J. Polym. Sci., Part A: Polym. Chem.* **2006**, *44*, 5182.

(42) Paddock, R. L.; Nguyen, S. T. *Macromolecules* **2005**, *38*, 6251.

(43) Niu, Y.; Zhang, W.; Pang, X.; Chen, X.; Zhuang, X.; Jing, X. *J. Polym. Sci., Part A: Polym. Chem.* **2007**, *45*, 5050.

(44) Cohen, C. T.; Thomas, C. M.; Peretti, K. L.; Lobkovsky, E. B.; Coates, G. W. *Dalton Trans.* **2005**, 237.

(45) Qin, Z.; Thomas, C. M.; Lee, S.; Coates, G. W. *Angew. Chem., Int. Ed.* **2003**, *42*, 5484.

(46) Guo, L.; Wang, C.; Zhao, W.; Li, H.; Sun, W.; Shen, Z. *Dalton Trans.* **2009**, 5406.

(47) Darensbourg, D. J.; Bottarelli, P.; Andreatta, J. R. *Macromolecules* **2007**, *40*, 7727.

(48) Darensbourg, D. J.; Phelps, A. L. *Inorg Chem* **2005**, *44*, 4622.

(49) Darensbourg, D. J.; Mackiewicz, R. M. *J. Am. Chem. Soc.* **2005**, *127*, 14026.

(50) Eberhardt, R.; Allmendinger, M.; Rieger, B. *Macromol. Rapid Commun.* **2003**, *24*, 194.

(51) Darensbourg, D. J.; Mackiewicz, R. M.; Rodgers, J. L.; Fang, C. C.; Billodeaux, D. R.; Reibenspies, J. H. *Inorg. Chem.* **2004**, *43*, 6024.

(52) Darensbourg, D. J.; Mackiewicz, R. M.; Rodgers, J. L.; Phelps, A. L. *Inorg. Chem.* **2004**, *43*, 1831.

(53) Li, B.; Wu, G.-P.; Ren, W.-M.; Wang, Y.-M.; Rao, D.-Y.; Lu, X.-B. *J. Polym. Sci., Part A: Polym. Chem.* **2008**, *46*, 6102.

(54) Aida, T.; Inoue, S. *Acc. Chem. Res.* **1996**, *29*, 39.

(55) Darensbourg, D. J.; Fitch, S. B. *Inorg. Chem.* **2009**, *48*, 8668.

(56) Nakano, K.; Hashimoto, S.; Nozaki, K. *Chem. Sci.* **2010**, *1*, 369.

(57) Vagin, S. I.; Reichardt, R.; Klaus, S.; Rieger, B. *J. Am. Chem. Soc.* **2010**, *132*, 14367.

(58) Darensbourg, D. J.; Mackiewicz, R. M.; Billodeaux, D. R. *Organometallics* **2005**, *24*, 144.

(59) Nakano, K.; Kamada, T.; Nozaki, K. *Angew. Chem., Int. Ed.* **2006**, *45*, 7274.

(60) Ren, W.-M.; Liu, Z.-W.; Wen, Y.-Q.; Zhang, R.; Lu, X.-B. *J. Am. Chem. Soc.* **2009**, *131*, 11509.

(61) Noh, E. K.; Na, S. J.; S, S.; Kim, S.-W.; Lee, B. Y. *J. Am. Chem. Soc.* **2007**, *129*, 8082.

(62) Min, S. S. J. K.; Seong, J. E.; Na, S. J.; Lee, B. Y. *Angew. Chem., Int. Ed.* **2008**, *47*, 7306.

(63) Na, S. J.; S, S.; Cyriac, A.; Kim, B. E.; Yoo, J.; Kang, Y. K.; Han, S. J.; Lee, C.; Lee, B. Y. *Inorg. Chem.* **2009**, *48*, 10455.

(64) Min, J.; Seong, J. E.; Na, S. J.; Cyriac, A.; Lee, B. Y. *Bull. Korean Chem. Soc.* **2009**, *30*, 745.

(65) Yoo, J.; Na, S. J.; Park, H. C.; Cyriac, A.; Lee, B. Y. *Dalton Trans.* **2010**, *39*, 2622.

(66) Aida, T.; Inoue, S. *Macromolecules* **1982**, *15*, 682.

(67) Fu, G. C. *Acc. Chem. Res.* **2000**, *33*, 412.

(68) Inoue, S.; Koinuma, H.; Tsuruta, T. *J. Polym. Sci., Part B* **1969**, *7*, 287.

(69) Inoue, S. *CHEMTECH* **1976**, *6*, 588.

(70) Kuran, W.; Listos, T. *Macromol. Chem. Phys.* **1994**, *195*, 1011.

(71) Yasuda, T.; Aida, T.; Inoue, S. *Makromol. Chem., Rapid Commun.* **1982**, *3*, 585.

(72) Yasuda, T.; Aida, T.; Inoue, S. *Macromolecules* **1983**, *16*, 1792.

(73) Yasuda, T.; Aida, T.; Inoue, S. *Macromolecules* **1984**, *17*, 2217.

(74) Shimasaki, K.; Aida, T.; Inoue, S. *Macromolecules* **1987**, *20*, 3076.

(75) Endo, M.; Aida, T.; Inoue, S. *Macromolecules* **1987**, *20*, 2982.

(76) Trofimoff, L.; Aida, T.; Inoue, S. *Chem. Lett.* **1987**, 991.

(77) Aida, T.; Kawaguchi, K.; Inoue, S. *Macromolecules* **1990**, *23*, 3887.

(78) Beletskaya, I.; Tyurin, V. S.; Tsivadze, A. Y.; Guilard, R.; Stern, C. *Chem. Rev.* **2009**, *109*, 1659.

(79) Lindsey, J. S.; Schreiman, I. C.; Hsu, H. C.; Kearney, P. C.; Marguerettaz, A. M. *J. Org. Chem.* **1987**, *52*, 827.

(80) Adler, A. D.; Longo, F. R.; Finarelli, J. D.; Goldmacher, J.; Assour, J.; Korsakoff, L. *J. Org. Chem.* **1967**, *32*, 476.

(81) Ballester, P.; Oliva, A. I.; Costa, A.; Deya, P. M.; Frontera, A.; Gomila, R. M.; Hunter, C. A. *J. Am. Chem. Soc.* **2006**, *128*, 5560.

(82) Adler, A. D.; Longo, F. R.; Kampas, F.; Kim, J. *J. Inorg. Nucl. Chem.* **1970**, *32*, 2443.

(83) Yan, G.-P.; Bischa, D.; Bottle, S. E. *Free Radical Biol. Med.* **2007**, *43*, 111.

(84) Abraham, R. J.; Medforth, C. J. *Magn. Reson. Chem.* **1987**, *25*, 432.

(85) Ballester, P.; Costa, A.; Castilla, A. M.; Deya, P. M.; Frontera, A.; Gomila, R. M.; Hunter, C. A. *Chem. - Eur. J.* **2005**, *11*, 2196.

(86) Huet, J.; Gaudemer, A.; Boucly-Goester, C.; Boucly, P. *Inorg. Chem.* **1982**, *21*, 3413.

(87) Kuran, W. *Appl. Organomet. Chem.* **1991**, *5*, 191.

(88) Kuran, W.; Listos, T. *Pol. J. Chem.* **1994**, *68*, 1071.

(89) Herrebout, W. A.; Clou, K.; Desseyn, H. O. *J. Phys. Chem. A* **2001**, *105*, 4865.

(90) Smith, J. G. *Synthesis* **1984**, 629.

(91) Klaus, S.; Lehenmeier, M. W.; Anderson, C. E.; Rieger, B. *Coord. Chem. Rev.* **2011**, *255*, 1460.

(92) Darensbourg, D. J.; Moncada, A. I.; Choi, W.; Reibenspies, J. H. *J. Am. Chem. Soc.* **2008**, *130*, 6523.

(93) Abraham, R. J.; Marsden, I.; Xiujing, L. *Magn. Reson. Chem.* **1990**, *28*, 1051.

(94) Yamamoto, K.; Hoshino, M.; Kohno, M.; Ohya-Nishiguchi, H. *Bull. Chem. Soc. Jpn.* **1986**, *59*, 351.

(95) Guo, X. M.; Jiang, C.; Shi, T. S. *Inorg. Chem.* **2007**, *46*, 4766.

(96) Okada, S.; Segawa, H. *J. Am. Chem. Soc.* **2003**, *125*, 2792.

(97) Akins, D. L.; Zhu, H.-R.; Guo, C. *J. Phys. Chem.* **1996**, *100*, 5420.

(98) Sakurai, T.; Yamamoto, K.; Naito, H.; Nakamoto, N. *Bull. Chem. Soc. Jpn.* **1976**, *49*, 3042.

(99) Iimura, Y.; Sakurai, T.; Yamamoto, K. *Bull. Chem. Soc. Jpn.* **1988**, *61*, 821.

(100) Sakurai, T.; Yamamoto, K.; Seino, N.; Katsuta, M. *Acta Crystallogr., Sect. B* **1975**, *B31*, 2514.

(101) Inoue, S. *J. Polym. Sci., Part A: Polym. Chem.* **2000**, *38*, 2861.

(102) Sugimoto, H.; Ohtsuka, H.; Inoue, S. *J. Polym. Sci., Part A: Polym. Chem.* **2005**, *43*, 4172.

(103) Anderson, C. E.; Vagin, S. I.; Hammann, M.; Zimmermann, L.; Rieger, B. *ChemCatChem* **2013**, *5*, 3269.

(104) Abraham, R. J.; Medforth, C. J. *Magn. Reson. Chem.* **1988**, *26*, 334.

(105) Fukuzumi, S.; Maruta, J. *Inorg. Chim. Acta* **1994**, *226*, 145.

(106) Del Gaudio, J.; La Mar, G. N. *J. Am. Chem. Soc.* **1978**, *100*, 1112.

(107) Del Gaudio, J.; La Mar, G. N. *J. Am. Chem. Soc.* **1976**, *98*, 3014.

(108) Epstein, L. M.; Straub, D. K.; Maricondi, C. *Inorg. Chem.* **1967**, *6*, 1720.

(109) Guyenne, S.; Leon, E. I.; Martin, A.; Perez-Martin, I.; Suarez, E. *J. Org. Chem.* **2012**, *77*, 7371.

(110) Sanchez-Eleuterio, A.; Quintero, L.; Sartillo-Piscil, F. *J. Org. Chem.* **2011**, *76*, 5466.

(111) Hernandez-Garcia, L.; Quintero, L.; Sanchez, M.; Sartillo-Piscil, F. *J. Org. Chem.* **2007**, *72*, 8196.

(112) Greene, F. D.; Savitz, M. L.; Osterholtz, F. D.; Lau, H. H.; Smith, W. N.; Zanet, P. M. *J. Org. Chem.* **1963**, *28*, 55.

(113) Gray, P.; Williams, A. *Chem. Rev.* **1959**, *59*, 239.

(114) Yan, G. P.; Bischa, D.; Bottle, S. E. *Free Radical Biol. Med.* **2007**, *43*, 111.

(115) Adler, A. D.; Longo, F. R.; Kampas, F.; Kim, J. *J. Inorg. Nucl. Chem.* **1970**, *32*, 2443.